

Molecular Identification and Characterization of the *PHOSPHATE DEFICIENCY RESPONSE* related genes, *PRT1* (*ATP-PHOSPHORIBOSYL TRANSFERASE 1*) and *ALMT1* (*ALUMINUM-ACTIVATED MALATE TRANSPORTER 1*)

Dissertation

To obtain the Doctoral Degree in the Natural Sciences (Dr. rer. nat.)

Submitted to

The Faculty of Natural Sciences I (Biological Science)

Martin Luther University, Halle-Wittenberg, Germany



Romel Ahmed

Born on 12.12.1976 in Comilla, Bangladesh

Halle (Saale), July 2015

Reviewers (Gutachter)

- (1) **Prof. Dr. Steffen Abel** (Leibniz Institute of Plant Biochemistry)
- (2) **Prof. Dr. Edgar Peiter** (Martin-Luther University),
- (3) **Dr. rer.nat. habil. Tamara Gigolashvili** (University of Cologne)
- (4) **Dr. Peter Doerner** (The University of Edinburgh)

Date of Defense: 28th September, 2015

DECLARATION BY THE CANDIDATE

I, Romel Ahmed, hereby declare that the work presented in this dissertation, entitled “Molecular Identification and Characterization of the *PHOSPHATE DEFICIENCY RESPONSE* related genes, *PRT1 (ATP-PHOSPHORIBOSYL TRANSFERASE 1)* and *ALMT1 (ALUMINUM-ACTIVATED MALATE TRANSPORTER 1)*”, is an authentic record of my own research conducted under the supervision of Professor Dr. Steffen Abel at the Department of Molecular Signal Processing, Leibniz Institute of Plant Biochemistry, Halle (Saale). I have not submitted the results embodied in this dissertation for the award of any other degree or diploma.

Place and Date:

Halle (Saale), 21-07-2015

(Romel Ahmed)

DECLARATION BY THE SUPERVISOR

This is to certify that the above statement made by the candidate is correct and true to the best of my knowledge.

Place and Date:

(Professor Dr. Steffen Abel)

Halle (Saale), 21-07-2015

Leibniz Institute of Plant Biochemistry (IPB)

DEDICATION

**THIS THESIS IS DEDICATED TO MY BELOVED PARENTS DR. DELOWER
HOSSEN AND HALIMA DELOWER**

Contents

CHAPTER I.....	1
1. INTRODUCTION.....	1
1.2 Plant adaptive responses to Pi deficiency	2
1.3 Local responses to Pi starvation	3
1.3.1 Modification of RSA.....	3
1.3.2 Local Pi sensing.....	5
1.4 Systemic responses to Pi starvation.....	6
1.4.1 Regulators of systemic responses	7
1.4.2. Phosphate transporters	9
1.4.3. Signaling molecules	10
1.5 Cross-talk between nutrients	12
1.6 Forward genetic approaches to isolate Pi-related mutants	12
2. THESIS OBJECTIVES.....	15
CHAPTER II.....	16
1. INTRODUCTION.....	18
2. RESULTS	22
2.1 General characterization of <i>pdr1</i>	22
2.2 Sensitivity of <i>pdr1</i> to external N	23
2.3. <i>pdr1</i> root growth is impaired under Pi starvation.....	24
2.4. <i>pdr1</i> is Pi deficient under high Pi condition.....	27
2.5 Genetic mapping and identification of the <i>PDR1</i> locus.....	28
2.6 Sequence analysis of <i>PDR1</i>	32
2.7 Validation of the <i>PDR1</i> locus.....	34
2.9 Altered RSA of <i>pdr1</i> plants and His-mediated normalization	43
2.10 Free His levels increase upon Pi starvation.....	46
2.11 The rescuing effect of His is local	47
2.12 His in -Pi+DNA medium rescues the <i>pdr1</i> phenotype by stimulating DNA decay.....	49
2.13 Accumulation of anthocyanin and starch in <i>pdr1</i> upon Pi starvation is ameliorated by external His.....	50
2.14 Induction of <i>PSI</i> genes in <i>pdr1</i> by external His	51
2.15 Sensitivity of WT and <i>pdr1</i> to a high external NO_3^-	54
2.16 NO_3^- and NH_4^+ content of <i>pdr1</i> were not different from the WT	55

2.17	Chlorophyll content of the <i>pdr1</i> mutants was not different from the WT	56
2.18	No difference in the content of glutamine, glutamate, asparagine and aspartate between WT and <i>pdr1</i> plants	57
2.19	Increased content of other free amino acids in <i>pdr1</i> compared to the WT	57
2.20	His supplement in N-deficient medium aggravate the growth.....	59
2.21	High His supplement drastically restrict the Arabidopsis growth	59
2.22	Effect of external amino acids on <i>pdr1</i> and WT root growth	60
3.	DISCUSSION	63
3.3	PDR1 is required to use organophosphate	67
3.4	The short root phenotype of <i>pdr1</i> on high Pi medium is linked to high NO ₃ ⁻	68
3.5	Effect of external amino acids on <i>pdr1</i> and WT, and specificity of His.....	70
3.6	Functionally active PDR1/ATP-PRT1 and ATP-PRT2 most likely have distinct functions in <i>planta</i> 72	
3.8	The effect of His is local.....	73
3.9	Crosstalk between Pi and N	74
CHAPTER 3.....		76
1.	INTRODUCTION.....	77
2.	RESULTS	81
2.1	Screening for <i>pdr2</i> suppressors	81
2.2	Five of the <i>pdr2</i> suppressor mutations are allelic to <i>LPR1</i>	82
2.3	Suppressor Line R01A1 carries a mutation in <i>AtALMT1</i>	83
2.4	Genetic analysis confirmed the <i>almt1</i> mutation in R01A1 as recessive	86
2.5	The mutation in <i>AtALMT1</i> in <i>pdr2</i> restores the meristematic function of <i>pdr2</i>	86
2.6	The mutation in <i>AtALMT1</i> in <i>pdr2</i> drives away iron accumulation of <i>pdr2</i>	89
2.7	The mutation in <i>AtALMT1</i> of <i>pdr2</i> prevents root callose accumulation	91
2.8	The <i>almt1</i> mutant is insensitive to low Pi	92
2.9	The loci of the four remaining <i>pdr2</i> suppressor lines are yet to be identified.....	93
3.	DISCUSSION	95
3.1	ALMT1 mediates the PDR2 responses under Pi starvation	96
3.1.1	Excluding the Fe uptake.....	96
3.1.2	Remobilization of internal iron.....	97
3.1.3	Remodeling membrane lipid composition	98
3.2.	Concluding remarks.....	100
4	EXPERIMENTAL PROCEDURES	101
4.1.	Plant Material	101

4.2.	Growth Conditions	101
4.3.	EMS Mutagenesis.....	102
4.4.	Purification of herring sperm DNA	103
4.5.	Genetic Mapping and identification of the <i>PDR1</i> locus	103
4.6.	Hydroponic culture for DNA utilization experiment.....	104
4.7.	Split-root experiments	104
4.8.	Quantitative analysis of cellular free Pi content.....	105
4.9.	Amino acids measurement	106
4.10.	Root growth analysis	106
4.11.	Root meristem size and cell elongation	106
4.12.	Starch staining	106
4.13.	Anthocyanin quantification	107
4.14.	Measurement of NO_3^- and NH_4^+ content	107
4.15.	Analysis of photosynthetic pigments (chlorophyll a and b).....	107
4.16.	RT- and qRT-PCR analysis.....	108
4.17.	Construction of transgenic plant (overexpression and promoter GUS/GFP lines)	108
4.18.	Subcellular localization study	111
4.19.	Promoter GUS/GFP study.....	111
4.20.	Histochemical staining procedures	112
4.21.	Al^{+3} sensitivity test.....	112
4.22.	Genotyping of <i>pdr1</i> and <i>almt1</i> mutants	112
5.	REFERENCES.....	113
	ACKNOWLEDGEMENTS	Error! Bookmark not defined.
	CURRICULUM VITAE.....	Error! Bookmark not defined.
	LIST OF ABBREVIATIONS.....	Error! Bookmark not defined.

CHAPTER I

Responses of Plants to Phosphate Limitation

1. INTRODUCTION

Plant roots sense the change of available nutrients in the rhizosphere and use this information as a cue to adapt their growth and metabolism. Adaptative growth responses include molecular and morphological changes that modify root cell division and differentiation as well as distinct physiological processes (Giehl et al., 2014). This enables plants to maximize the acquisition of nutrients from the rhizosphere (Poethig, 2013; Lastdrager et al., 2014). Among the nutrients, nitrogen (N) and phosphate (Pi) are the most limiting in natural conditions and are thus critical for plant growth and development (Frink et al., 1999; Abel, 2011)

N is a basic element for amino acid and protein synthesis; hence, it is the top most important inorganic nutrient for plants. Plants take up N from the rhizosphere in the form of nitrate (NO_3^-) and ammonium (NH_4^+); however, NO_3^- is the most preferred form of N, especially in the temperate environments. The high solubility of NO_3^- and NH_4^+ limits N bioavailability because of accelerated leaching and loss by denitrification (Vance, 2001). After N, phosphorus (P) is the second most limiting nutrient in the rhizosphere. P in the form of inorganic phosphate (Pi) is a vital structural constituent of essential biomolecules and energy-rich compounds, such as nucleic acids, sugar phosphates, phospholipids and phosphoproteins, nucleoside triphosphate (ATP/GTP/CTP/UTP) or NADPH (Czarnecki et al., 2013). It constitutes a major node in metabolism and is an important signaling molecule modulating multiple cellular functions in signal transduction pathways and gene expression (Abel, 2011). However, the chemistry of Pi makes its bioavailability inadequate in many ecosystems (Abel, 2011). So, the supply of Pi in the soil and its demand by plants as well as the ways plants cope with Pi shortage are important issues discussed in the following introductory sections. Here, I mostly focus on the recent development in the Pi field as the focus of my doctoral research was on the identification and characterization of the Pi regulatory genes, *PDR1* and *PDR2*. Because the *pdr1* mutation points to a link between Pi and N sensing, I also discuss the crosstalk between the two nutrients.

1.1 Pi in the plant and rhizosphere

Plants need an adequate supply of P in its inorganic and fully oxidized form (H_2PO_4^- , HPO_4^{2-} or Pi) as plant growth is tightly dependent on Pi and is a vital component for cellular growth and metabolism. In plants, the total P concentration is in the range of 0.5 to 5 mg g^{-1} dry weight while the metabolically active Pi pool is in the order of 0.1 to 0.8 mg g^{-1} (Vance, 2010; Veneklaas et al., 2012). The total P pool in plant cells consists of free Pi and esterified P compounds, such as nucleic acids, phospholipids and low molecular mass metabolites (Vance, 2010; Malboobi et al., 2014). The larger pool are nucleic acids, mostly RNA (40-60%) (Veneklaas et al., 2012). Plants need to maintain Pi in the range of 5 to 20 mM in the cytoplasm to ensure metabolic functions (Malboobi et al., 2014) while the Pi availability in the rhizosphere seldom exceeds 10 μM (Abel, 2011), usually it is between 0.1 and 1 μM (Veneklaas et al., 2012). The poor mobility and low solubility of Pi, its conversion to organic forms by microorganisms and high propensity of Pi in soil to form complexes with metals (Al, Fe, Ca and Mg) makes a substantial amount of this nutrient much less available for the plant (Abel, 2011). Consequently, one important adaptive response to cope with low Pi availability in the rhizosphere is the modification of root system architecture (RSA) as a visible morphological marker.

1.2 Plant adaptive responses to Pi deficiency

Alterations of RSA in response to Pi starvation are mainly to forage the available Pi from the top soil layers reviewed (Abel, 2011; Peret et al., 2011) and such a modification appears to be locally regulated by available Pi in the rhizosphere, which is known as a local response (Ticconi and Abel, 2004; Reymond et al., 2006; Sanchez-Calderon et al., 2006; Svistoonoff et al., 2007; Abel, 2011) On the other hand, low internal Pi concentrations in plants elicit the systemic responses affecting metabolic adjustments, such as secretion of organic acids, up-regulation of Pi transporters etc. (Thibaud et al., 2010). A comprehensive transcriptome study of split root experiments conducted by Thibaud et al., (2010) revealed the regulation of genes by local growth response is clearly distinct from the systemically controlled genes. The same study estimated that about 70% of the total Pi-responsive genes are regulated by local responses of the root tips to the external Pi while internal Pi content accounts for induction of the remaining fraction of the genes by systemic regulation in the Arabidopsis plant.

1.3 Local responses to Pi starvation

1.3.1 Modification of RSA

Understanding the regulation of organogenesis, particularly the development and structure of the root system under nutrient starvation is necessary to identify precisely the defects caused by mutations in Pi responsive genes. The availability of nutrients in the rhizosphere has a profound effect on the RSA, which is determined by the spatial configuration through modification of cell elongation, lateral root branching and root hair spacing which has an immense impact on the growth and development of a plant (Giehl et al., 2014); Satbhai et al., 2015).

The primary root (PR) is the major determinant of the RSA in *Arabidopsis* because the post embryonic development of lateral roots (LR) and root hair formation (emergence, length and density) largely depends on the growth behavior of the PR, particularly upon Pi starvation. The fate of the root length in turn depends on the rate of cell division, expansion and differentiation while the former occurs in the root apical meristem (RAM), which consists of stem cell niche (SCN) and the meristematic active zone. The SCN comprises vascular initials, pericycle initials, cortex/ endodermis initials and epidermis/root cap initials around the organizing center called quiescent center (QC) in the tip of the growing roots (Dolan et al., 1993). Figure 1-1 depicts the distinct developmental zones of a root; the zone of the meristem, elongation and differentiation and the SCN around the QC. Mitotic activity of the stem cells generates transient amplifying cells which determine the meristem size. If the QC is eliminated as for example by laser ablation, the stem cells start to differentiate causing the subsequent reduction of the meristem and eventually leading to an irreversible root growth arrest (vandenBerg et al., 1997). Cell identity within the root stem cell niche is determined by a number of genes like, *SCARECROW (SCR)* and *SHORT-ROOT (SHR)* which encode GRASS transcription factors (Helariutta et al., 2000; Sabatini et al., 2003). The *RETINOBLASTOMA-RELATED (RBR)* gene, which is the orthologue of tumor suppressor gene *RETINOBLASTOMA (RB)* in human is also known to negatively control the G1/S transition (Kuwabara and Gruissem, 2014). Proximal to meristematic zone is the elongation zone where cells undergo elongation upon the cessation of the division, thus the length of meristematic zone is in between the position of SCN and initiation of first elongating cell. As the cell goes further away from the SCN, its dividing capability decreases and eventually stop the division to start elongation (Petricka et al., 2012a) which ultimately goes for the differentiation for acquiring tissue-specific characteristics (Perini et al., 2012). During

differentiation, LR and root hairs are developed thus giving a particular shape of the three dimensional structure in the soil.

Such a phenotypic plasticity to change RSA largely confers the adaptive advantages over the nutrient limitation condition. However, the degree of plasticity depends on the type of a particular nutrient deficiency, the type of species and also differs within the species based on the accessions (Rosas et al., 2013). There are excellent reviews highlighted the recent development of the effect of nutrient availability on RSA [reviewed in (Forde and Lorenzo, 2001; Lopez-Bucio et al., 2003; Malamy, 2005; Osmont et al., 2007; Giehl et al., 2014; Satbhai et al., 2015)]. For example, N deficiency promotes the elongation of PR and LR without having less effect on the density of LR (Lopez-Bucio et al., 2003; Gruber et al., 2013). On the contrary, the attenuation of primary root (PR) and stimulation of LR together with the profuse root hair formations are the typical responses of *Arabidopsis thaliana* to Pi starvation (Ticconi et al., 2004; Gruber et al., 2013). A suit of studies revealed that the drastic reduction of the PR under Pi limiting condition results from the reduction in cell elongation as well as cell-cycle activity in the root meristem (Lopez-Bucio et al., 2003; Sanchez-Calderon et al., 2005).

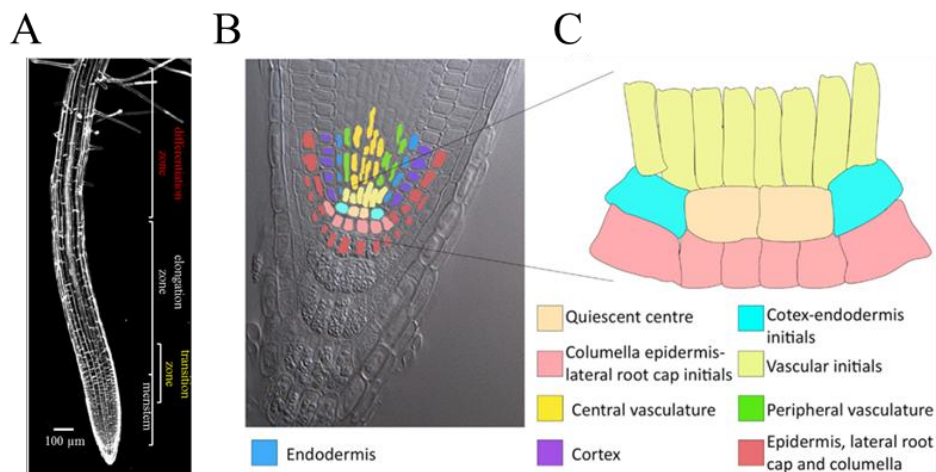


Figure 1-1: Confocal longitudinal section of an Arabidopsis root tip. The left image in (A) shows the Arabidopsis root tip highlighting three distinct developmental zones: the meristematic zone with transition zone, the elongation zone and the differentiation zone. The middle image in (B) shows the color tracing of root tip and (C) shows the magnification of the stem-cell niche (SCN) (Azpeitia et al., 2013).

1.3.2 Local Pi sensing

The root tip is the primary site of external Pi sensing as documented in split-root experiments of *Arabidopsis* where roots were grown partly on high Pi and partly on low Pi. This kind of experiments demonstrated the locally restricted attenuation of PR growth and increase of phosphatase activity as soon as they come in contact with the low Pi concentrations (Liu et al., 2010; Zhang et al., 2014). Although, in split root assays, the shoots and upper part of the roots remain in contact with high Pi, arresting PR growth irrespective of the internal Pi status indicates two important notions. First notion is the necessity of physical contact of the root with the low Pi to activate the response machinery and the second one is the possible Pi sensing site located in the root tip. Numerous studies from mutant analysis, natural variation, and transcriptomic assays indicate that the soil Pi status close to the root tip modulate the RSA of *Arabidopsis* regardless of internal Pi concentration (Chevalier et al., 2003; Ticconi and Abel, 2004; Svistoonoff et al., 2007; Thibaud et al., 2010). However, how does the root tip sense the external Pi remained a paradox. The pioneering molecular insight into the Pi sensing by the root tip has been exemplified by the isolation of *PHOSPHATE DEFICIENCY RESPONSE 2 (PDR2)*. *PDR2* encodes the single P5-type ATPase (AtP5A) in *Arabidopsis* and the mutant is hypersensitive to low Pi showing very short PR growth due to the loss of quiescent center even though the total Pi content in the mutant is not different from the WT, providing evidence of its function as to maintain and fine-tune meristematic activity by monitoring the external Pi status and finally reshaping RSA (Ticconi et al., 2009). *PDR2* was shown to be required for the proper post-translational expression of *SCR* (Ticconi et al., 2004) which on the other hand was previously shown to down-regulate *RBR* gene and the association of *RBR* in the maintenance of root stem-cell (Wildwater et al., 2005) further link the *PDR2* as a Pi-sensitive checkpoint in root development.

The quantitative trait loci of *LPR* were identified using recombinant inbred line population between two *Arabidopsis* ecotypes Bay and Sha (Reymond et al., 2006). In contrast to the *pdr2* mutant phenotype, disruption of the function of *LOW PHOSPHATE ROOT (LPR1* and *LPR2)* displays insensitive root phenotype characterized by a long root on low Pi (Svistoonoff et al., 2007). *LPR1* and its paralogue *LPR2* encode multicopper oxidases expressed in the root tip, including the meristem and root cap (Svistoonoff et al., 2007; Ticconi et al., 2009). The authors (Svistoonoff et al., 2007) also showed that the necessity of the root tip to come physically in contact with the low Pi medium to show the phenotype that further confirmed the location of the possible sensing site at the root tip. The *low-phosphorus insensitive (lpi)* mutants isolated by forward genetics approaches showed long root under Pi limiting growth

medium and are phenotypically similar to *lpr* mutants (Sanchez-Calderon et al., 2006). While the locus of *lpi* remained unidentified till date, further studies with *pdr2* and *lpr* mutant confirmed the epistatic relation of *PDR2* and *LPR1*, indicating that they act in the same regulatory pathway (Ticconi et al., 2009; Müller et al., 2015).

This was further strengthened by the observation that both *LPR1* and *PDR2* are located in the endoplasmic reticulum (ER) and their expression domain overlaps in the root meristematic region (Ticconi et al., 2009). The recent research showed the RAM adjustment is dependent of iron (Fe) in the low Pi medium (Müller et al., 2015). Indeed, multiple lines of evidences suggested earlier that the modulation of RSA upon Pi starvation is the result of complex Pi-Fe interaction (Svistoonoff et al., 2007; Ward et al., 2008; Müller et al., 2015). The recovery of the PR elongation by the reduction of Fe concentration in the low Pi medium was shown by (Svistoonoff et al., 2007). In agreement with this observation, Müller and associates clearly demonstrated the arrested root growth of wild-type (WT) under low Pi condition was due to over accumulation of Fe particularly in the transition zone between dividing and elongating cells of the root (Müller et al., 2015). The authors also showed upon Pi deficiency *pdr2* mutant accumulated more Fe in contrast to the WT and insensitive mutant *lpr1* showed no accumulation of Fe in the RAM while impeded root of *pdr2* rescued if Fe was removed from the -Pi containing media. Thus, Fe dependent low Pi inhibitory effect on the WT and hypersensitive mutant *pdr2* root growth (Müller et al., 2015) strongly support the earlier findings (Svistoonoff et al., 2007). However, in addition to Fe, the presence of other ions in the low Pi medium has also been implicated in triggering significant morphological changes of root system under Pi-deficient condition (Jain et al., 2009) that urge the consideration of the potential connections of Pi with other ions to decipher the Pi sensing and/or signaling mechanisms in controlling the RSA. Apart from the role of external Pi availability in prompting the local responses, internal Pi content in the plant also triggers the so called systemic responses.

1.4 Systemic responses to Pi starvation

A well-known Pi starvation response is the accumulation of starch and anthocyanin in leaf (Bariola et al., 1999; Ticconi et al., 2001; Jiang et al., 2007), replacement of phospholipids with sulfolipid and galactolipids (Yu et al., 2002), secretion of enzymes like ribonucleases (RNases), nucleases, phosphodiesterases, acid phosphatases (APases) and organic acids to scavenge and recycle Pi from internal and external sources (Ticconi and Abel, 2004; Richardson et al., 2009; Liang et al., 2010; Liu et al., 2012).

Plants maximize the Pi uptake from the unusual sources upon Pi starvation like organically bound P that is most abundant in the rhizosphere (Richardson, 2009). One of the strategies is the induction and secretion of acid phosphatases (APases) to release Pi from the P bound complexes (Tran et al., 2010). Several APases from plants have been biochemically and molecularly characterized (Zhang et al., 2014), 11 of them were shown to be up-regulated upon Pi-starvation (Haran et al., 2000; Li et al., 2002). Similarly, plants secrete organic acids from root cells like citrate and malate into the rizosphere to mobilize Pi from metal bound complexes, thus, increasing the pool of available soil Pi (Vance et al., 2003; Ticconi and Abel, 2004; Fang et al., 2009; Richardson, 2009; Plaxton and Tran, 2011).

Another hall-mark response of plants is the induction and secretion of nucleases (RNases/DNases) in Pi-limiting condition. For example, Nürnberger et al., (1990) found low Pi-dependent secretion of RIBONUCLEASE1 (RNS1) correlated with an increasing degradation of extracellular RNA in a suspension-cultured tomato cells. Similarly, by keeping the external Pi concentration constant in the medium, but decreasing the internal Pi concentration by Pi sequestration (incubating the cells with D-mannose and other metabolites), resulted in an increased expression of various RNases (Kock et al., 1998). It has been suggested that the induction and secretion of RNases might be the common strategy of plant to cope with the Pi limited conditions (Tran and Plaxton, 2008). Indeed, the supply of RNA and DNA as a source of Pi was reported to restore the WT (Col-0) root growth (Ticconi and Abel, 2004) indicating the ability of plants to use the available soil nucleic acids.

1.4.1 Regulators of systemic responses

Several transcription factors (TFs) belong to the family of MYB, WRKY and BHLH have been isolated and characterized that are known to be induced only on Pi starvation. *PHOSPHATE STARVATION RESPONSE 1 (PHR1)* which was isolated in an EMS mutant screen (Rubio et al., 2001) belongs to the family of MYB TFs and was shown to regulate a set of *PSI* genes. The orthologues of *PHR1* were identified in rice (*OsPHR2*) and bean (*PvPHR1*) and it was demonstrated that they shared similar function (Valdes-Lopez et al., 2008; Zhou et al., 2008). PHL1 (PHR1 like) along with PHR1 also shows major regulatory roles as the activation and repression of typical *PSI* genes are affected in the double mutants of *phr1phl1* (Bustos et al., 2010). Most of the PHR1 regulated genes were shown to harbor the PHR1 DNA binding motif “GNATATNC” which is called P1BS PHR1 binding sequences (Rubio et al., 2001; Hammond et al., 2003; Misson et al., 2005; Fang et al., 2009). PHR1 is

negatively regulated by SPX1 (SPX domain-containing protein 1), and is sumoylated by SIZ1, SUMO E3 ligase (Miura et al., 2005; Miller et al., 2010). The *siz1* mutant shows an altered Pi-dependent modulation of the RSA, altered *PSI* gene expression and anthocyanin accumulation (Miura et al., 2005). Another MYB transcription factor, *MYB62* is upregulated upon Pi starvation and repress the expression of a number of the *PSI* genes, including gibberellin biosynthetic genes (Devaiah et al., 2009). The same authors showed that over expression of *MYB62* affects the RSA, Pi uptake and acid phosphatase activity.

Basic helix-loop-helix (bHLH) and zinc finger containing transcription factors are also reported to be involved in Pi starvation responses and modulating RSA [reviewed in Chiou and Lin 2011)]. The mutant of *bhlh32* shows significantly increased expression of *PSI* genes, more anthocyanin and Pi accumulation and root hair formations under Pi-sufficient condition compared to the WT (Chen et al., 2007). Similarly *ZAT6*, a TF of a zinc finger family serves as a negative regulator upon Pi starvation. It is induced upon Pi starvation and over expression of this gene inhibits the transcripts of many *PSI* genes and attenuates the PR growth (Devaiah et al., 2007c).

Among the 74 members of the family of WRKY transcription factors in Arabidopsis, a number of them have been implicated in regulating *PSI* genes in addition to the wide array of responses of this family to biotic and abiotic stresses [reviewed in Chiou and Lin 2011)]. *WRKY6*, -42, and -75 are playing a role in fine tuning of the Pi homeostasis in plants in Pi sufficient and deficient condition (Devaiah and Raghothama, 2007; Chen et al., 2009; Su et al., 2015). For example, *WRKY6* and its orthologue *WRKY42* suppress the expression of *PHO1*, an important gene for Pi translocation from root to shoot and this only happen in Pi sufficient condition. Thus, they help the plant to avoid the accumulation of Pi at a toxic level in the shoot. Interestingly, the binding of these TF on the promoter of *PHO1* is abolished at low Pi conditions due to the degradation of their proteins via 26s proteasome-mediated proteolysis (Chen et al., 2009; Su et al., 2015). On the contrary, *WRKY75* is upregulated in Pi starvation and positively regulates a number of *PSI* genes, including phosphatase, *MT4/TFS1*-like genes and high affinity Pi transporters *PHT1* (Devaiah and Raghothama, 2007).

The involvement of several SPX domain-containing protein in Pi perception and maintaining a steady state level of cellular Pi have been reviewed recently (Secco et al., 2012a). The name SPX derived after the suppressor of yeast *gpa1* (*Syg1*), the yeast phosphatase 81 (*Pho81*) and the human XENOTROPIC AND POLYTROPIC RETROVIRUS RECEPTOR 1 (*Xpr1*). The

presence of the domain is, so far reported in almost all major eukaryotes from *Caenorhabditis elegans* and *Drosophila* to mammals (Stefanovic et al., 2011). It is well studied in yeast while in plants which possess the domain were reported to play important roles in fine tuning Pi homeostasis through physical interaction with other proteins (Duan et al., 2008; Hurlimann et al., 2009; Zhou and Ni, 2010; Puga et al., 2014). Depending on the presence of additional domain, SPX domain containing protein in plants is classified into four families, namely SPX, SPX-EXS, SPX-MFS and SPX-RING (Secco et al., 2012b). There are four (AtSPX1-AtSPX4) and six (OsSPX1- OsSPX6) proteins belonging to the SPX family in Arabidopsis and rice, respectively (Duan et al., 2008; Wang et al., 2009). AtSPX1, AtSPX2 and AtSPX3 were reported to be induced by Pi starvation and regulate plant adaptation to Pi starvation by inducing a number of *PSI* genes (Duan et al., 2008). A recent study deciphers the molecular mechanism of SPX1 function showing the inhibition of PHR1 activity by direct binding of SPX1 to PHR1 in a Pi dependent fashion in vitro and in vivo (Puga et al., 2014). At high external Pi, the interaction is most prominent, thus fine-tuning the Pi uptake to alleviate the Pi toxicity while diminishing interaction at low Pi relieve the PHR1 repression to cope with the challenge of limited Pi by activating the major *PSI* genes (Puga et al., 2014). The authors show that double mutants of *SPX1* and *SPX2* accumulate more cellular Pi in compared to the WT when grown on a high Pi medium which indicates the disruption of the normal fine tuning activity of SPX1/PHR1 to maintain the Pi homeostasis (Puga et al., 2014). *AtPHO1* and *AtPHO1:HI* belongs to SPX-EXS class known to be induced upon Pi-starvation while AtNLA, which belongs to SPX-Ring class was reported to be repressed upon Pi starvation in Arabidopsis (Peng et al., 2007; Kant et al., 2011; Rouached et al., 2011; Stefanovic et al., 2011). Disruption of the function of PHO1 shows typical Pi starvation responses like short root, anthocyanin accumulation and induction of Pi starvation associated genes, while over-expression diminish those phenotypes under low Pi conditions (Poirier et al., 1991; Hamburger et al., 2002; Rouached et al., 2011).

1.4.2. Phosphate transporters

All the steps of cellular and molecular responses in Pi deficient condition described above are an attempt to maintain the Pi homeostasis in the plant by maximizing the acquisition, subsequent allocation among different tissues, partitioning between subcellular compartments and mobilization within the plant that require the concerted action of multiple membrane Pi transport systems. The Arabidopsis genome possesses five Pi transporter family; PHT1,

PHT2, PHT3 and PHT4 and plastidic phosphate translocator (PPT) of which the acquisition and mobilization of Pi are largely accomplished by nine members of *PHT1* gene family (Nussaume et al., 2011). Until now, the functional characterization was performed for five PHT1 members, i.e. AtPHT1;1 and AtPHT1;4 (Shin et al., 2004), AtPHT1;5 (Nagarajan et al., 2011) and AtPHT1;8 and AtPHT1;9 (Remy et al., 2012). They are expressed in diverse tissues preferentially in the roots and function as high affinity or low affinity transporters depending on the endogenous Pi status of the plant (Poirier and Bucher, 2002; Nussaume et al., 2011). For example, PHT1;1 and PHT1;4 are the significant contributors of Pi uptake that account for the 75% of the total Pi uptake and are expressed predominantly in the root (Shin et al., 2004; Misson et al., 2005; Catarecha et al., 2007; LeBlanc et al., 2013) while the role of PHT1;5 is Pi distribution which is expressed in the shoots (Nagarajan et al., 2011). PHT1;8 and PHT1;9 were also shown to be expressed in roots and enhanced Pi uptake upon Pi-depletion (Remy et al., 2012). The additive function of those transporters was demonstrated in double homozygous mutants of *pht1;8 pht1;9* (Remy et al., 2012) and *pht1;1 pht1;4* (Shin et al., 2004) which showed a massive decrease in Pi allocation. Fontenot et al. (2015) demonstrated that Arabidopsis PHT1;1 and PHT1;4 form homomeric and heteromeric complexes and substitution of 312 tyrosine of PHT1;1 by aspartate augment the Pi uptake when expressed in yeast cell, likely by the disruption of homomeric interaction. Only one known member of the PHT2 family, PHT2;1 is characterized so far and was shown to encode a low affinity Pi transporter localized to chloroplasts. PHT2;1 share the similarity to PHO4 transporter of *Neurospora crassa* and *pho89* transporter of *Saccharomyces cerevisiae* (Versaw and Metzberg, 1995; Martinez and Persson, 1998). The functions of this transporter is to translocate Pi within the aerial parts of the plant, thus plays a role in the allocation of Pi within the plant (Daram et al., 1999; Versaw and Harrison, 2002). The three PHT3 members were predicted to encode mitochondrial Pi-transporters. However, none of them are functionally characterized yet (Takabatake et al., 1999). The PHT4 family comprises six members, all of which encode low affinity Pi transporter which mediate Pi transport between cytosol and plastids (Guo et al., 2008). There are 16 members PPT family in Arabidopsis (Knappe et al., 2003), but functional characterization is yet to be done.

1.4.3. Signaling molecules

A number of studies indicated that Pi acts as a signaling molecule in addition to its nutrient role. Evidence for the signaling function of Pi comes from experiments using phosphite (Phi)

as a supplement under low Pi conditions. Phi is a non metabolizable analog of Pi. Because plants can not discriminate between Phi and Pi, it is taken up and accumulates in the cytoplasm (Danova-Alt et al., 2008). It is believed that Phi accumulation mimics Pi sufficiency. Indeed, Phi application was found to suppress typical Pi deficiency response reaction like changes in the root morphology, starch and anthocyanin accumulation as well as the induction of several *PSI* genes (Ticconi et al., 2001). The recent evidence is the SPX1/PHR1 interaction, SPX1 is the competitive inhibitor of PHR1 and the interaction is dependent on Phi or Pi (Puga et al., 2014). Similar results also reported from *Saccharomyces cerevisiae* (McDonald et al., 2001), thus it gives a compelling evidence to support the notion that Pi act as a signaling molecule.

Over the last few years, the discovery of plant miRNAs has given new insight in regulating the adaptive responses to Pi starvation. By definition, miRNAs are the non-coding small RNA comprises 20-22 nucleotides that regulate the expression of target genes via post-transcriptional or translational gene silencing (Carthew and Sontheimer, 2009). In Arabidopsis, miR399 species are known to be up-regulated upon Pi starvation and targets *PHO2* mRNA for degradation. *PHO2* encodes for a ubiquitin-conjugating E2 enzyme (UBC24), which represses a number of *PSI* genes (Fujii et al., 2005; Aung et al., 2006; Bari et al., 2006). Loss of function of *PHO2* leads to the excessive accumulation of Pi in the shoots to the toxic level on Pi sufficient conditions due to a constitutive activation of-deficiency response (Delhaize and Randall, 1995; Aung et al., 2006; Bari et al., 2006). On the other hand, *AT4/IPS1* non-coding RNAs induced by Pi starvation found to counteract the miRNA399 activity by so called target mimicry (Franco-Zorrilla et al., 2007; Abel, 2011). Interestingly, *PHO2*, miRNA399 and *AT4/IPS1* are transcriptionally regulated by PHR1 (Rubio et al., 2001; Bari et al., 2006; Lin and Chiou, 2008; Valdes-Lopez et al., 2008; Zhou et al., 2008; Abel, 2011). So, a complex miR399-*PHO2* signaling pathway works in plant to communicate Pi status between shoot and root that triggers the signal for further induction of the required genes for Pi uptake, allocation and remobilization. This signaling pathway seems to be conserved across species as the evidences have come from wheat, barley, bean, rice and arbuscular mycorrhiza (Valdes-Lopez et al., 2008; Branscheid et al., 2010; Hackenberg et al., 2013). Additional miRNAs were also reported to be induced upon Pi-limitation across the plant species such as miR156, miR169, miR158, miR163, miR319, miR395, miR398, miR447, miR778, miR827, miR866 and miR2111 (Fujii et al., 2005; Pant et al., 2009; Hammond and White, 2011).

1.5 Crosstalk between nutrients

In silico analysis of publicly available micro array data recently demonstrated that a subset of common genes are regulated by diverse nutrients (Giehl et al., 2014) suggesting the existence of a crosstalk. The replacement of phospholipids by sulfolipids upon Pi starvation is the example of interdependency and coordinated control mechanism of nutrient homeostasis in plant (Yu et al., 2002). Recently, it has been found that highest Arbuscular mycorrhizal formation and free Pi concentrations in *M. truncatula* grown on a double nutrient deficient medium of Pi and N compared to a single deficient low Pi medium (Bonneau et al., 2013). Evidence of a crosstalk system involving different nutrient availability signals and carbon and nutrient metabolism have also been demonstrated in some other works (Wang et al., 2003; Wu et al., 2003; Belal et al., 2015). Briat et al. (2015) recently reviewed the cross-talk between several nutrients like Pi, S, Zn and Fe mediated by PHR1. Furthermore, a cross-talk between phosphate and zinc signaling is well documented [reviewed in (Kisko et al., 2015) and Fe dependent low Pi root growth inhibition is demonstrated recently (Müller et al., 2015). Excessive Pi accumulation in Arabidopsis leaf of *nla* (*nitrogen limitation adaptation*) mutant plant suggested the interplay between Pi and N (Kant et al., 2011). The *NLA* was identified from a mutant that showed an early senescence phenotype due to weak adaptation to low nitrate (Peng et al., 2007). It encodes a protein containing an N-terminal SPX domain and a C-terminal RING domain possessing putative ubiquitin E3 ligase activity (Peng et al., 2007; Lin et al., 2013). Intriguingly, *NLA* is the target of Pi starvation-induced miR827, loss of function of which resulted in the increase of several Pi-transporter proteins (Lin et al., 2013). Further experiments showed (Park et al., 2014) that *NLA* regulate phosphate homeostasis in Arabidopsis by recruiting PHO2 (PHOSPHATE2) to degrade the PHT2. It is clear that there exist a central level of coordination and cross-talk in plant system to maintain the nutrient homeostasis, there is still insufficient knowledge to explore the molecular mechanism of sensing and signaling of this complex pathway and their ultimate effects on plant development. Various genetic approaches have been undertaken in the last decades to understand the molecular and physiological events responsible for sensing and signaling mineral resources by isolating and characterizing the related mutants.

1.6 Forward genetic approaches to isolate Pi-related mutants

Forward genetic screening for the mutants in altered responses to phosphate starvation has led to the identification of a number of genes. Although substantial progress has been made in the last decades to elucidate some of the important genes involved in transporting (e.g.,

PHT1.1, PHT1.9), transcribing (PHR1, PHL1) and sensing (SPX domain containing protein), much of the players in the Pi network is still to be explored. Particularly, the signaling pathway is still elusive other than identification of *PDR2* and *LPR1* involved in local Pi sensing and a PHR1-IPS1-miR399-PHO2 in systemic signaling cascade. Thus, understanding of sensing and responding of plants to the external and internal Pi at the molecular level is of paramount importance.

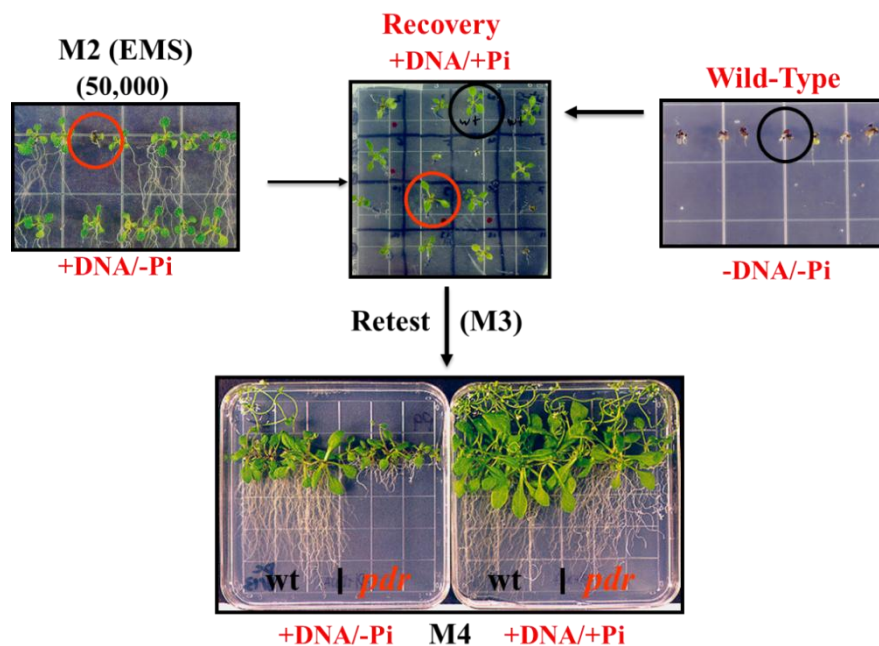


Figure 1-2. Conditional genetic screen of *phosphate deficiency response* (*pdr*) mutants isolated by Chen et al., (2000). Arabidopsis WT and EMS mutants were grown on the square agar plate containing -DNA/-Pi and +DNA/-Pi medium respectively. The putative mutants denoted by the red circle in the left upper panel were transferred to the +Pi/+DNA for recovery (center panel) which were then transferred to the soil. As a control, WT seedlings were grown on -P-DNA medium (upper right panel) were also transferred to +Pi/+DNA medium for the recovering. Red and white circles denote *pdr* mutant and WT respectively. M3 seeds were harvested from the recovered plants and M4 plants were used for the comparative root growth assay with the WT (lower panel).

In an effort to dissect Pi sensing, Abel and colleagues devised a genetic screen (Fig. 1-2) to isolate mutants which are affected in the reorganization of the root system architecture in Arabidopsis under Pi limitation (Chen et al., 2000; Ticconi et al., 2001). The authors devised the screening strategy using DNA/RNA as a sole source of P based on the fact that WT plants can use organophosphate when Pi is limiting. The EMS mutagenized M2 seeds were grown on -Pi/+DNA containing agar plate along with the WT (Fig. 1-2). The mutants that were not

able to sustain the growth were transferred to +Pi+DNA medium for the recovering which were then transferred to the soil for M3 generation. The M3 was then re-tested on the identical (-Pi+DNA) growth medium for the inheritance of the phenotype. M4 plants were used for the comparative root growth study with WT plants on a low Pi and DNA-containing low Pi growth medium (Fig. 1-2). The ultimate result of the screen was the isolation of 22 putative *pdr* mutants that were categorized into two classes. Class I mutants, typified by *pdr1*, impaired in root growth on the nucleic acid and or low Pi containing growth medium hypothesized to be defective in Pi mobilization. Class II mutants, typified by *pdr2* are not affected in Pi mobilization, but showed a conditional root growth phenotype. Loss-of-function *pdr2* plants are not able to adapt to Pi limiting condition and show a very short PR, exhausted QC and loss of RAM activity while no discernible root phenotype observed under +Pi conditions. However, the total Pi content and induction of *PSI* genes in *pdr2* was not affected. Based on this, it was assumed that there must be a local signaling mechanism which triggers changes in the RSA upon Pi starvation.

2. THESIS OBJECTIVES

I have pursued a two-pronged approach to dissect molecular mechanisms of plant responses to phosphate (Pi) starvation using EMS-induced mutagenized Arabidopsis populations.

Project 1: The first project was aimed at the identification and characterization of the *PDR1* gene.

Earlier studies indicated that two factors contribute to the conditional short root phenotype of *pdr1*: a decreased sensitivity to low Pi and an increased sensitivity to high nitrate and other nitrogen compounds. Thus, my research goals were as follows:

- To confirm the previous results and to extensively phenotype *pdr1* under supply of different P and N sources.
- To identify the underlying causal SNP in *pdr1* by de novo next generation sequencing.
- To clone the *PDR1* gene and characterize it, for example, by monitoring the spatio-temporal expression patterns during plant development (qRT-PCR; transgenic reporter lines expressing promoter GUS/GFP constructs), by studying the subcellular localization of the encoded PDR1 protein, and by analyzing the root meristem, root system architecture, Pi-uptake, and accumulation of anthocyanins or starch.

Project 2: The second project was to isolate and identify suppressors of the *pdr2* mutation.

The extremely short root phenotype of *pdr2* on low Pi medium and its epistatic relation with *lpr1/lpr2* mutations were confirmed in earlier studies (Ticconi et al., 2009; Müller et al., 2015). In addition to the genetic interaction of *PDR2* and *LPR1/LPR2* there could be a complex network either upstream or downstream of *PDR2* regulating the adaptive responses via local signaling upon Pi starvation. A further study to identify and characterize the unknown molecules in the *PDR2* signaling pathway would contribute to a better understanding the molecular mechanism that governs the local responses to Pi starvation. Therefore, a number of priority works have been set up:

- To establish a *pdr2* suppressor screen using *pdr2-1/ProCycB1::GUS* lines
- To isolate and verify potential *pdr2* suppressor mutants
- To characterize a promising suppressor line and identify the locus

CHAPTER II

PHOSPHATE DEFICIENCY RESPONSE 1 (PDR1) Encodes ATP-PHOSPHORIBOSYL TRANSFERASE 1 (ATP-PRT1) and Reveals a Link Between Histidine Biosynthesis, Phosphate Signaling and Nitrogen Sensing in Arabidopsis thaliana

ABSTRACT

Plant root is the unique sensor to sense the nutrient availability in the soil and responds accordingly to modulate the RSA for the adaptation to the changing conditions. The *Phosphate deficiency response 1 (pdr1)* mutant was found to lose the ability to elicit the typical response to Pi deficiencies and to N-sufficient growth condition. The mutant was isolated from the screening of EMS mutagenized mutant population on the nucleic acid supplemented growth medium (Chen et al., 2000) and it carries a mutation in one of the first enzymes of Histidine (His) biosynthetic gene, *ATP-PRT1 (ATP- Phosphoribosyl Transferase I)*. The Subcellular localization study shows that the protein is exclusively localized in the plastids. The mutant seedlings on low Pi and DNA containing Pi source medium showed impinged root growth. The phenotype was found to be associated with the alteration of a subset of key *Phosphate Starvation Induced (PSI)* genes expression required for the hydrolysis of the DNA in the growth medium to mine and uptake the Pi. The loss of this intrinsic ability of *pdr1* resulted in the reduction of meristem size including the loss of meristem activity and early differentiation as revealed by histochemical and cell biological assays. Biochemical analysis showed that *pdr1* contained around 50% less free His in the shoots of +Pi/+N and -Pi grown seedlings while in the roots of +Pi/+N, the content was found to be equivalent compared to the wild type (WT). Strikingly, under Pi-deficit conditions, WT root induced the accumulation of fivefold more His than the Pi-sufficient growth conditions, whereas *pdr1* mutant roots showed no more accumulation suggesting the possible role of His under Pi starvation conditions. *pdr1* also showed higher accumulation of starch and anthocyanins compared to the WT control. Nutrient specificity tests showed that increased sensitivity of *pdr1* to high NO_3^- above 250 μM while below this threshold, root growth was found to be promoted more than the root of WT counterpart. Specificity of *pdr1* to N sensitivity was further determined under different N sources. While it showed the similar pattern of sensitivity relative to WT to all the tested N sources, no sensitivity was observed under the amino acid asparagine (Asn) supplemented growth condition which serves as a N

source. The equivalent PR growth for both WT and *pdr1* was recorded when 1 mM Asn was substituted the NO_3^- in the growth medium. The exogenous supplementation of 1 μM His was found to rescue the *pdr1* root phenotype under both Pi/+N and -Pi conditions as the over expression did. Further split root experiments displayed the effect of His is local rather than systemic as root tip must be in contacts with the His supplemented medium to be rescued. Given that His is not a nutrient as the presence of 3 μM His in N-deficient medium was found to have a negative effect on root growth and 1 mM concentration restricted the growth of both WT and *pdr1*, the rescue of other N sources by a very low concentration (1 μM) of His indicates its regulatory function resembling the functionality of hormone molecules. His is likely the hub, coordinating the interaction of a number of unknown molecules to fine-tune the root meristem activities. Thus, the challenges that remain to be tackled is to search for the means by which His can rescue the root phenotype in the presence of organophosphate and high N. Future work is expected to decipher the mystery of underlying His mediated molecular mechanism.

1. INTRODUCTION

Phosphorus (P), preferentially taken by the plant as an orthophosphate anion (Pi; H_2PO_4^- or HPO_4^{2-}), plays a decisive role for its growth and development. P exists in soil in two forms, inorganic phosphate (Pi) or organophosphates. However, the high capacity of Pi to form complexes with a number of cations and its incorporation into organic compounds renders its bioavailability in the soil less than 10 μM (Hinsinger, 2001; Abel, 2011), despite a large amount of total P in the soil (Raghothama, 1999; Poirier and Bucher, 2002). The second source of P in soil is organophosphates that need to be hydrolyzed prior to uptake by the plants. Available data suggest that soil contains more organophosphate than the free orthophosphate (Richardson, 2009), such an ecological paradox has elicited the question if a plants can also use the organic phosphate. Though the use of organic P by the plants is well-known, the underlying molecular mechanism is poorly understood. Most researches to date has been focused extensively on the developmental strategies of plants in response to Pi deficiency that resulted in the identification of key regulatory players like PDR2 (Ticconi et al., 2004), LPR1 (Svistoonoff et al., 2007), several transcription factors, like PHR1 (Rubio et al., 2001), PHL1 (Bustos et al., 2010), SPX domain containing protein AtSPX1-SPX4 (Duan et al., 2008), WRKY75 (Devaiah et al., 2007), ZAT6 (Devaiah and Raghothama, 2007) and MYB62 (Devaiah et al., 2009) and several miRNA and antagonists of miRNA399 (Bari et al., 2006; Chiou et al., 2006; Franco-Zorrilla et al., 2007) as well as several transporters [reviewed in (Nussaume et al., 2011)]. Thus, the research has been driven as to understand how the root explores available soil Pi but has not focused much on how roots mine to make the soil Pi available.

The plant's ability to explore the soil P is not only depending on the modification of RSA or association with mycorrhiza, but also depends on its capacity to find the adequate Pi sources and to convert it into a useable form. The correlation of molecular responses with the organic P in the rhizosphere that shares more than 50% of the total P has not been a subject of priority research. Considering the rapid declining of Pi pool in nature (Cooper and Carliell-Marquet, 2013) and major P pool in the soil is organically bound (Richardson, 2009), dissecting the molecular mechanism for the recycling and reusing this P by the plant is of paramount importance. Traditionally it has been known that only plant associated microorganisms break down the organic P and release the Pi, but limited research in the last decades experimentally confirmed that independent of microorganisms, plant by itself can also use the organic sources of P. A first hint came in 1988 from the study of (Goldstein et al., 1988) under Pi

starvation that showed the acid phosphatase activity determined by histochemical staining in the roots of tomato was negatively correlated with the concentration of Pi in the media. Followed by this, several mutants, for example *pup1*, *pup3*, *pho3* showing less APases activities have been identified in Arabidopsis (Trull and Deikman, 1998; Zakhleniuk et al., 2001; Tomscha et al., 2004). The less Pi content in *pup1* and *pup3* mutants was found to be associated with the less APases activities when grown in a peat-vermiculite mix soil (Tomscha et al., 2004). This indicates that plants can use organic phosphate though it is inconclusive as the growth medium of this study also partly contained inorganic phosphate with the organic one. Thus, experimentally it was unconfirmed if plants indeed can use the organic phosphate till the pioneer work of Abel and his colleagues came to light in 2000 (Chen et al., 2000). The authors performed conditional genetic screening to isolate Arabidopsis mutants that fail to grow on medium containing nucleic acid as the only P source. The advantage of this screening over the colorimetric or histochemical detection of root enzyme activities is the identifications of defects of the molecules implicated in the regulatory pathway as inability to utilize nucleic acid implies impairment in many enzyme activities. *pdr1* and *pdr2* are among the mutants isolated in this screen showing impaired growth in nucleic acid containing Pi source medium. The locus of the *pdr2* mutants was cloned and characterized (Chen et al., 2000; Ticconi et al., 2004) while the locus of *pdr1* was remained to be identified. *pdr1* mutant showed a severe PR growth defect on low Pi and low Pi containing DNA medium and comparatively shorter PR on +Pi with respect to the WT as characterized by Delatorre, (2002). The reduced use of DNA by *pdr1* compared to WT was demonstrated by gel electrophoresis evaluating the sample from the DNA supplied growth medium. Delatorre, (2002) then performed northern analysis for the expression of genes coding for a ribonuclease (*AtRNS2*; Bariola et al., 1999), an acid phosphatase [*AtACP5*; (Del Pozo et al., 1999)], a high-affinity Pi transporter [*AtPT2*; (Muchhal et al., 1996)], and a non-coding RNA [*AtAt4*; (Shin et al., 2006)]. The blot was performed for the shoots and roots of WT and *pdr1* seedlings grown on +Pi and -Pi. The steady-state transcript levels of all the tested genes increased in WT plants grown under P-limiting conditions, particularly in the roots, while the expression of the corresponding genes in *pdr1* was absent or much less prominent than that observed in WT plants. In addition, two typical markers, starch and anthocyanin accumulation under Pi starvation was also measured that showed higher accumulation in both cases under -Pi and -Pi containing DNA medium. The results were consistent with the low free and total Pi content in the root of *pdr1* compared to the WT grown under -Pi and DNA containing -Pi medium. The nutrient specificity of root growth inhibition of *pdr1* mutant was then examined.

PR of wild-type seedlings grown on $-Pi$, $-S$, or $-Fe$ medium were 40-60% shorter than on complete medium. Likewise, although PR growth of *pdr1* was generally suppressed when compared with WT on complete medium, it was significantly more inhibited on $-Pi$ (by about 80%) than on $-S$ or $-Fe$ medium. The decrease of *pdr1* PR growth on a low S and low Fe was in similar rate of decrease in WT suggesting its root growth phenotype is not specific to $-S$ and $-Fe$. Surprisingly, removal of NO_3^- ($-N$) normalize the *pdr1* root phenotype with respect to WT. This observation suggests that a short root phenotype of *pdr1* in $+DNA/-Pi$ was caused by reduced utilization of external DNA in Pi limiting conditions and by an inhibitory effect of external NO_3^- on PR growth. There is a growing evidence recently documented concerning a crosstalk between the nutrients such as interdependency and interconnection between Pi and S (Yu et al., 2002; Rouached et al., 2011), Pi and N (Kant et al., 2011; Bonneau et al., 2013; Park et al., 2014; Medici et al., 2015), Pi and Fe (Müller et al., 2015) and between Pi, S, Zn and Fe under the control of PHR1 (Briat et al., 2015). This suggests the existence of a complex genetic interplay between nutrients causes a higher level of complexity that needs to be addressed to decipher the natural adaptation strategies. Here I present detailed characterization and identification of this novel *pdr1* mutant locus. *PDR1* was identified as an *ATP-phosphoribosyl transferase 1*, *ATP-PRT1* (At1g58080) by whole genome re-sequencing followed by fine mapping. ATP-PRT1 is the first committed catalyzing enzymes for His biosynthesis and it has second isoform, ATP-PRT2. In general, His biosynthesis pathway is very much conserved across the all organisms (Muralla et al., 2007). In Arabidopsis, there are 8 steps catalyzed by 11 different enzymes and the corresponding genes have been identified, designated as HISN numbering 1 to 8 sequentially (Muralla et al., 2007) while in yeast they are simply named as HIS gene with corresponding number. Several mutants in Arabidopsis His biosynthetic pathway like the mutant of HisN6, HisN3 has already been isolated. The studies showed the disruption of function of His yielded either embryonic, seedling lethality or severe disturbance of meristem activity as for example *emb296* of HisN6 and *apg10* of HISN3 (Tzafrir et al., 2004; Noutoshi et al., 2005). In addition to lethality, experimentally it is also very hard to distinct metabolic and regulatory functions of this amino acid that explains why the regulatory role of His is still elusive to date. Nonetheless, a leaky mutant *hpa* of HisN6 depicts the role of His in maintaining the meristem activity of Arabidopsis (Mo et al., 2006). However, no report is known yet as to the role of His in regulating nutrients in the plants, even though some reports have been shown the link of His biosynthetic genes in regulating the phosphate pathway in *Saccharomyces cerevisiae* (Arndt et al., 1987; Denis et al., 1998; Pinson et al., 2000; Pinson et al., 2009). The results

presented here demonstrate the interconnection of His biosynthetic pathway with nutrients that mediates a cross-talk between Pi and N. *PDR1/ATP-PRT1* is therefore the first report to the best of our knowledge revealing a novel link in regulating the root meristem activity by maintaining the Pi and N homeostasis in Arabidopsis

2. RESULTS

2.1 General characterization of *pdr1*

The *pdr1* mutant was back-crossed to WT (Col-0) three times prior to a detailed phenotypic characterization. To determine the mode of inheritance of the *pdr1* short root phenotype, back-crossed populations were subsequently analyzed. The corresponding F1 generation showed a WT phenotype on $-P_i+DNA$ medium while the resultant inbred F2 progenies segregated as a single recessive Mendelian trait with a ratio of 3:1 (showing 227 F2 plants with a long PR and 73 F2 plants with a short PR) on the same growth medium ($-P_i+DNA$). The data represent the χ^2 value 0.79 that was not a significant deviation from the expected value (P value $0.37 > 0.05$). A similar segregation ratio was also observed for the $-P_i$ grown back-crossed (3-times) F2 population, further validating that the *pdr1* mutation is a single recessive allele. The PR growth of *pdr1* on $+P_i$ medium was found to be similar to WT, just after 2-3 days of germination, (Fig. 2-1A), however, in the following days, a slower root growth of *pdr1* was observed. After 6 days of germination, *pdr1* had only one third of the PR growth of WT (Fig. 2-1B). Interestingly, after three weeks of germination, *pdr1* PR together with the lateral root growth was found to be enhanced in the complete growth medium ($+P_i+N$), thus the difference of fresh weight biomass of *pdr1* with the WT was found to be marginal (Fig. 2-1C & 2-1D). When WT and *pdr1* seedlings were transferred after 10 days of germination from $+P_i$ grown plate to the soil in the greenhouse, the shoot phenotype of both genotypes was similar (Fig. 2-1E). To obtain a comprehensive picture of the P_i effect on *pdr1*, I quantified the PR lengths of 6 days old seedlings grown on $+P_i$, $-P_i$, $-P_i+DNA$ medium (Fig. 2-1F & 2-1G). A 50% reduction of the *pdr1* PR length compared to the WT root grown on $-P_i$ was observed. The provision of DNA in the $-P_i$ medium promoted the WT root growth to a comparable level with the $+P_i$ grown WT root while *pdr1* showed no more significant improvement, rather it phenocopied its $-P_i$ growth, thus making a 6-fold difference with the WT (Fig. 2-1F & 2-1G). This is suggestive to the intrinsic capacity of the WT to use the organic P while the mutation in *pdr1* locus lost this ability. Interestingly, the slow growth of *pdr1* on P_i sufficient medium (Fig. 2-1B) put forward a question whether *pdr1* was constitutively P_i -deficient or not specific to P_i only. Earlier experiments by Delatorre (PhD Thesis, 2002) showed a similar response of *pdr1* PR growth like WT on $-Fe$ and $-S$ media, but a striking observation was the enhanced sensitivity of *pdr1* root growth to high NO_3^- on

+Pi media. This pointed out the additional possible link of N to short root *pdr1* phenotype on a complete growth medium (+Pi/+N).

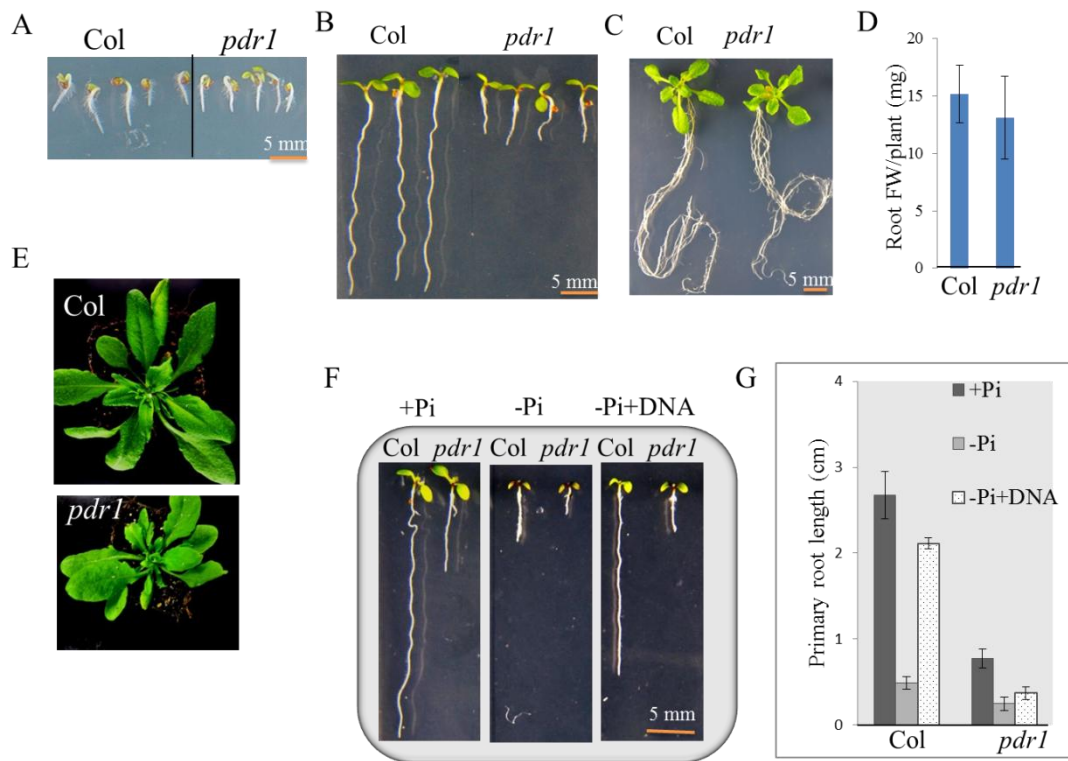


Figure 2-1: General phenotypes of the *pdr1* mutant.

(A-D) Growth parameters of *pdr1* compared to WT at an early and prolonged period of growth on vertically oriented agar plates. Images of WT and *pdr1* seedlings grown on +Pi/+N for (A) 2 days, (B) 6 days, and (C) 25 days after germination. (D) shows biomass of roots as fresh weight (FW) from 25 days old seedlings, values are the mean \pm SD of 10 independent roots.

(E) 3 weeks old soil grown *pdr1* seedlings showed a similar shoot phenotype compared to the WT.

(F) Representative images of root growth and (G) PR lengths of 6 days old WT (Col-0) and *pdr1* seedlings grown vertically oriented on agar plates containing +Pi, -Pi and -P+DNA medium. Filter-sterilized purified herring sperm DNA was substituted for Pi and added to the autoclaved medium to a final concentration of 0.4 mg mL^{-1} .

2.2 Sensitivity of *pdr1* to external N

To further understand the effect of NO_3^- , a dose response study was carried out to compare the PR growth of WT and *pdr1* seedlings (Fig. 2-2A & 2-2B). The PR length of WT increased with the increasing concentration from 0 to 10 mM of KNO_3 in the growth media. In contrast to the WT, *pdr1* showed significantly longer roots up to 0.1 mM KNO_3 provision followed by

a drastic decrease at and above this concentration (Fig. 2-2B). Likewise, the sensitivity of *pdr1* was tested in response to NH_4Cl and $(\text{NH}_4)_2\text{SO}_4$ containing N source media (Fig. 2-2C & 2-2D). NH_4^+ as a sole source of N inhibited the WT PR growth progressively with the increasing concentration as consistent with previous study (Li et al., 2014) and *pdr1* showed sensitivity in a like manner of NO_3^- .

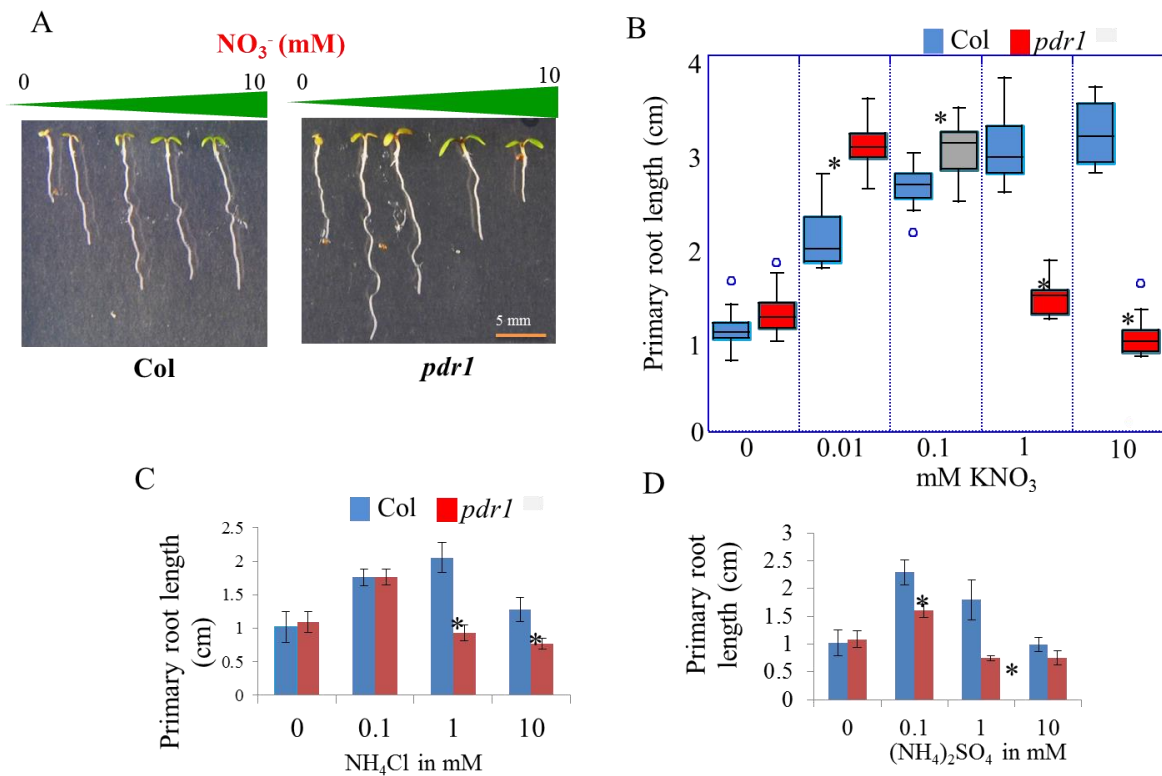


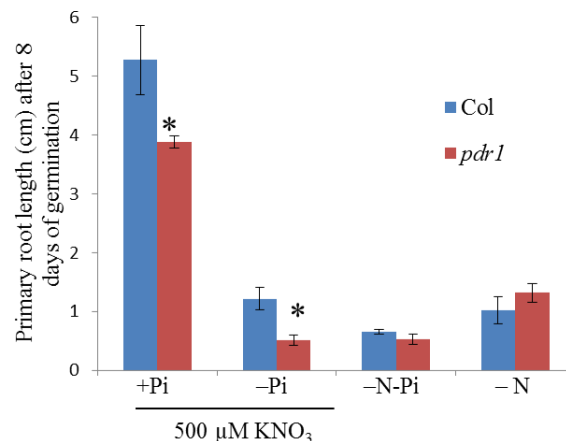
Figure 2-2. Sensitivity of *pdr1* to nitrate and ammonia. WT and *pdr1* plants were grown on +Pi medium containing different concentrations of NO_3^- and NH_4^+ . (A) Representative images after 4 days of germination, (B) PR of 8 days old seedlings grown on different concentrations of KNO_3 (B), NH_4Cl (C), and $(\text{NH}_4)_2\text{SO}_4$ (D) containing medium. Values are the mean \pm SD of 18-30 independent roots. *, Difference between WT plant and *pdr1* mutant was significant by t-test ($P < 0.05$).

2.3. *pdr1* root growth is impaired under Pi starvation

The association of high N with the short root phenotype of *pdr1* prompted us to determine the tolerable concentration of N in the growth media for *pdr1* root growth to evaluate the effect of Pi on *pdr1* PR growth. 500 μM of KNO_3 in the Pi medium was found to reduce the PR of *pdr1* to 22% (Fig. 2-3) compared to the 66% reduction on 7 mM KNO_3 containing +Pi medium (Fig. 2-1G). Under this NO_3^- containing -Pi media, *pdr1* showed more than twofold reduced root growth compared to the WT. To completely minimize the masking effect of N

on Pi phenotype of *pdr1*, I carried out the root growth assays on different Pi regimes ranging from 0 to 500 μM in the presence of 250 μM KNO_3 (Fig. 2-4) The supply of 250 μM KNO_3 was set to be sufficient for non-limited equal root growth for both *pdr1* and WT, without being luxurious. Under this growth condition, the provision of Pi below 100 μM clearly showed significantly reduced PR growth of *pdr1* in comparing to the WT when grown continuously (Fig. 2-4A & 2-4B). But, above 200 μM Pi catering was enough to rescue the PR of the mutant compared to the corresponding root of WT under similar growth condition (Fig. 2-4B). Pi-dependent similar PR growth of *pdr1* was further confirmed by an additional transfer experiment where seedlings were grown on +Pi media for 5 days before transfer to 0 to 500 μM Pi medium in presence of 250 μM KNO_3 . Under this experimental condition, *pdr1* needed 500 μM Pi to minimize the PR growth difference to a non-significant level compared to the WT (Fig. 2-5A). The reason for slow PR growth in transfer experiment could be earlier inhibitory experience of *pdr1* on a high NO_3^- before transfer. However, when transferred to low NO_3^- (250 μM), and increased the Pi provision to 100 μM , the meristem activity of *pdr1* enhanced resulting in complete restoration of the *pdr1* meristem size (Fig. 2-5B). Early disorganization of the *pdr1* meristem compared to WT on Pi below 50 μM was patently visible (Fig. 2-5C).

Fig. 2-3. PR growth responses to 500 μM KNO_3 containing growth media. WT and *pdr1* plants were grown continuously for 8 days after germination on +Pi and -Pi under 500 μM KNO_3 , -N and -N-Pi medium. Values are the mean \pm SD of 18-30 independent roots. *, difference between WT plant and *pdr1* mutant was significant by t-test ($P < 0.05$).



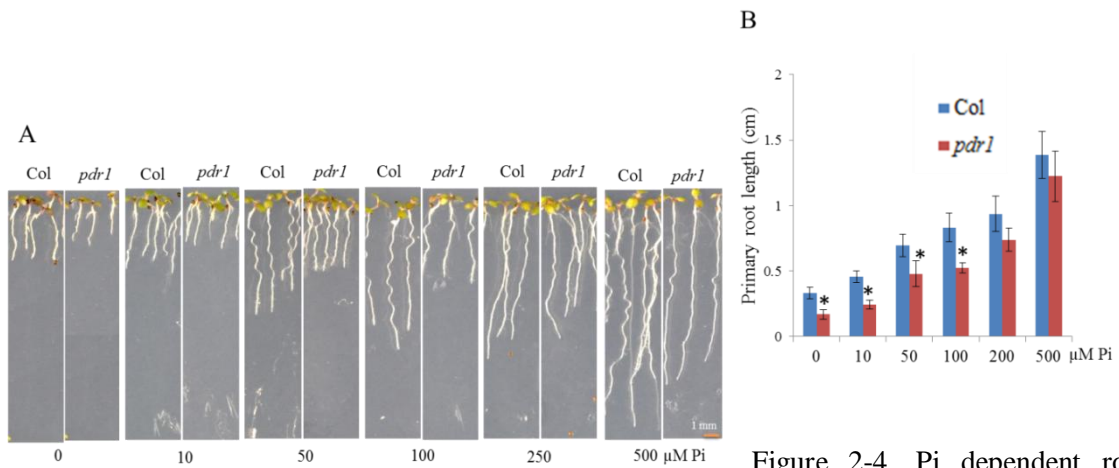


Figure 2-4. Pi dependent root growth of WT and *pdr1*.

Continuous growth of WT and *pdr1* for 8 days on different Pi concentrations (0-500 μM) in the presence of 250 μM KNO_3 . A) Representative images of the seedlings. B) PR length. Values are the mean \pm SD of 20-25 independent roots. *, difference between WT plant and *pdr1* mutant was significant

by t-test ($P < 0.05$).

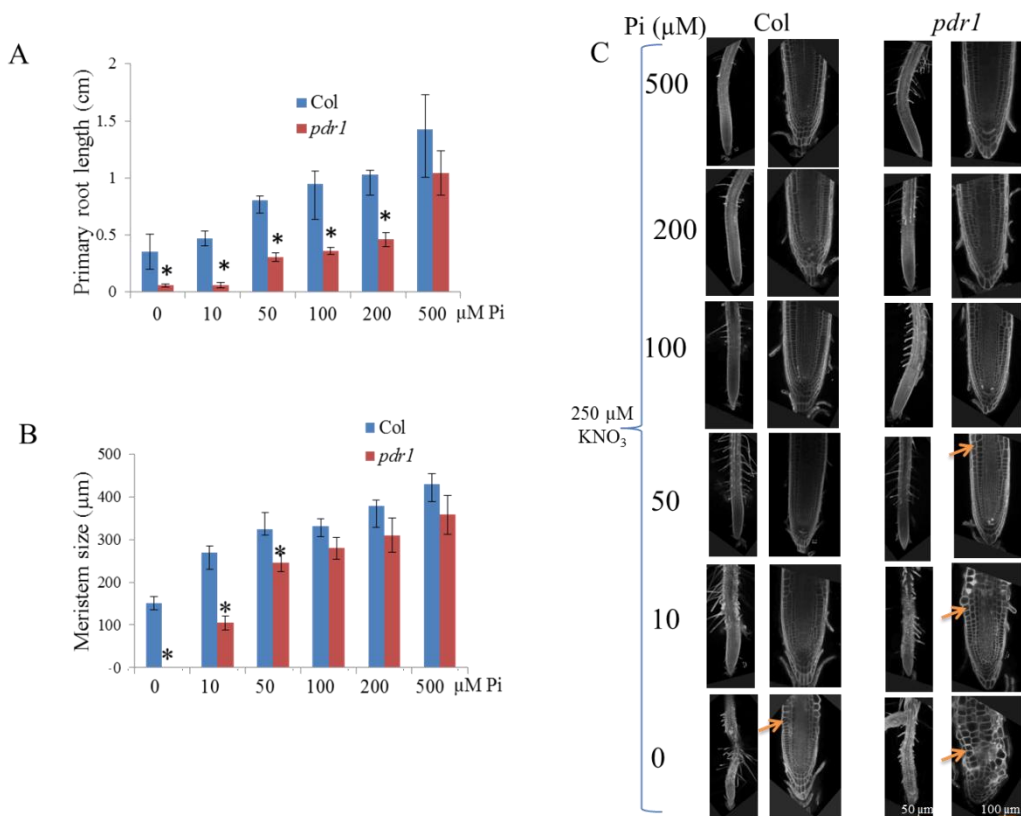


Figure 2-5. Pi dependent root growth of WT and *pdr1*. Plants were germinated and grown for 5 days on +Pi (200 μM) before transfer to different Pi regimes (0-500 μM) under constant level of 250 μM KNO_3 . (A) PR length (cm) and (B) size of primary root meristems (μm), and (C) propodium iodide (PI) staining of the root meristems. The arrows point to disorganized meristematic and differentiated cells. Values are the mean \pm SD of 10-15 independent roots for PR and 7 for determining meristem

size *, difference between WT plant and *pdr1* mutant was significant by t-test ($P < 0.05$).

2.4. *pdr1* is Pi deficient under high Pi condition

The obvious sensitivity of *pdr1* PR on low Pi prompted us to further investigate whether the mutant showed any defect in Pi content. Free Pi content in the shoots of *pdr1* was significantly lower when compared to the WT for both high and low Pi grown seedlings (Fig. 2-6A). By contrast, root Pi content was not different between the genotypes on high or low Pi (Fig. 2-6B). No significant difference in Pi content between WT and *pdr1* grown on -Pi condition was most likely because of no Pi in the media. However, the disparity in free Pi content in a high Pi condition indicated the defects of *pdr1* in the appreciation of Pi from the +Pi medium or translocation of Pi from root to shoot. The striking difference in the Pi content of *pdr1* shoots and roots was also found earlier compared to WT when seedlings were grown on DNA containing -Pi medium (PhD thesis, Delatorre, 2002). Under this growth condition, WT was found to increase free and total Pi to more than fivefold compared to -Pi while *pdr1* showed a very insignificant rise of Pi content, in spite of the presence of DNA in the media (PhD thesis, Delatorre, 2002).

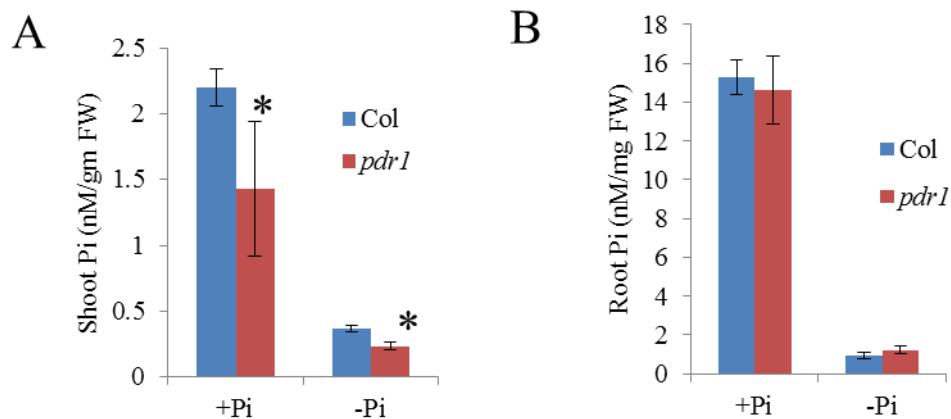


Figure 2-6. Free Pi content in the shoot and root of WT and *pdr1* mutants. Plants were grown on + Pi and after 5 days of germination transferred to +Pi and -Pi. After 3 days of transfer, free Pi content of (A) shoot and (B) root was determined. Values are the mean \pm SD of 4 independent samples. *, difference between WT and *pdr1* mutant was significant by t-test ($P < 0.05$).

2.5 Genetic mapping and identification of the *PDR1* locus

The *PDR1* locus was identified by whole genome re-sequencing followed by fine mapping. To obtain a chromosomal map position for the *pdr1* mutation, homozygous *pdr1* plants (third backcross) were out-crossed with the polymorphic mapping ecotype of accession Landsberg *erecta* (Ler-0). The resulting F1 progeny of this cross was subsequently selfed to establish a segregating F2 generation. The short root phenotype of the recessive *pdr1* mutant was scored on -Pi medium. Based on the short root *pdr1* phenotype, 50 individual F2 plants were selected and transferred to soil for bulk genomic DNA isolation. F3 progeny from each of the 50 individual F2 plants was scored again for the short root phenotype on -Pi and +Pi/+N to confirm that the causative mutation was homozygous in the sequencing pool. Ten F3 plants from each of the 50 F2 plants were used for the fine mapping. Leaf tissues of the 50 F2 plant were pooled to isolate bulk genomic DNA. After quantifying the extracted DNA and testing for its integrity (0.8% agarose gel), a total of 76 µg DNA was sent to the Beijing Genome Institute (BGI) at Hongkong for whole genome resequencing on the Illumina Hiseq2000 sequencing platform with 60X coverage.

The sequencing reads (79.87 million) were aligned onto the publicly available data of the reference Col-0 genome (Tair10) using SOAP2 (<http://soap.genomics.org.cn/soapaligner.html>). The obtained reads had a coverage rate of 99.82% with a sequencing depth of 57.44 and effective depth of 52.79. The SNP (single nucleotide polymorphism) variation of sequenced genome of *pdr1* pool DNA was detected by using SOAPSnp (<http://soap.genomics.org.cn/soapsnp.html>). As the polymorphic alleles were introduced by the mapping ecotype background of Ler-0, they appear at a frequency of ~50% in the pool of mapping population and are distributed randomly except at the neighboring chromosomal segment of the causal variant where non reference (Ler-0) allele frequency converged to zero. SNP frequency (number of SNP from the *pdr1* and Ler-0 at a particular coordinate) distributions were plotted against the coordinates of all five chromosomes (Fig. 2-7A). Homogenous distribution of SNP frequencies was found throughout all but chromosome 1 (Fig. 2-7A). The frequency decreased dramatically at the lower arm of chromosome 1 between coordinates 19 to 27 million bp due to the strong diminution of the mapping ecotype (Ler-0) alleles. Very low distribution of SNPs in this region indicated that the tightly linked *pdr1* locus co-segregates with Col-0 SNPs with high frequency (close to 1) at this region is presumably from the *pdr1*. I delimited 28 SNPs with a cutoff value of frequency >90% in this region with the presumption that the putative causal mutation was located in this region. The

28 SNPs were found in 28 different genes in the corresponding 8 million bp region. The SNPs located in the coding sequences (CDS) and in the promoter region showing EMS induced G-to-A or C-to-T nucleotide changes were extracted. I excluded the SNPs corresponding to Col-Ler natural SNPs, intergenic regions and chemically induced synonymous changes. I wended up with 5 SNPs having mutations in the exons of 5 different genes, namely *At1G53700*, *At1G58080*, *At1G59700*, *At1G61310* and *At1G66180* spanning the region between 20048586 to 24648813 bp on chromosome 1 (Fig. 2-7B). I attempted to identify the *PDR1* locus by isolating homozygous T-DNA insertion lines for four of the five genes, but none of them showed a short root phenotype on either -Pi or +Pi media. I excluded *At1G58080*, considering its distinct function in His biosynthesis.

In parallel, I performed fine mapping of the candidate regions by genotyping pooled and non-pooled 50 F2 individuals and around 500 F3 plants generated from the 50 F2 progeny (10 of each). Taking the advantage of the Ler-0 alleles in the mapping population that serve as a genetic marker, I used the Arabidopsis 1001 genome website to map the insertion/deletion (INDEL) between Col-0 and Ler-0 at different chromosomal positions within the candidate region of the chromosomal segment for genotyping the simple sequence length polymorphism (SSLP). Initially, based on the genotype of the original 50 F2 pooled DNA that was used for whole genome re-sequencing; the candidate region was delineated between 18.56 and 26.72 million bp. To narrow down the candidate region, each individual of 50 F2 and 500 F3 was further scored for the homozygous Col-0, Ler-0, and heterozygous genotype and calculated recombination frequency (RF) at 14 different chromosomal positions (Fig. 2-7C). I found an absence of recombination events between 21.31 and 21.51 million bp. Interestingly, within this 200 kb contig I found *At1g58080* which was one of the five candidate genes earlier identified based on the whole genome re-sequencing. I then PCR-amplified and sequenced this gene from genomic DNA prepared from the *pdr1* and WT that revealed a single nucleotide change from C to T in *pdr1* (Fig. 2-7D). The presence of the SNP was also confirmed by derived cleaved-amplified polymorphic sequences (dCAPS). The SNP changed the arginine (Arg or R) residue at the 109 position to a lysine (Lys or K) residue (Fig. 2-7D) located at the second exon of *ATP-PHOSPHORIBOSYL TRANSFERASE 1 (ATP-PRT1)*, which encodes the first committed enzyme of the His biosynthetic pathway. Earlier, it was also reported that functional disruption of many, if not all the His biosynthetic genes in Arabidopsis showed a huge developmental effect, including root meristems (Noutoshi et al., 2005; Mo et al., 2006 ; Ingle 2015).

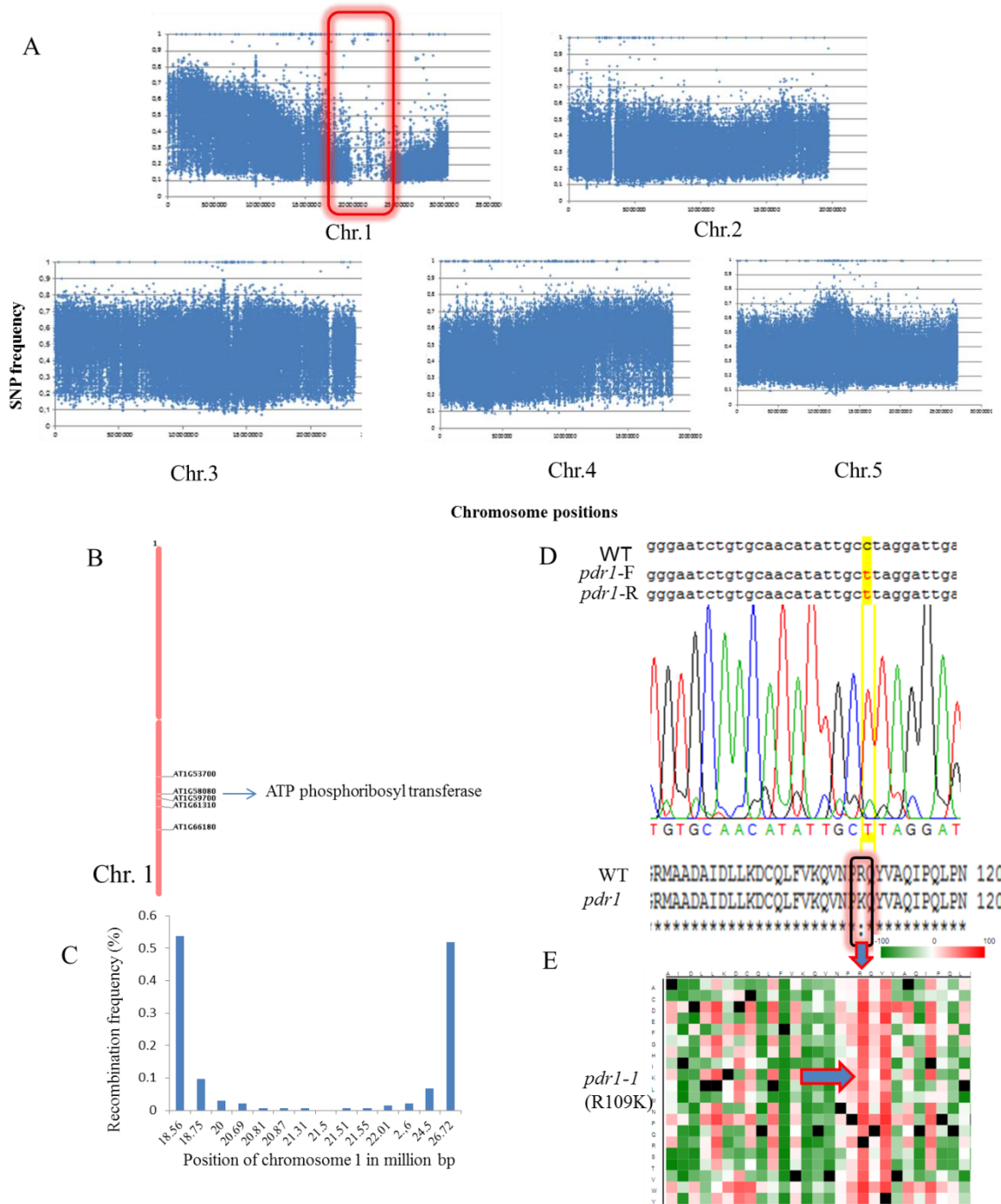


Figure 2-7. Identification of the *PDR1* locus by whole genome resequencing. (A), SNP distribution on all five chromosomes, the highlighted region of chromosome 1 shows the candidate region (upper left figure). (B), five candidate genes showing homozygous SNPs. (C), the Recombination frequency in the candidate region. (D), chromatogram shows the C-to-T nucleotide change that corresponds to the R-to-K substitution. (E), effect of the Arg residue caused by the *pdr1-1* mutation as predicted by Predict Protein (<https://www.predictprotein.org/>).

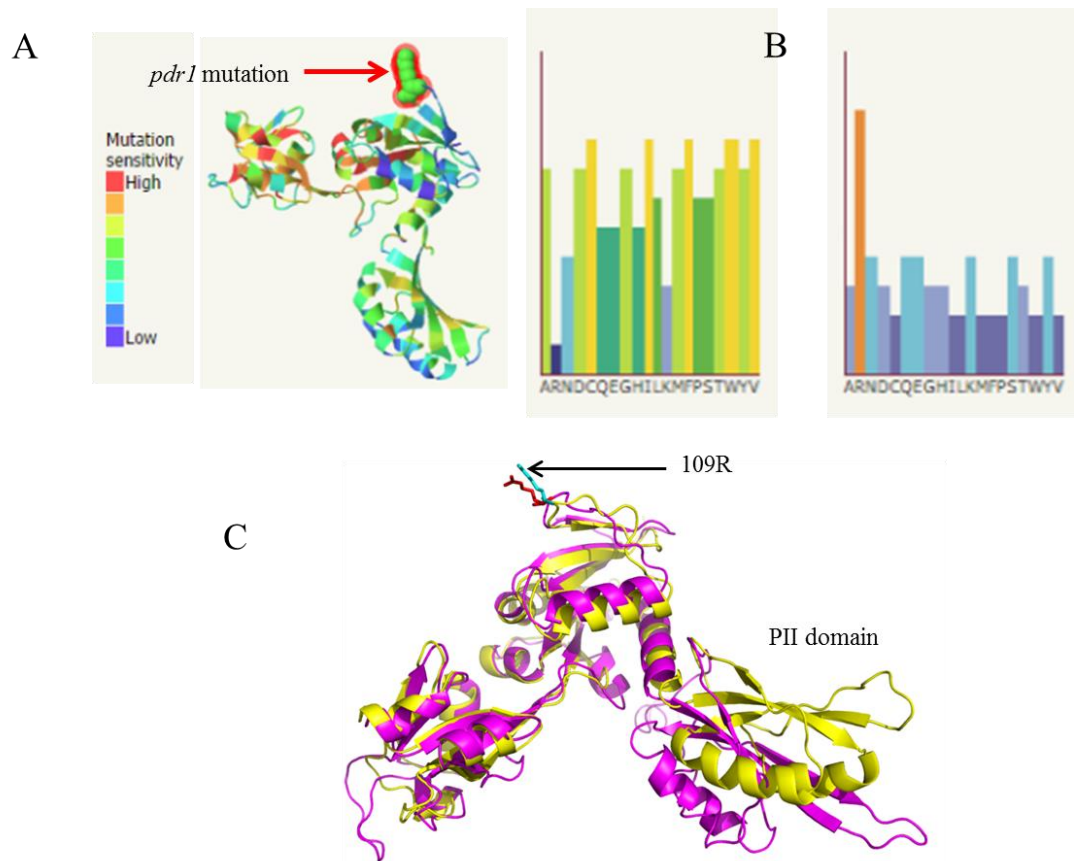


Figure 2-8. (A-B) Prediction of functional effect due to single amino acid variant. Predicted by *SusPect* using the Phyre Investigator user interface (Yates et al., 2014; <http://www.sbg.bio.ic.ac.uk/suspect>). The left panel in (A) shows the mutational analysis graph representing the predicted effect of the *pdr1* mutation (highlighted by arrow and red circle), which is likely to have an intermediate effect on functionality which is shown in the bar diagram. The right panel in (A) shows the mutational effect due to substitution of R (black bar) by any other amino acids. (B) Shows the sequence profile graph representing residue preferences in a protein at a particular sequence position. (C) Homology model of ATP-PRT1 (magenta) superimposed with 2VD3 (yellow), which is the structure of histidine inhibited Hisg from *Methanobacterium Thermoautotrophicum* (sequence identity of 32%). The arrow points the Arg at position 109 that is replaced by lysine in PDR1/ATP-PRT1. The superimposition shows the almost similar match of the two catalytic domain and the C-terminal PII domain.

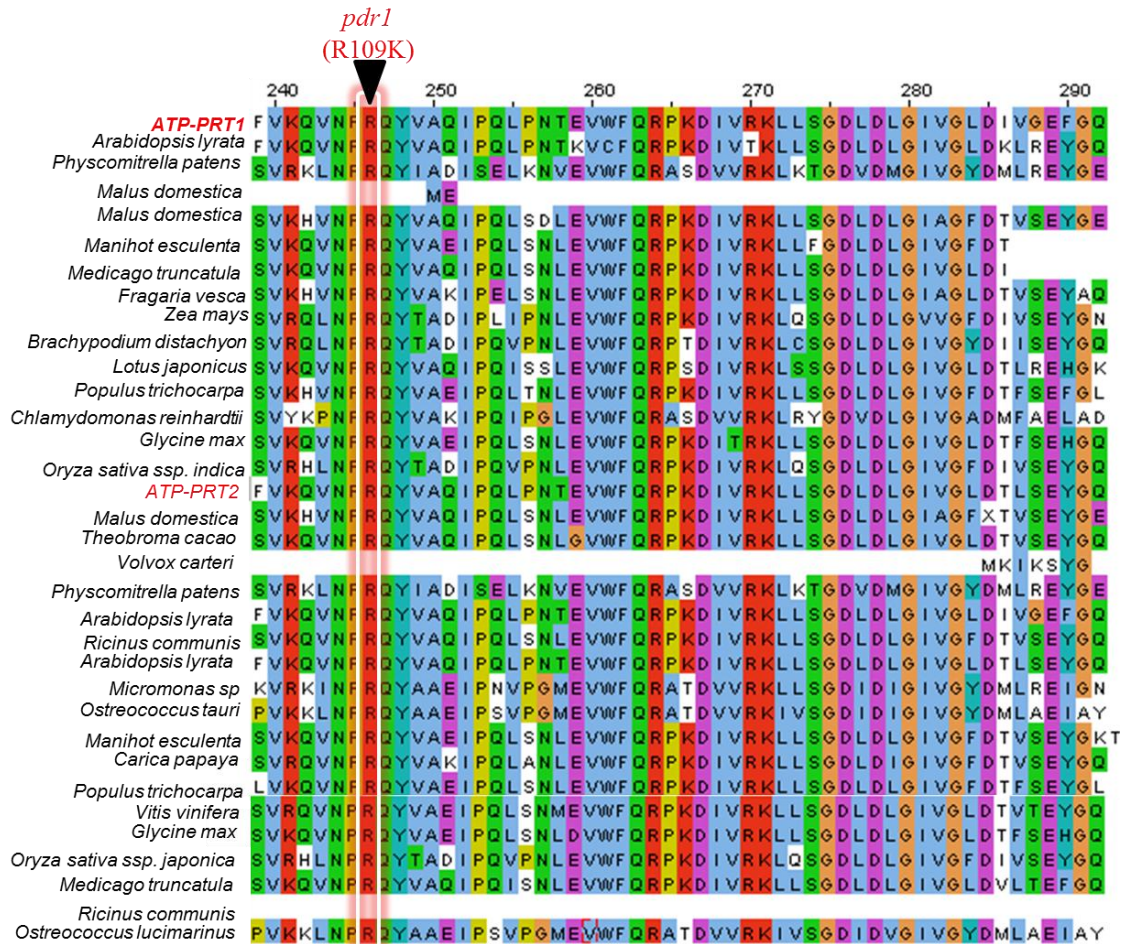


Figure 2-9. Multiple sequence alignment of plant ATP-PRT1 homologs around the site of the *pdr1* mutation. The arrow indicates the Arg-to-Lys substitution at position 109.

2.6 Sequence analysis of *PDR1*

As the R and K amino acid side chains share similar biochemical properties, it was intriguing to know how important is the R-to-K substitution at this position of the protein. In general, R residue was experimentally proven to confer a higher stability to protein structure than K thanks to its guanidinium group that allows three possible directions of interaction through its three asymmetrical nitrogen atoms (N ϵ , N η 1, N η 2) while K interacts only in one direction (Borders et al., 1994; Donald et al., 2011; Sokalingam et al., 2012). The functional effect of the R residue affected by the *pdr1* mutation was predicted by *predict protein*, a web-based tool (<https://www.predictprotein.org/>) that revealed an intermediate effect of this residue if substituted by K (Fig. 2-7E). The prediction was based on the evolutionary information, structural features, solvent accessibility and available annotation. The likelihood of phenotypic effect due to *pdr1* mutation was also analyzed using the Phyre Investigator user

interface, *SusPect* [(Yates et al., 2014); <http://www.sbg.bio.ic.ac.uk/suspect>] and extracted a similar result (Fig. 2-8A & 2-8B). Multiple sequence alignments showed that the R residue at 109 position of ATP-PRT1 is indeed evolutionary conserved in all the homologous genes of 34 plant species quizzed (Fig. 2-9). This indicated the relevance of the R residue for the functionality of the protein; otherwise, it would have not been conserved. There is a second isoform of *ATP-PRT1/PDR1* (Fig. 2-10) in the genome of Arabidopsis, encoded by AT1G09795 (*ATP-PRT2*; *HisN1b*), which shares overall amino acid identity of 74.6%. Most of the dissimilarities are in the predicted signal peptide region at the N-terminal part, and the promoter region of *ATP-PRT2* is much shorter (266 bp) than the *ATP-PRT1* (30810 bp). The neighboring upstream gene of *ATP-PRT2* is AT1G09794 (Cox19 family protein) which is reported to be not expressed as shown in the EST database of TAIR. Both *ATP-PRT1* and *ATP-PRT2* are functionally active as demonstrated by the complementation of the *his1* mutant of *Saccharomyces cerevisiae* (Ohta et al., 2000). Despite the presence of a functionally active second isoform of *ATP-PRT1*, why the *pdr1* mutation showed the severe phenotypic effect is an appealing question on the subject warranting further investigation.

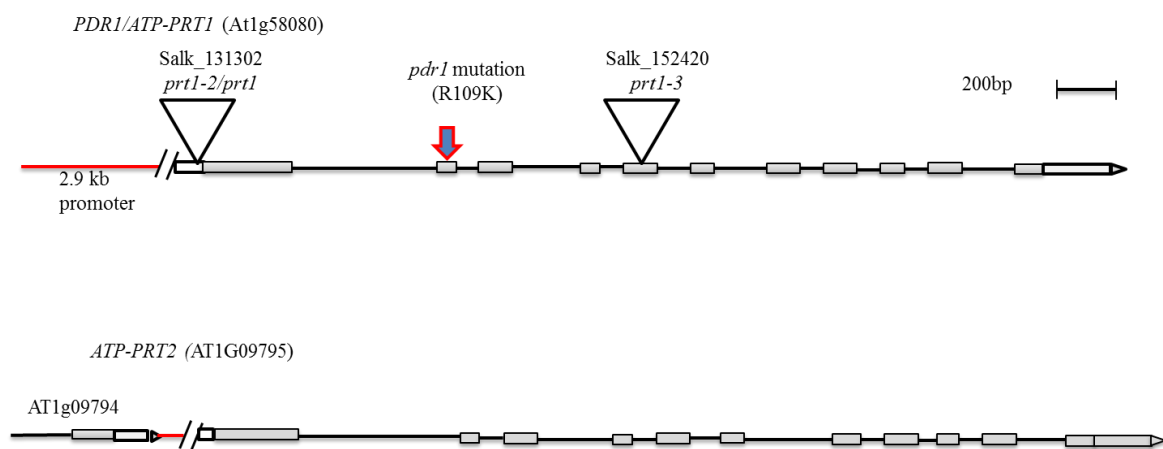


Figure 2-10. Models of the two Arabidopsis *ATP-PRT* genes, *AtATP-PRT1* (At1g58080) and *AtATP-PRT2* (AT1G09795). White boxes represent 5' UTR (left) and 3' UTR (right), gray boxes and black lines represent exons and introns, respectively. Red lines represent the promoter region (not drawn to the scale). The positions of the *pdr1-1* EMS mutant allele and of the two T-DNA insertion alleles in *AtATP-PRT1*, Salk_131302 and Salk_152420, are indicated by triangular marks. The two genes share 74.6% amino acid sequence identity. The nearby upstream gene of *ATP-PRT2* is At1g09794, which is not expressed according to EST data.

2.7 Validation of the *PDR1* locus

To confirm that the *pdr1* mutation was indeed in the *ATP-PRT1* locus, a homozygous T-DNA insertion line, Salk_131302 (insertion site is very close to the ATG start codon), was isolated (Fig. 2-10) for crossing with *pdr1*. Hereafter, this insertion line is designated as *prt1-2* or simply *prt1*, which also shows a severely impaired root phenotype. The semi-quantitative and qRT-PCR confirmed it as a knock-down allele (Fig. 2-11A 2-11B). The resultant F1 progeny of *pdr1* and *prt1-2* crosses showed a short root phenotype, indicating that the *pdr1* and *prt1* mutations are allelic (Fig. 2-11C).

Molecular complementation of the *pdr1* mutant with the WT copy of *ATP-PRT1* and *ATP-PRT2* cDNA was undertaken to further validate the *PDR1* locus. The full length cDNA of *ATP-PRT1* and *ATP-PRT2* was cloned and after subsequent checking of the sequence to avoid any mutation in the ORF, I used the clone in the sense orientation to fuse it with the 35S promoter of the *Cauliflower mosaic virus* together with the marker gene *GFP* (*CaMV Pro35S::ATP-PRT1~GFP*) using the Gateway-compatible binary destination vectors pB7WGF2. The constructs were then transformed into the *pdr1* mutant via *Agrobacterium* and ten stably transformed T2 lines were assayed that showed an apparent rescue of the *pdr1* short root phenotype on +Pi and -Pi by the overexpression of either *ATP-PRT1* or *ATP-PRT2* (Fig. 2-11C).

As *PDR1/ATP-PRT1* is the first enzyme of His biosynthesis and known to play a dominant role in regulating His production (Ingle, 2015), I tested whether His supplementation in the media can rescue the short root phenotype of *pdr1* grown on +Pi, -Pi, and -Pi+DNA medium. I observed the complete restoration of *pdr1* short root phenotype to WT by just using 3 μM of His supplementation (Fig. 2-12A). To evaluate if *pdr1* shows a dose response to different concentrations of His, I tested the plant on +Pi medium supplemented with 500 nM to 50 μM His. To my surprise, I found that even 500 nM partially rescued the *pdr1* short root phenotype while 1 μM was optimal for the full restoration of *pdr1* and the corresponding optimal concentration was 3 μM for rescuing *prt1-2* (Fig. 2-12B). Comparatively higher concentration of His requirement for the knock-down line can be explained by the more severe root phenotype of the *prt1-2* than that of *pdr1* (Fig. 2-12A).

To confirm the specificity of His in restoring the phenotype, I further tested the root growth on each of the 20 amino acid supplemented +P media (Fig. 2-13A) and did not find any of the single amino acid supplements (5 μM) to rescue the phenotype except for His (Fig. 2-13).

Additionally, supplement of D-His (5 μ M) was also found to have no effect to rescue the *pdr1* short PR (Fig. 2-13A). The metabolite of the fourth His biosynthetic enzyme, 5'-Phosphoribosyl-4-carboxamide-5-aminoimidazole (AICAR), was also tested, but neither of the tested concentrations (10, 20 and 50 μ M) in +Pi and -Pi media were able to rescue the phenotype (Fig. 2-14). In yeast, the expression of Pi transporter *PHO84* was found to be positively correlated with the increasing concentration of AICAR under Pi starvation (Pinson et al., 2009). Probably, the highest concentration (50 μ M) I applied to the growth medium was not enough or simply it was not hydrolyzed or taken up.

As imidazole is a functional group of His (Ingle, 2011), I supplemented this or imidazole acrylic acid in the growth medium (+Pi) at a concentration of 10, 20 or 50 μ M. None of the concentration of both molecules showed rescuing effect on *pdr1* PR (Fig. 2-15). I also checked if external adenine could rescue the *pdr1* phenotype under Pi starvation considering the fact that His biosynthesis is tightly linked with the nucleotide metabolism (Alifano et al., 1996 ; Ward and Ohta, 1999; Boldt and Zrenner, 2003). Any rescuing effect was not observed at low (100 μ M) or high (1 mM) concentrations; rather high concentration drastically reduced the growth, including the root of WT, *pdr1* and *prt1-2* (Fig. 2-16). Above results explicitly showed that only His supplementation can chemically complement the *pdr1*. The third allele *prt1-3* is presumably a knock-out line showed a seedling-lethality (Fig. 2-17) that indicate His is vital for plant growth and development.

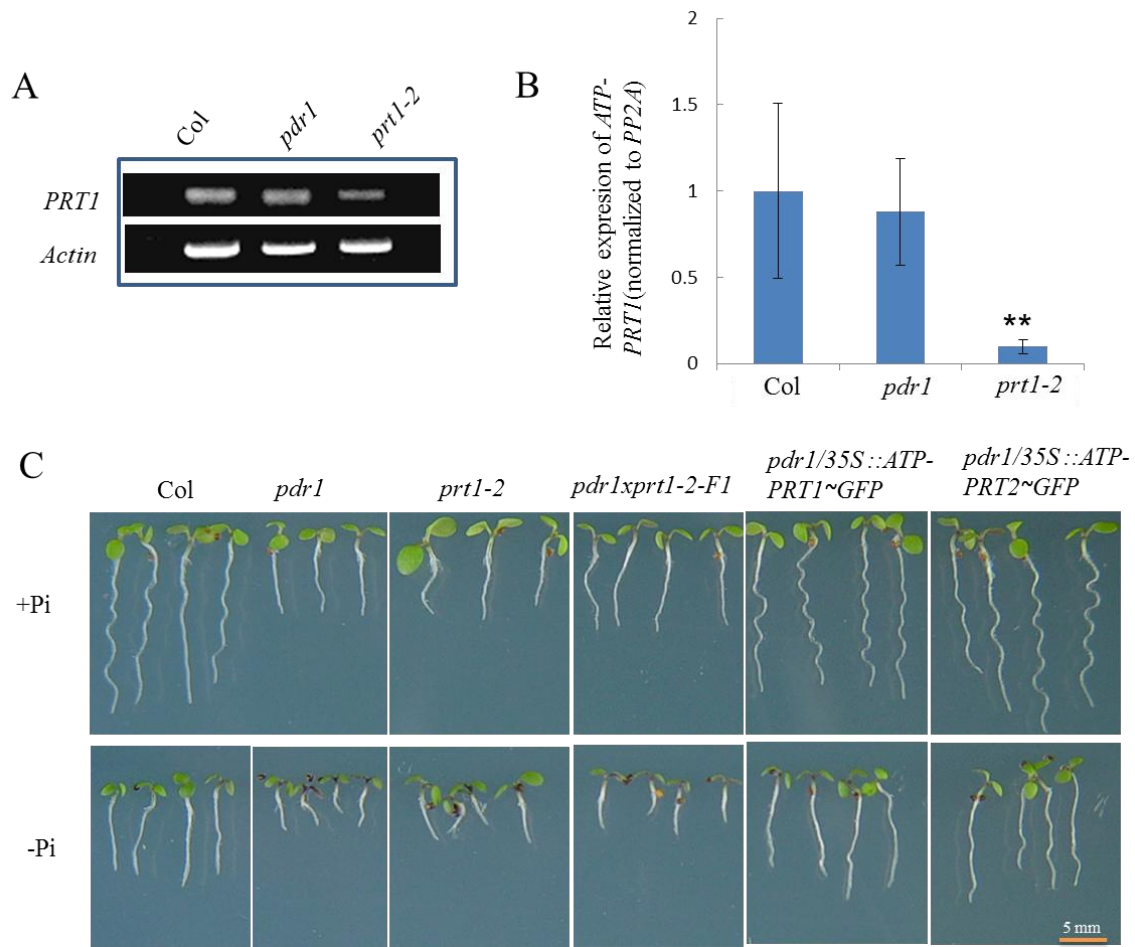


Figure 2-11. Validation of the *PDR1* locus. (A) Detection of *PRT1* mRNA by semi-quantitative RT-PCR analysis using *Actin* expression as loading control. (B) Quantitative RT-PCR analysis of *PRT1* mRNA expression normalized with *PP2A*. (C) Allelism test by crossing *pdr1-1* and *prt1-2*, and molecular complementation of *pdr1-1* by overexpressing the WT *ATP-PRT1* and *ATP-PRT2* under control of the CaMV 35S promoter in the *pdr1-1* mutant. Shown are representative image of 4 days old seedlings grown on +Pi and -Pi. Values are the mean \pm SD of 3 independent samples. *, difference between WT plant and *prt1-2* mutant was significant by t test ($P < 0.05$).

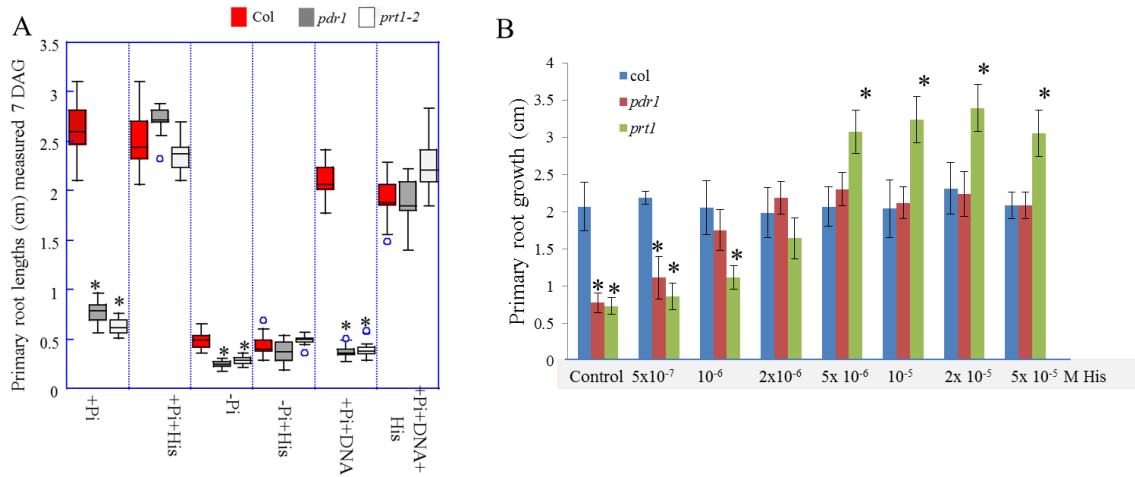


Figure 2-12. (A) Chemical complementation of the *pdr1* short root phenotype by supplementation with 3 μ M His. PR lengths of 7 days old WT(Col-0), *pdr1-1* and *prt1-2* seedlings grown vertically on agar plates containing +Pi, +P+His, -Pi, -Pi+His, -Pi+DNA, and -Pi+DNA+His media. (B) Dose response of WT, *pdr1-1* and *prt1-2* seedlings to various His concentrations 0.5-50 μ M. Seeds were germinated and grown for 7 days on vertically oriented agar plates containing +Pi medium supplemented with the respective concentration of His. Values are the mean \pm SD of 25-30 independent roots. *, difference between WT plant and *pdr1* mutant was significant by t-test ($P < 0.05$).

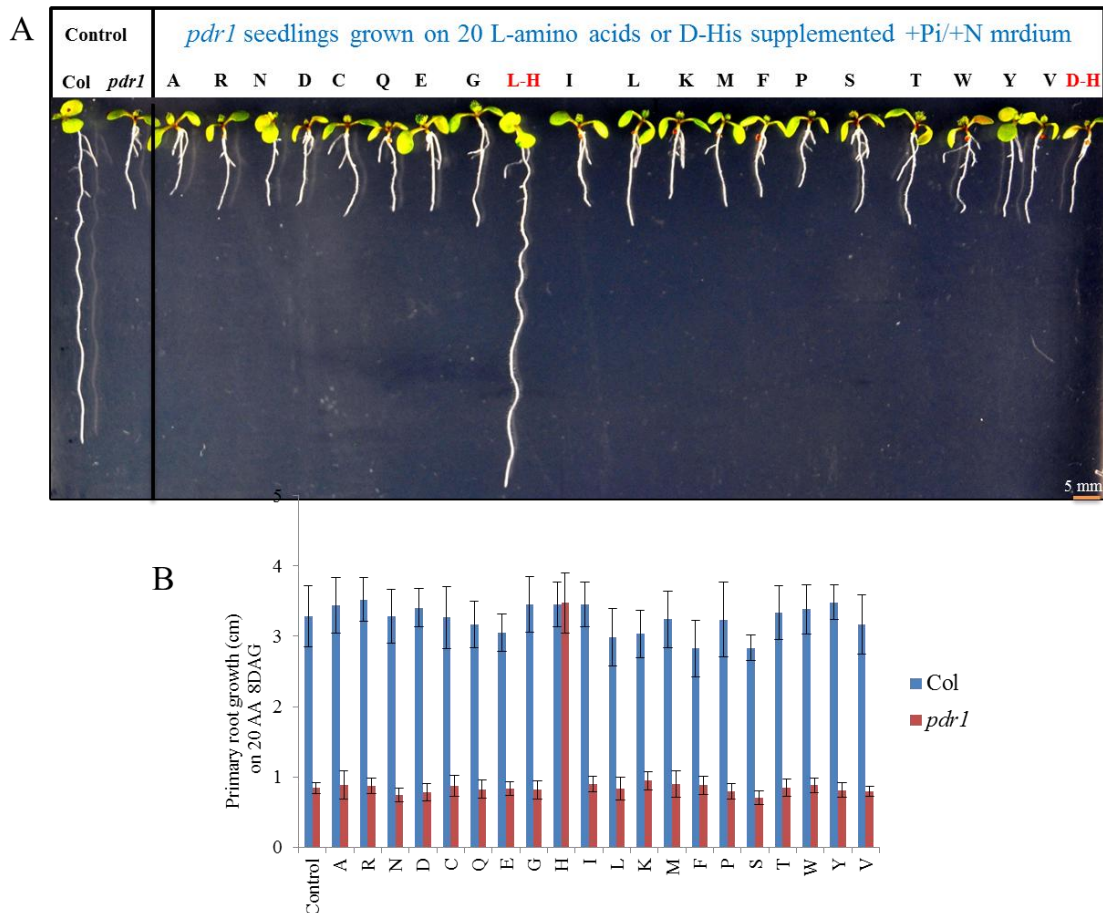


Figure 2-13. Chemical complementation of the *padr1* short root phenotype is specific for L-His. WT and *padr1* seedlings were grown for 8 days on +Pi medium supplemented with filter-sterilized L-amino acids or D-His (5 μ M each). (A) Images of *padr1* seedlings representative for each amino acid supplementation. (B) Quantification of WT and *padr1-1* PR length for each treatment. Values are the mean \pm SD of 25-35 independent roots.

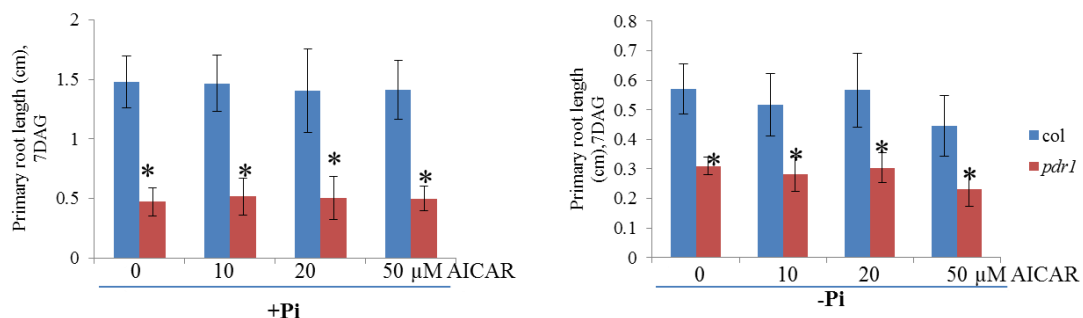


Figure 2-14. Response of WT and *padr1-1* roots to 10-50 μ M AICAR (5'-Phosphoribosyl-4-carboxamide-5-aminoimidazole). Seeds were germinated and grown for 7 days on vertically oriented agar plates containing the complete growth medium (+Pi, left graph) or -Pi (right graph) supplemented with the respective concentration of AICAR. Values are the mean \pm SD of 25-38 independent roots. *, difference between WT and *padr1* mutant was significant by t-test ($P < 0.05$).

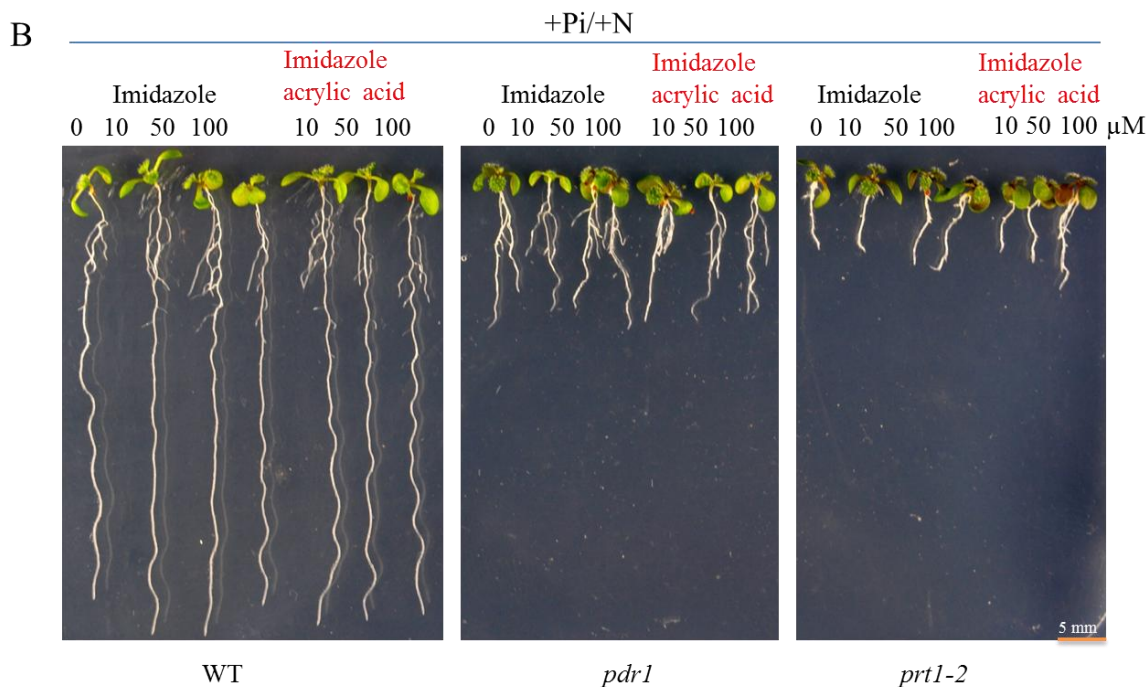
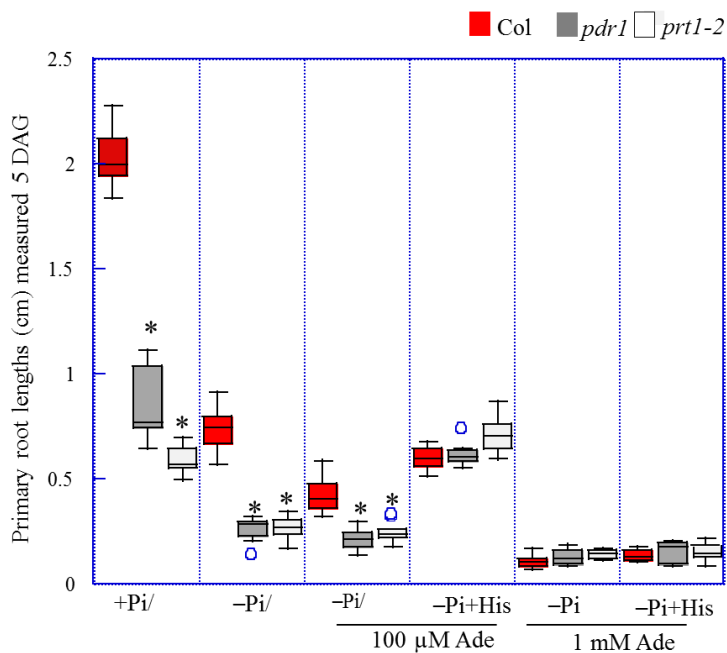


Figure 2-15. The response of WT, *pdr1-1* and *prt1-2* seedlings to different concentrations (10-100 μ M) of imidazole and imidazole acrylic acid. Representative images are shown after 7 days of germination.

Figure 2-16. The response of WT, *pdr1-1* and *prt1-2* seedlings to adenine (Ade). PR length was measured after 5 days of germination (DAG) of plants continuously grown on the indicated media (His was used at 10 μ M). Values are the mean \pm SD of 10-15 independent roots.

*, difference between WT and *pdr1* mutant was significant by t-test ($P < 0.05$).



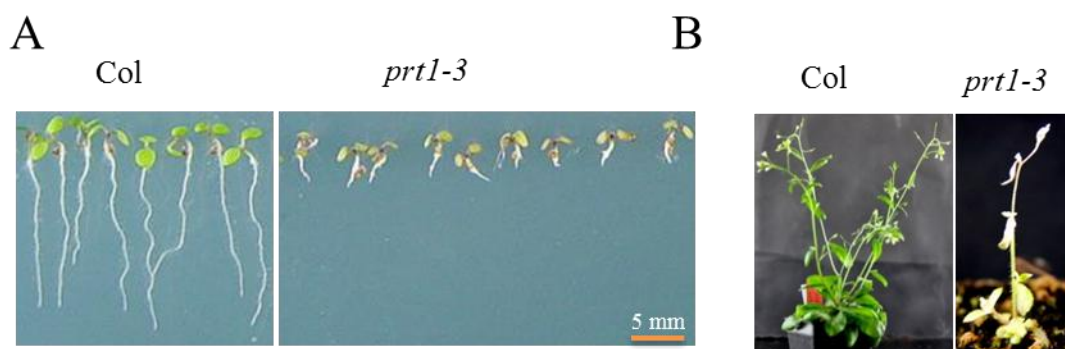


Figure 2-17. His is vital for plant survival. The presumed knock-out line of *ATP-PRT1*, *prt1-3* (Salk_152420) is seedling-lethal. (A) 6 days old WT and *prt1-3* seedlings grown vertically on +Pi agar plates. (B) 4 weeks old seedlings of WT and *prt1-3* in soil showing the seedling lethality of the knock-out line.

2.8 Subcellular localization and expression of PDR1/ATP-PRT1 and ATP-PRT2

The PDR1/ATP-PRT1 and ATP-PRT2 proteins are likely to be localized in the plastids as predicted by web based tools [PlantLoc; (Tang et al., 2013)]. To test this, the 3' end of the coding region of *PDR1/ATP-PRT1* and *ATP-PRT2* was fused with the GFP reporter gene and expressed under the control of *CaMV* 35S promoter. The transgenic plants are referred hereafter as *pdrl/Pro35S:ATP-PRT1-GFP* and *pdrl/Pro35S:PRT2-GFP* in the subsequent discussion. Plastid targeted virulence strain EHA105 was used as positive control. The subcellular localization of PDR1/ATP-PRT1 and ATP-PRT2 was tested in a transient expression system of tobacco leaves. The localization of GFP fused protein was visualized under the confocal scanning laser microscopy after 3 days of infiltration. The results showed the expression of both the PDR1/PRT1 and PRT2 were exclusively localized in the plastids (Fig. 2-18). I also checked the localization of the protein in stably transformed *Arabidopsis pdrl* mutant plants that showed similar results (Fig. 2-19). To more precisely determine the cells that express *PDR1/ATP-PRT1* and *ATP-PRT2* in the various tissues, transgenic plants expressing the gene encoding β -glucuronidase (GUS) under the control of the native promoters were generated. I generated homozygous single-copy *ProPRT1::GUS/GFP* lines while isolation of *ProPRT2::GUS/GFP* plants is still in progress. Analysis of expression profile of 5 days old seedlings showed the GUS activity in the vascular system of the matured part of the roots as well as in the shoot and leaves (Fig. 2-20). The presence of GUS staining was also evident in the emerging lateral roots. No GUS staining was detected at the root tip or

in the elongating zone of the root (Fig.2-20). More careful evaluation is necessary on different NO_3^- and Pi regimes for spatial and temporal expression. Promoter GUS in WT and *pdr1* should also be checked in the presence of His under the experimental condition of +Pi/+N and -Pi. Considering the dominant role of PDR1/ATP-PRT1 in modulating root growth as displayed by EMS (*pdr1*), knock-down (*pdr1-2*) and knock-out (*pdr1-3*) mutants, despite of the presence of the second isoform *ATP-PRT2*, future experiment should also be focused on the expression map of both isoforms.

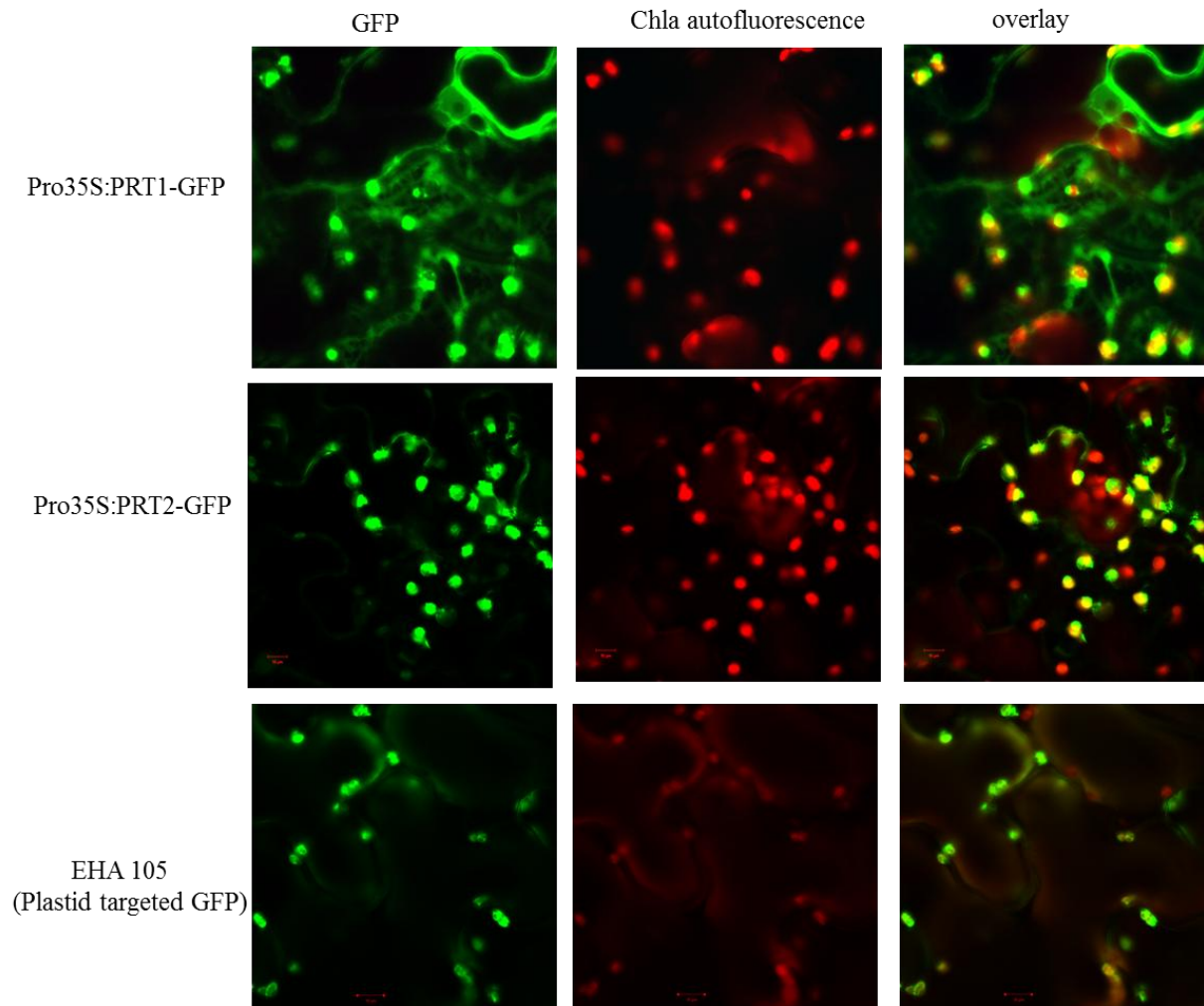


Figure 2-18. Subcellular localization of ATP-PRT1~GFP and ATP-PRT2~GFP in *N. benthamiana*. Tobacco leaves were transiently transfected with *Agrobacterium* strains harboring plasmids supporting expression of GFP-tagged ATP-PRT1 and ATP-PRT2 under the CaMV 35S promoter. The EHA105 vector construct encoding a plastid-targeted GFP was used as a positive control. Images were taken 3 days after infiltration under the confocal scanning laser microscopy.

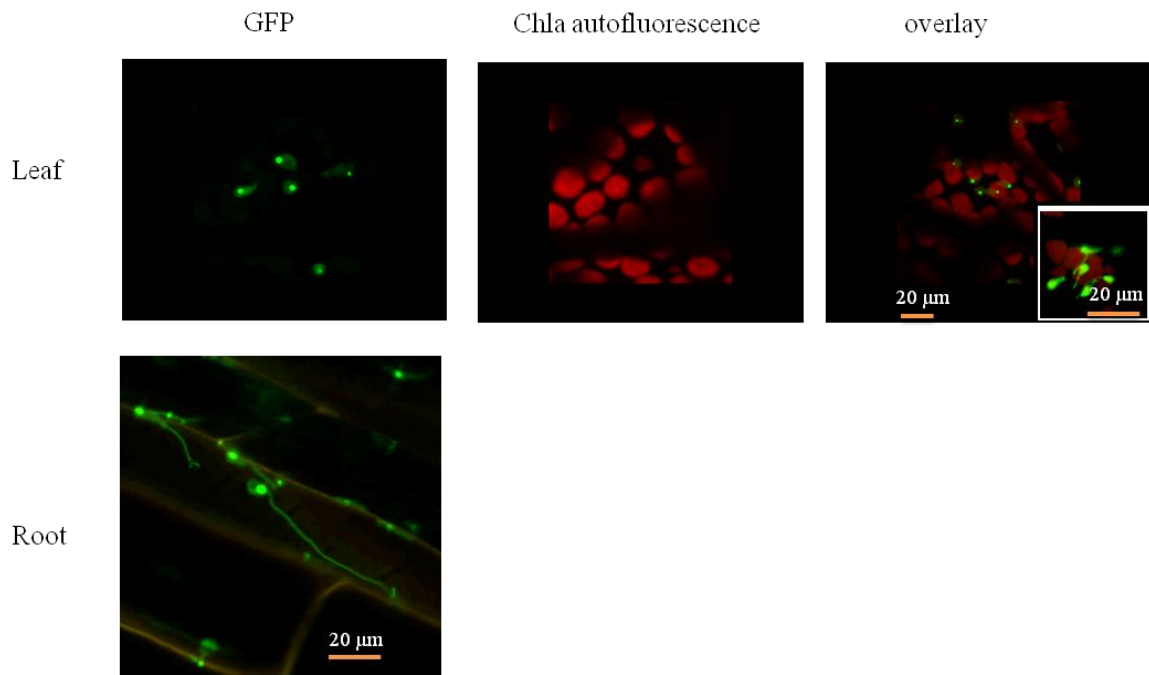


Figure 2-19. Subcellular localization of *ATP-PRT1~GFP* in stably transformed, homozygous transgenic *Arabidopsis* lines. The upper panel shows GFP fluorescence in leaf plastids. The inset shows a higher magnification. The lower panel indicates localization of the fusion protein in root plastids.



Figure 2-20. Histochemical analysis of *ProATP-PRT1::GUS/GFP* expression in homozygous transgenic WT plants grown on +Pi medium. GUS activity was observed after 5 days of germination.

Scale bar represents 100 μm .

2.9 Altered RSA of *pdr1* and His-mediated normalization

The typical response to the Pi-starved condition is the modulation of RSA for the adaptation to the changing conditions (Abel, 2011). The most visible phenotype is the immediate reduction of PR growth followed by the prolific growth of LR along with the profuse root hair development (Williamson et al., 2001; Peret et al., 2014). Therefore, in addition to PR, I evaluated the Pi deficient effect on the LR growth of *pdr1* compared to the WT in the presence or absence of His in the media. The account of the emergence of LR per unit length (cm) of the PR in Pi-sufficient *pdr1* was found to be 3-fold more than that of WT grown on the identical condition (Fig. 2-21A and 2-21B). Likewise, on low Pi condition, the events of LR emergence were double in *pdr1* than in WT (Fig. 2-21B). In both Pi and -Pi condition, His supplementation reduced the LR emergence of *pdr1* to the WT level (Fig. 2-21B) likely by directing the genetic set up to focus towards the PR development. Consequently, the total root length (sum of the PR and LR) of *pdr1* on His supplemented +Pi and -Pi media enhanced significantly to the equal length of WT (Fig. 2-21C). In spite of the higher events of LR emergence in *pdr1*, the growth was slower than that of the WT in the absence of His, thus making the total root length of *pdr1* significantly shorter than the corresponding parameter of WT (Fig.2-21C). To check if the shoot is equally affected by the *pdr1* mutation, shoot and root fresh weight (FW) were measured for the WT and *pdr1* plants grown on +Pi, -Pi, -Pi+His and +Pi+His for 4 days after transferring 5 days old seedlings from the +Pi medium. The results showed that only root was affected by the mutation in *pdr1* while shoots remained unaffected both on +Pi and -Pi conditions (Fig. 2-22).

The shorter root of *pdr1* plants in contrast to WT may be attributed to a decrease in root cell division and/or cell elongation. To scan the meristem activity of *pdr1*, I crossed *pdr1* with a transgenic Arabidopsis line expressing a *ProCycB1::GUS* fusion gene, a reporter for cell cycle activity (Colón-Carmona et al., 1999). WT and *pdr1* seedlings were continuously grown for 5 days on +Pi, -Pi, -Pi+DNA and -Pi+DNA medium for GUS staining. The difference in staining pattern and intensity was very conspicuous between WT and *pdr1* root grown on -Pi; *pdr1* showed much fainter staining than the WT (Fig. 2-23). Provision of DNA in the -Pi improved the activity of *ProCycB1::GUS* of WT root while *pdr1* showed no obvious upturn. Interestingly, His supplementation in the -Pi+DNA containing media fostered the meristem activity of the *pdr1* similar to WT as indicated by the elevated GUS staining in the root (Fig. 2-23). Although, I did not see any difference in staining intensity between WT

and *pdr1* grown on +Pi media, the staining of *pdr1* at the close proximity of the root tip was noted (Fig. 2-23) suggesting also the less root meristem activity of the mutant under +Pi/+N condition.

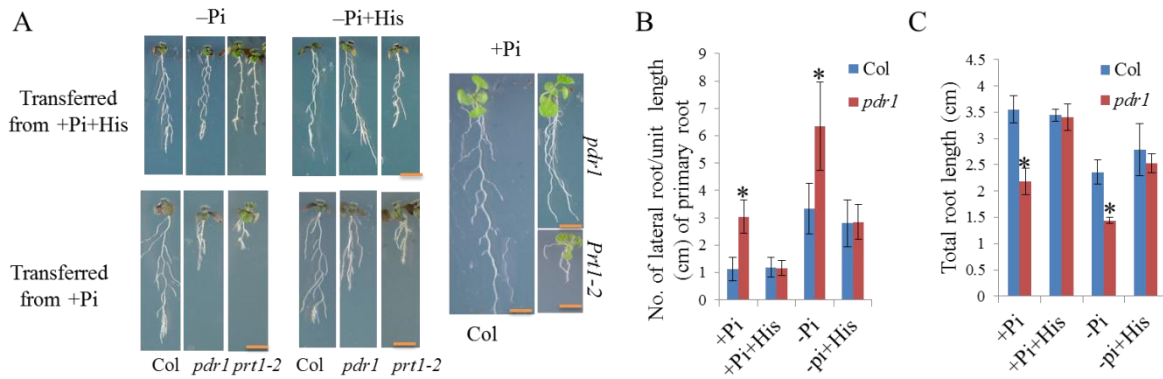


Figure 2-21. Effect of His (3 μ M) on RSA. WT, *pdr1-1* and *pri1-2* seeds were germinated and grown vertically for 5 days on +Pi and +Pi+His containing agar plates prior to transfer to +Pi, +Pi+His, -Pi and -Pi+His. (A) Representative images of seedlings 5 days after transfer. (B) Number of lateral roots per cm PR length. (C) Total root length (primary plus lateral roots), calculated 5 days after transfer. *, difference between WT plant and *pdr1* mutant was significant by t-test ($P < 0.05$).

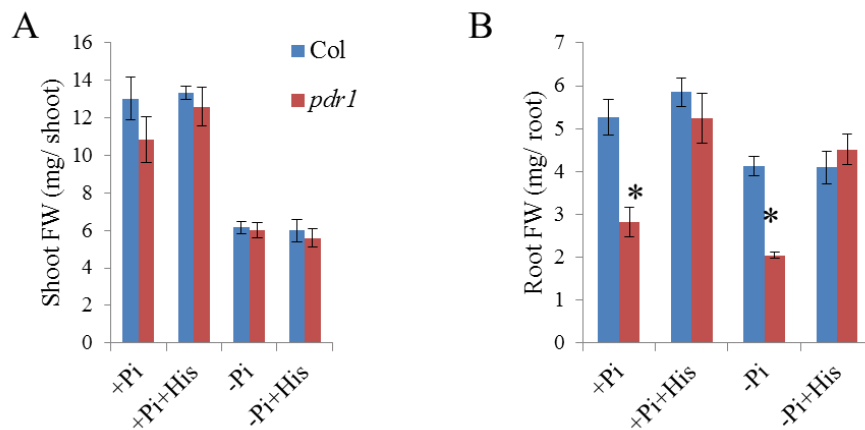


Figure 2-22. The *pdr1* mutation lowers root biomass, which is restored by His supplementation (3 μ M). (A) Shoot and (B) root biomass of WT and *pdr1* plants were measured 4 days after transfer from +Pi (5 days old seedlings) to +Pi, -Pi, -Pi +His and +Pi+His. Values are the mean \pm SD of 25-30 independent roots. *, difference between WT and *pdr1* mutant was significant by t-test ($P < 0.05$).

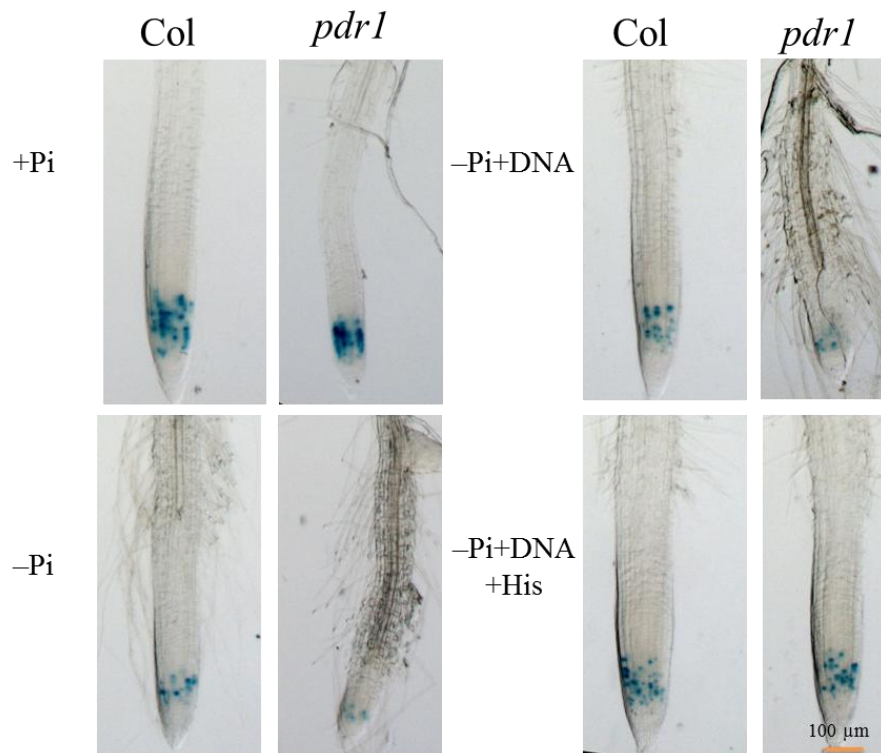


Figure 2-23. Histochemical analysis of *ProCyCB1::GUS* expression in WT and *pdr1-1* seedlings after germination and continuous growth on vertically oriented agar plates for 5 days on the indicated media. Filter-sterilized purified herring sperm DNA was substituted for Pi and added to the autoclaved medium to a final concentration of 0.4 mg mL^{-1} . His was used at $3 \text{ } \mu\text{M}$.

In addition to the marker gene assay, I performed propidium iodide (PI) cell wall staining to analyze the cellular response of WT and *pdr1* PR grown on +Pi, -Pi, and -Pi+His for three days after transferring 5 days old seedlings from +Pi media (Fig.2-24). As shown in Fig (2-24A), the meristem size of *pdr1* was significantly shorter (56%) than the WT seedlings grown on -Pi. In medium with high Pi, *pdr1* also showed 45% shorter meristem as expected due to the shorter root growth of *pdr1* on high Pi. Similarly, the shorter elongation zone and less number of elongating epidermal cells in the trichoblast cell-file were recorded for *pdr1* compared to the WT grown on both +Pi and -Pi (Fig. 2-24C). Conversely, $3 \text{ } \mu\text{M}$ His supplementation in -Pi and -Pi+DNA containing medium restored those cell parameters of *pdr1* like WT (Fig. 2-24).

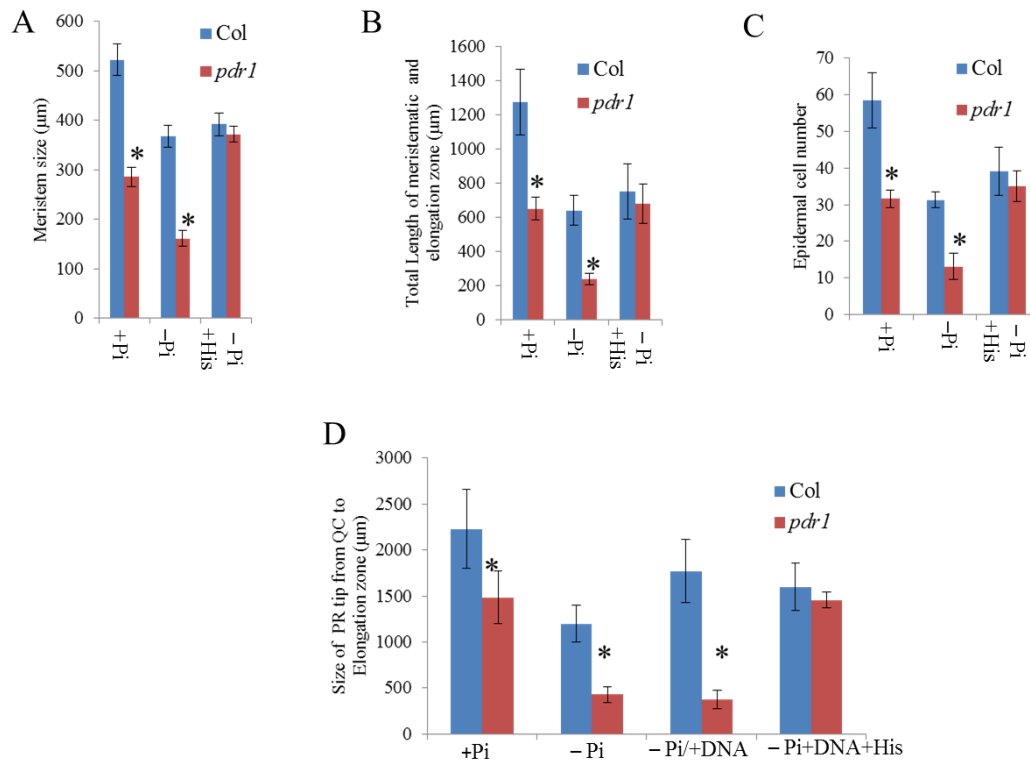


Figure 2-24. His supplementation (3 μM) restores *pdr1* root meristem parameters on $-\text{Pi}$ medium. WT and *pdr1* seedlings were grown on vertically oriented agar plates for 5 days on $+\text{Pi}$ medium prior to transfer to $+\text{Pi}$, $-\text{Pi}$ and $-\text{Pi}+\text{His}$ media for another 4 days. (A) Meristem size. (B) Total length of the meristematic and elongation zone. (C) Number of epidermal cells in the meristematic zone. (D) Total length of the meristematic and elongation zone after continuous growth (6 days) on the indicated media. Values are the mean \pm SD of 7-10 independent roots. *, difference between WT and *pdr1* mutant was significant by t-test ($P < 0.05$).

2.10 Free His levels increase upon Pi starvation

To further understand the role of His in modulating the RSA upon Pi starvation, I measured free His content in *pdr1* and WT along with other amino acids. Plants were grown on a complete medium for five days before transferring to respective $+\text{Pi}$ and $-\text{Pi}$ medium. Three days after transfer to $+\text{Pi}$, the content of free His in both WT and *pdr1* was found to be same in the roots, most likely because of the compensatory effect of the second active copy, *ATP-PT2* (Ohta et al., 2000). For the shoots, *pdr1* had significantly less free His (around 50% reduction) both on $+\text{Pi}$ and $-\text{Pi}$ condition than the corresponding WT (Fig. 2-25A). However, after 3 days of Pi starvation, the content in WT root increased by fivefold compared to the $+\text{Pi}$ grown corresponding root (Fig. 2-25B). By contrast, the *pdr1* roots showed no further accumulation of the free His in response to Pi deficiency. The elevated level of His upon Pi

starvation in the WT suggests the link of His with the Pi starvation responses. The failure of *pdr1* to accumulate the free His on Pi challenged condition implicated the *ATP-PRT1* in P-starvation responses despite the presence of second active isoform *ATP-PRT2*. This reflects the distinct physiological role of the two isoforms of *ATP-PRT* genes, although both are biochemically active (Ohta et al., 2000).

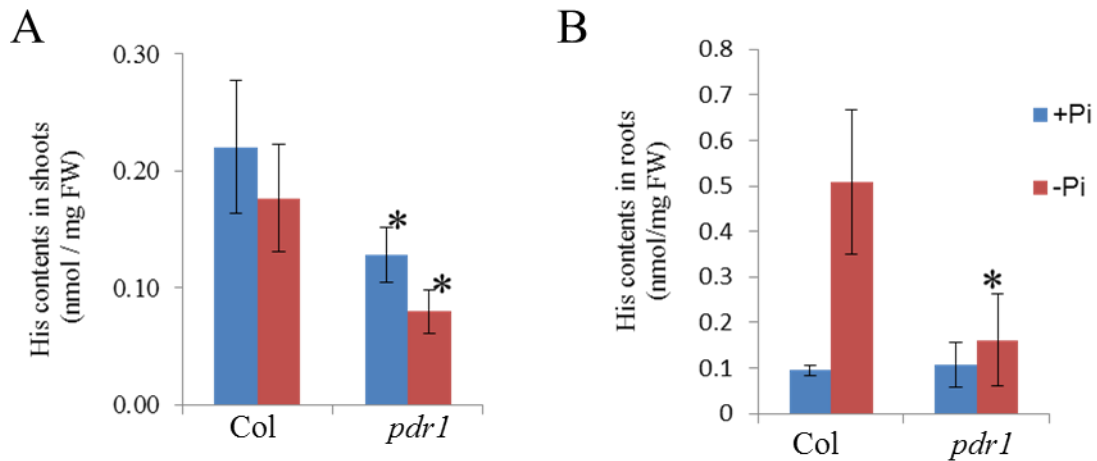


Figure 2-25. Free His content of WT and *pdr1* shoots and roots. Plants were grown on +Pi for 5 days and then transferred to +Pi or –Pi medium. After two days, roots and shoots were separated, weighed, and processed for His determination according to the method described by Ziegler and Abel (2014). His content of shoots (A) and root (B). Values are the mean \pm SD of 4 independent measurements. *, difference between WT and *pdr1* mutant was significant by t-test ($P < 0.05$).

2.11 The rescuing effect of His is local

It is unlikely that *pdr1* short root phenotype, especially under high Pi, is due to a global His starvation as I found no significant difference of free His content in root of *pdr1* mutant from that of the WT (Fig. 2-25B) grown on a complete medium (+Pi/+N). The next question has turned up as to why *pdr1* PR is shorter than WT even though no significant effect was noticed in the aerial part of the *pdr1* seedlings grown in the agar plate under +Pi and –Pi conditions (Fig. 2-22A). One likely hypothesis is the localized shortage of His in the meristem of *pdr1*. This prompted us to scale carefully whether the effect of His is local or systemic in rescuing the root phenotype. We then performed the split-root and transfer experiments that endorsed the notion of local effect (Fig. 2-26). In a split-root experiment, the *pdr1* root phenotype was found to be rescued when the root tip was in contact with His-containing media (Fig. 2-26A & 2-26B) irrespective of the presence or absence of His on the upper part of shoot and root. This was confirmed in both +Pi and –Pi growth conditions. Furthermore, I grew the plants on the

media with or without 3 μM His supplementation and then transferred 5 days after germination (DAG). After transfer, *pdr1* PR found to sustain the WT like growth only on the His supplemented media independent of its earlier growth condition (+His or -His) while PR growth was arrested on +P-His media even though they were grown on a His supplemented medium before transfer (Fig. 2-26C). A similar result was also observed for the second allele of *pdr1*, *pri1-2* (SALK_131302) line that has further substantiated the hypothesis of local than the systemic effect of His.

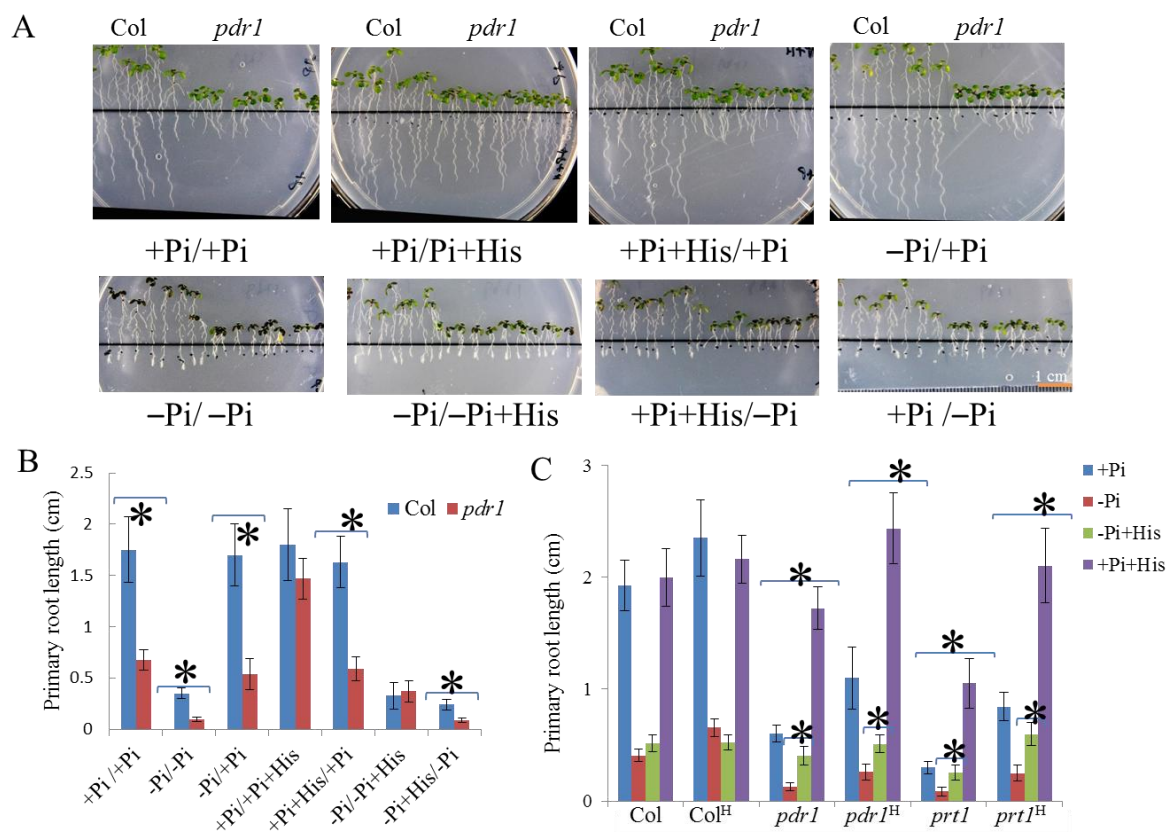


Figure 2-26. (A, B) Root growth response of *pdr1* and WT to 3 μM external His in split-root assays. WT and *pdr1* plants were grown on +Pi for 6 days after germination on vertically oriented square agar plates. Subsequently, the seedlings were transferred to agar-split round plates in such a way that the shoot and most part of the primary root were placed on the upper and just the primary root tips (~1 mm) on the lower compartment. The media composition of each compartment (i.e., +Pi, -Pi, +Pi+His, or -Pi+His) is given above the figure plates (upper/lower compartment). (A) Images were taken 4 days after transfer, and (B) the PR lengths was measured after 3 days of transfer. (C) Root growth response of *pdr1* and WT after transfer to different media. Plants were grown on +Pi or +Pi+His (indicated by H superscript) agar for 5 days prior to transfer to +Pi, -Pi, -Pi+His, +Pi+His. PR lengths (cm) was measured 3 days after transfer were. Filter-sterilized 3 μM L-His was supplemented in the respective autoclaved medium. Values are the mean \pm SD of 15-20 independent roots. *, Difference between WT and *pdr1* mutant was significant by t-test ($P < 0.05$).

2.12 His in $-Pi+DNA$ medium rescues the *pdr1* phenotype by stimulating DNA decay

How does His rescue the *pdr1* root growth phenotype in $-Pi+DNA$ medium is an intriguing question. Previously, Delatorre (PhD Thesis, 2002) showed that, unlike WT, *pdr1* seedlings do not efficiently degrade external DNA when grown in hydroponic culture. To test if His stimulates hydrolysis of external DNA, WT and *pdr1* plants were grown in hydroponic cultures of $-Pi+DNA$ medium or $-Pi+DNA$ medium supplemented with 10 μM His (Fig. 2-27). As expected, *pdr1* root growth was severely impaired in the $-Pi+DNA$ containing medium while His feeding rescued root growth as it was also observed on solid agar media. To confirm that the rescuing effect was linked to the hydrolysis of DNA in the His supplemented medium, gel electrophoresis was performed every 5 days to visualize the remaining DNA in the medium. In the absence of His supplement, the use of DNA by *pdr1* was exceedingly less than the WT (Fig. 2-27A). By contrast, I found the rapid hydrolysis of the DNA by *pdr1* in the His supplemented media compared to the $-Pi+DNA$ medium as reflected by the decreasing residual DNA over the 20 days of growth periods (Fig. 2-27A). This could be due to the His mediated activation of the nucleolytic enzyme secretion by *pdr1* in the media to hydrolyze the DNA to forage the Pi.

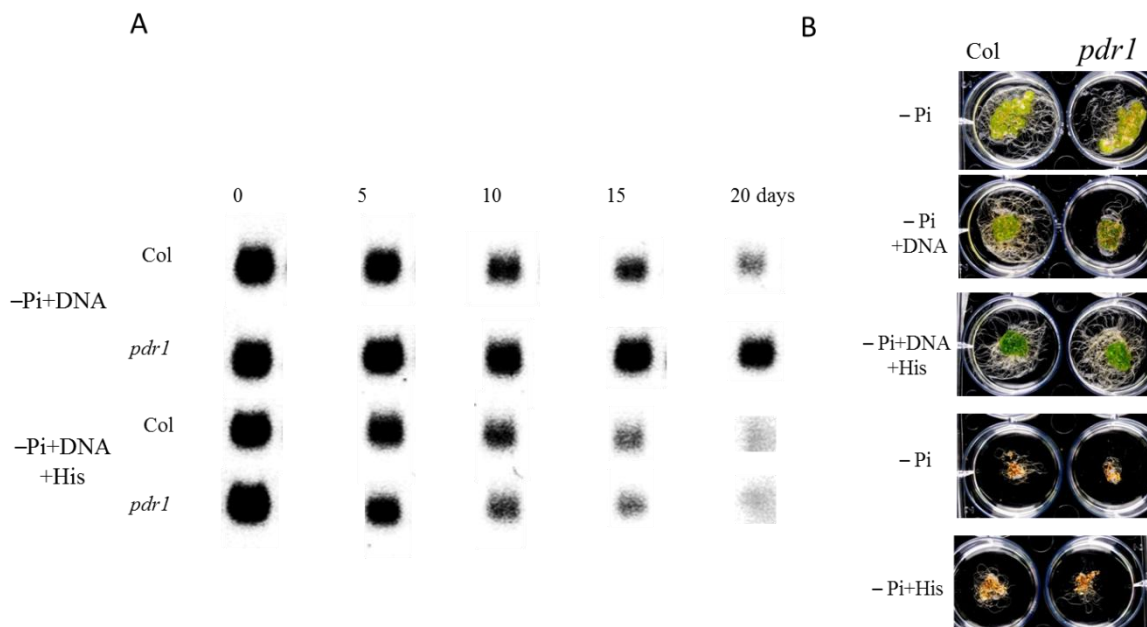


Figure 2-27. DNA utilization by *pdr1* compared to WT in a hydroponic culture. (A) Gel images showing the utilization of exogenous DNA by WT and *pdr1* seedlings as a source of Pi. Plants were grown on $-Pi+DNA$ (0.4 mg mL^{-1}) with or without 10 μM His for 20 days and samples were collected every 5 days for visualizing by gel electrophoresis. All the cultures were repeated three times and representative images are shown here. B) Images of the seedlings grown on respective media after 20 days of germination.

2.13 Accumulation of anthocyanin and starch in *pdr1* upon Pi starvation is ameliorated by external His

The leaf turns to purple in color upon Pi starvation, a visible phenotype mostly due to accumulation of anthocyanin pigments (Vance et al., 2003; Fang et al., 2009), presumably to protect nucleic acids and chloroplasts from ultraviolet (UV) light and photoinhibitory damage respectively (Zeng et al., 2010). Elevated anthocyanin production was also observed in *Arabidopsis* when RNS1, a secreted ribonuclease, is suppressed by antisense technology (Bariola et al., 1999). To gain insight into the correlation of PDR1 function with anthocyanin accumulation, I compared the content of this pigment in response to Pi starvation between WT, *pdr1* and *pri1-2* seedlings grown on +Pi, -Pi, -Pi+His and +Pi+His containing medium (Fig. 2-28A). The result showed higher accumulation of anthocyanin in the leaves of WT seedlings grown on -Pi (8 fold) than those on +Pi (Fig. 2-28A). By contrast, Pi-challenged *pdr1* and *pri1-2* seedlings accumulated 63% and 42% more of this pigment, respectively compared to WT (Fig. 2-28A). While exogenous His on +Pi had no obvious effect on anthocyanin accumulation, supplement of His in a -Pi medium reduced the accumulation of this pigment to half of the content observed on -Pi medium (Fig. 2-28A) for all the three genotypes. Likewise, I also observed the less starch staining of *pdr1* leaves when His was supplied in the -Pi+DNA medium when compared to the strong staining of the *pdr1* plants grown on the similar growth condition in the absence of His (Fig. 2-28B). The results suggest that PDR1 functions in controlling a wide array of responses to Pi-starvation.

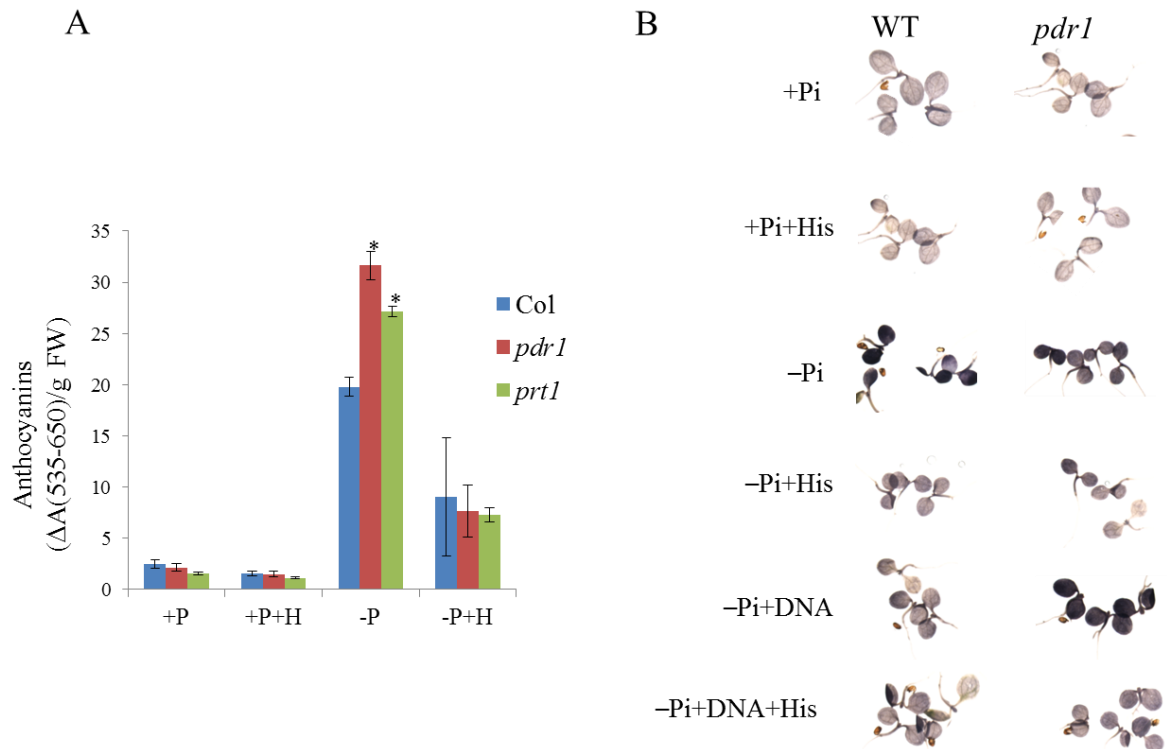


Figure 2-28. Starch and anthocyanin accumulation in WT and *pdr1* seedlings. (A) Accumulation of anthocyanin in seedlings grown on +Pi, +Pi+His, -Pi, -Pi+His for 3 days after transfer of 5 days old seedlings from +Pi. (B) Starch staining of 6 days old seedlings grown on +Pi, -Pi+His, -Pi, -Pi+His, -Pi+DNA and -Pi+DNA+His, n= 3, representative images are shown. Filter-sterilized His (3 μ M) was used as a supplement. Purified herring sperm DNA was substituted for Pi and added to the autoclaved medium to a final concentration of 0.4 mg mL⁻¹. Values are the mean \pm SD of 4 independent samples. *, difference between WT and *pdr1* mutant was significant by t-test (P < 0.05).

2.14 Induction of *PSI* genes in *pdr1* by external His

The shorter PR of *pdr1* under low Pi and -Pi+DNA conditions suggests that *PSI* genes in *pdr1* are defective in the expression that modulate the mitotic activity and meristem maintenance. Indeed the reduced expression of *ProCycB1::GUS* and shorter meristem size of *pdr1* corroborate the reduced expression of a subset of *PSI* genes as shown in the northern blot analysis by Delatorre (PhD thesis, 2002). To test whether His supplementation has any effect on the expression of the *PSI* genes, I performed qRT-PCR for key *PSI* gene expression in the WT and *pdr1* root tips (approximately 0.5cm) grown on +Pi, -Pi and -Pi+His for two days after transfer of 5 days old plants from the +Pi (200 μ M) medium. As expected, Pi starvation induced the expression of *AtACP5*, *AtAT4*, *AtPT2* and *AtRNase2* in the roots of WT

(Fig. 2-29). Roots of *pdr1* seedlings also showed an induction upon Pi starvation, but in contrast to the WT, expression of all the four genes was significantly reduced to 50%. However, no significant difference was found for any of the interrogated genes between WT and *pdr1* root when grown on +Pi. Remarkably, the transcript level of *RNase2* in WT and *pdr1* roots grown on His supplemented –Pi media increased approximately to fivefold. His supplementation in low Pi was also found to increase the transcript of *AtACP5* by 35% and *AtAt4* by 46% in *pdr1* compared to WT, though the increases were not statistically significant (Figure 2-29). No additional effect was found in inducing the expression of *AtPT2* of *pdr1* roots grown on a His containing low Pi medium under our growth conditions. I further checked the expression of *SPX3* which was found to be expressed very low in *pdr1* root, around 6-fold less than that of WT seedlings and His did not trigger the expression (Figure 2-29) indicating that His has no global effect of inducing all *PSI* gene expression upon Pi limitation rather the effect seems to be more specific.

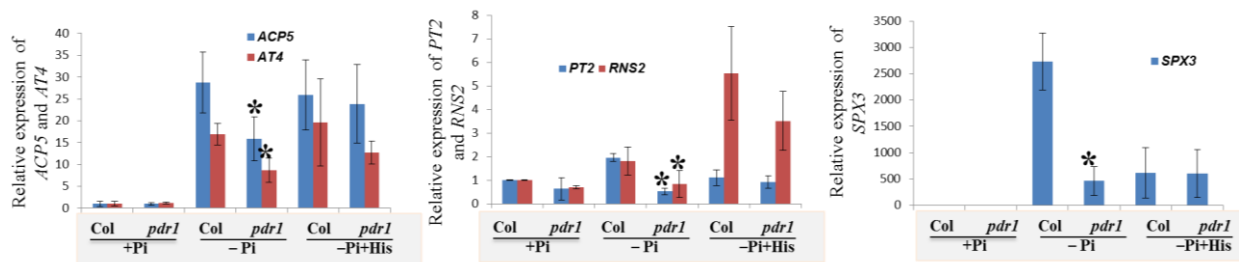


Figure 2-29. Transcript levels of a subset of *PSI* genes. WT and *pdr1* plants were germinated and grown for 5 days on 200 μ M containing +Pi medium, then transferred to +Pi, –Pi and His (3 μ M) supplemented –Pi medium. Two days after transfer, PR tips (approximately 5 mm) were harvested and processed for qRT-PCR analysis. Data were normalized with respect to *PP2A* to calculate the relative expression of *AtACP5*, *AtAt4*, *AtPT2*, *AtRNase2* and *AtSPX3*. * indicates a significant difference from the WT according to a two-sample t-test ($P < 0.05$), values are the means \pm SD of three replicates.

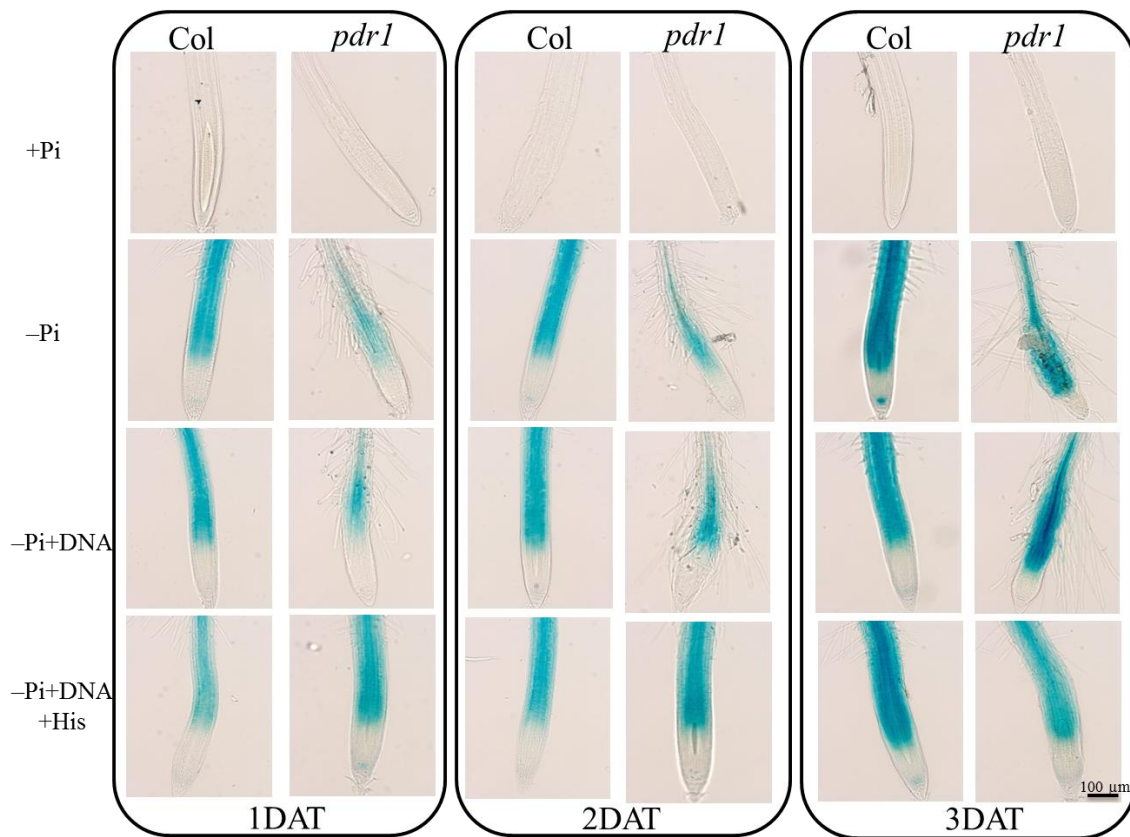


Figure 2-30. *ProAtACP5::GUS* expression in transgenic WT and *pdr1* PR. WT and *pdr1* plants were germinated and grown for 5 days on 200 μ M containing +Pi medium and then transferred to +P, -Pi, -Pi+DNA or -Pi +DNA+His (3 μ M) media. Histochemical GUS staining was performed for up to 3 days after transfer. Representative images of stained roots are shown here.

For the cross-validation that mutation in *pdr1* indeed caused an altered expression of the *PSI* genes, constructs containing the promoters of the *AtACP5* fused to the *GUS* reporter gene was introduced into the *pdr1*. I studied the GUS activity of *pdr1* compared to WT roots grown on +Pi, -Pi, -Pi+DNA and -Pi+DNA+His containing media for three different time points of 24, 48 and 72 hours after transferring 5 days old seedlings from +Pi (200 μ M Pi) (Fig. 2-30). After 20 minutes of incubation in staining solution at 37°C, an intense staining of Pi-challenged WT roots was documented that was not surprising as reported elsewhere (Olczak et al., 2003; Duan et al., 2008) while remarkably low activity of GUS was observed for the *pdr1* in all the time points examined (Fig 2-30). Addition of DNA in the low Pi media found to have no effect on inducing the *AtACP5::GUS* expression in *pdr1* roots for the first 48 hours, though after 72 hours, a slight increase of the expression was observed (Fig. 2-30). His supplement in the DNA containing low Pi medium stimulated the expression of GUS even at the earlier time point of transfer (Fig. 2-30). Compared to the WT, less GUS activity and His mediated normalization of the expression in the roots of *pdr1* is consistent with the results of

qRT-PCR and northern analysis. Thus, it is obvious that His has a pivotal role in the induction of a subset of *PSI* gene expression under Pi starvation; however, the underlying molecular mechanism remains elusive.

2.15 Sensitivity of WT and *pdr1* to a high external NO_3^-

pdr1 sensitivity to NO_3^- was confirmed by a dose response study (Fig. 2-2A and 2-2B). To gain more insight into the growth response of WT and *pdr1* to high concentration of NO_3^- , 10 μM to 100 mM were supplied in the media. WT PR was found to be restricted at or above 25 mM NO_3^- , and at 100 mM NO_3^- , the root growth was reduced so drastically that reminiscence the *pdr1* phenotype at 1 mM NO_3^- (Fig. 2-31A). However, the response of *pdr1* at all the tested concentrations above 10-100 mM remained almost constant as it does at the 1 mM concentration showing no further inhibition suggesting that the inhibitory effect on *pdr1* is not due to toxicity. The sensitivity of *pdr1* and *prt1-2* to glutamine (Gln) and glutamate (Glu) were also tested by a dose response experiments (0-10 mM). Compared to the NO_3^- , PR of WT was found to be shorter on the medium with both amino acids (AA) substitution (Fig. 2-31B). In contrast to the restricted PR growth of WT on high concentration of Glu, the corresponding concentration of Gln showed longer root of WT (Fig. 2-30B). However, the PR of *pdr1* and *prt1-2* showed the similar degree of inhibition compared to the WT as caused by the NO_3^- (Fig. 2-31B).

The complete contrasting root phenotype of *pdr1* and its functionally weak active allele *prt1-2* at the low and high concentration of N in comparison to the corresponding WT spark the question if Arabidopsis has two distinct signaling pathways for low and high N regulation. As such, it is not unreasonable to postulate that the high N regulatory mechanism in *pdr1* is switched off, hence showing the inhibitory effect at the transition point of 0.25 mM and remained unresponsive above the higher concentrations.

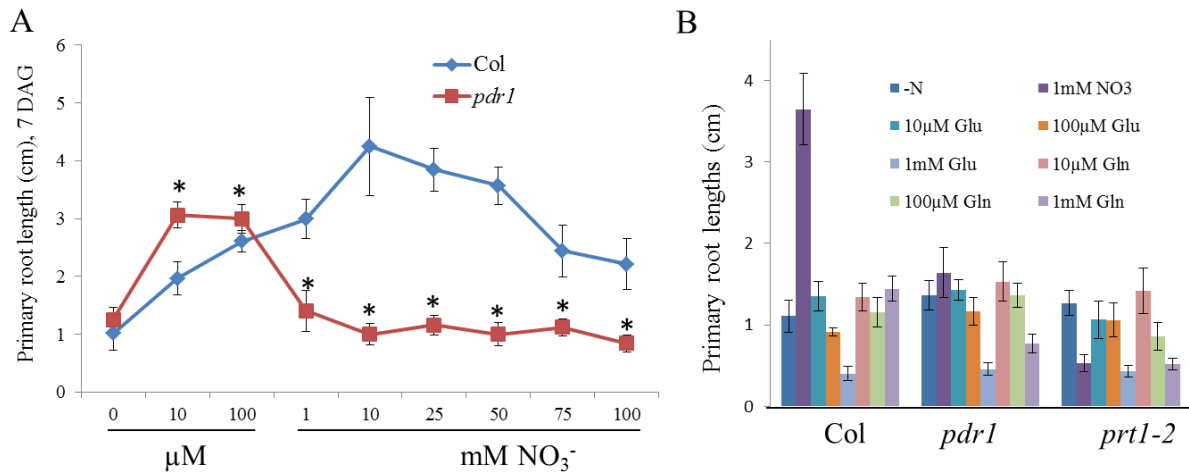


Figure 2-31. Response of WT, *pdr1-1* and *prt1-2* to high nitrate doses and different N sources. (A) PR lengths of 7 days old plants grown on +Pi medium containing 0 to 100 mM KNO_3 . (B) PR growth in response to different concentrations of KNO_3 , Glu and Gln. Plants were grown for 10 days on +Pi/-N media without or with the indicated N supplements. Values are the mean \pm SD of 20 independent roots. *, difference between control (1 mM KNO_3) and high KNO_3 of WT roots was significant by t-test ($P < 0.05$).

2.16 NO_3^- and NH_4^+ content of *pdr1* were not different from the WT

The inhibitory root growth of *pdr1* to high N could be due to its inability to uptake N from the growth medium or the assimilation of more NH_4^+ that caused the toxicity (Li et al., 2014). To test this, I measured the content of NO_3^- and NH_4^+ of the shoot and root of WT and *pdr1* mutant plants (Fig. 2-32). Plants were grown for 8 days on a complete medium (7 mM KNO_3) in the presence or absence of 3 μM His to measure the NO_3^- content in root and shoot separately according to the method described by Cataldo et al. (1975). NO_3^- content of the plants grown on N-deficient medium was measured as a negative control. The results showed no significant difference of NO_3^- content in roots and shoots in between the WT and *pdr1* grown on a complete medium, irrespective of the His supplement (Fig. 2-32A). His supplement in the media had no effect compared to the control indicating no obvious role of His in the uptake of the NO_3^- or downstream metabolic processes. I also measured the NH_4^+ content according to Baethgen and Alley (1989) that also showed no significant difference in between the WT and mutant (Fig. 2-32B) that rejects the possibility of NH_4^+ toxicity. Based on this observation, it could be inferred that *pdr1* is not impaired in the assimilation or

translocation of nitrogen and the impaired root phenotype is independent of the status of N content.

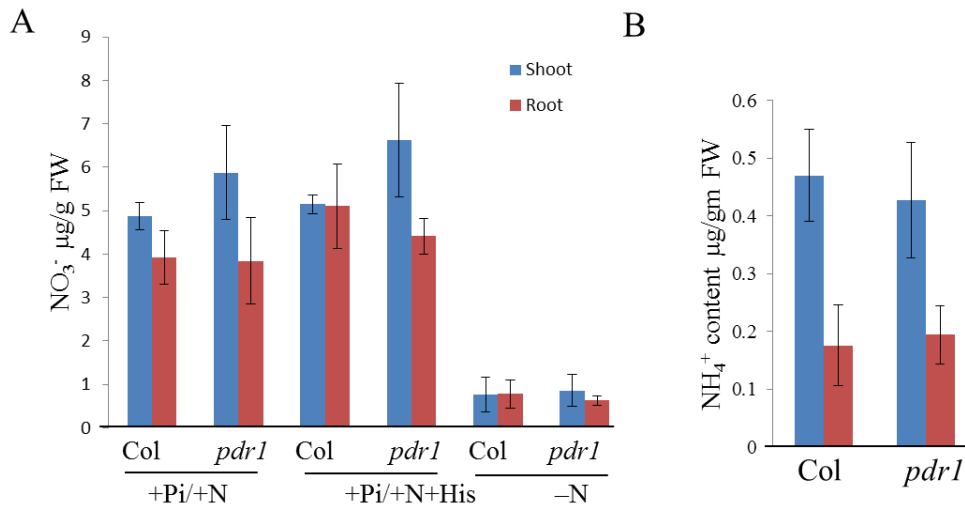
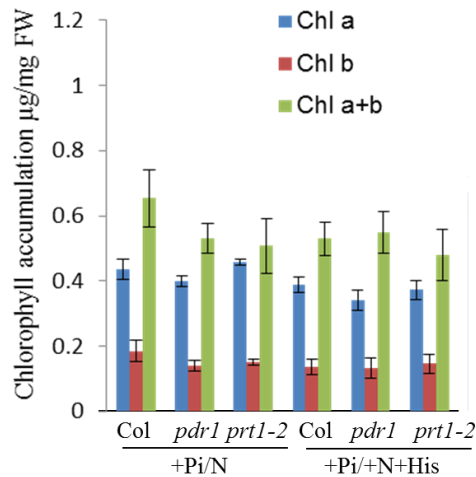


Figure 2-32. Free nitrate and ammonia content. (A) WT, *pdr1-1* and *pdr1-2* plants were grown continuously for 8 days on vertically oriented agar plates containing +Pi/+N, +Pi/+N+His (3 □M) and -N before measuring the NO₃⁻ in shoots and roots. (B) NH₄⁺ content in the roots and shoots. Measurement was done after 2 weeks growth on +Pi/+N. Values are the mean ± SD of 20 independent roots. Values are not significantly different from the control (Col+Pi) as displayed by t-test (P < 0.05).

2.17 Chlorophyll content of the *pdr1* mutants was not different from the WT

Since the photosynthetic apparatus contains a massive amount of N in plants, any appreciable deficiency of N should result in the aberrant formation of chlorophyll (Bojović and Marković, 2009; Maruta et al., 2010). Therefore, I examine if the mutation in *PDR1/ATP-PRT1* had any deficiency of the chlorophyll content that could reflect the N starvation. The Chl a and Chl b were measured in WT, *pdr1* and *pdr1-2* leaves, according to the method described (Ni et al., 2009). There was no significant differences in chlorophyll content between the genotypes irrespective of His in the medium (Fig. 2-33). Thus, the data further confirmed that *pdr1* is not starving any N nutrient; as such, the short root phenotype is independent of N content in the plant.

Figure 2-33. Chlorophyll content in WT, *pdr1-1* and *prr1-2* plants grown continuously for 8 days on vertically oriented agar plates containing +Pi/+N, +Pi/+N+His (3 □M). Values are not significantly different from the control (Col+Pi) as displayed by t-test ($P < 0.05$).



2.18 No difference in the content of glutamine, glutamate, asparagine and aspartate between WT and *pdr1*

The growth and development of plants are effected by the assimilation of inorganic N to amino acids (Hageman and Lambert, 1988). Gln and Glu are the assimilated products of inorganic N which serve as the N donors in the biosynthesis of essentially all amino acids, nucleic acids, and other N-containing compounds such as chlorophyll (Lea, 1993). Therefore, I measured all the amino acids, including Gln, Glu, Asn and Asp (Fig. 2-34) to test whether the *pdr1* phenotype on high N was the result of limiting downstream assimilation process. The content of both Gln and Glu showed no obvious difference in the shoot rather it increased to 2-fold in the roots of *pdr1*, both of which are known to form Asp and Asp, and these four amino acids are used to translocate organic N from sources to sinks (Mifflin and Lea, 1980; Peoples and Gifford, 1993). No significant difference of Asp content was found between the WT and *pdr1* while the content of Asn increased significantly in the shoots and roots of *pdr1* than its corresponding WT counterpart (Fig. 2-34). The higher or equivalent accumulation of all four AA in *pdr1* with respect to the WT had led us to annul the possibility of any defect in the assimilation of inorganic N in *pdr1*.

2.19 Increased content of other free amino acids in *pdr1* compared to the WT

To determine whether the mutation at *pdr1* locus affect His levels, I measured the content in WT and *pdr1* according to the method described (Ziegler and Abel, 2014). The content of His in *pdr1* roots was not different from that of WT plants grown on a complete medium (Fig. 2-25). This is obvious because of the compensatory effect of the second active copy, *ATP-PRT2* (Ohta et al., 2000). To get further insight into the global effect of *pdr1* mutation on the other free amino acids, I concurrently measured the contents of each amino acid in the roots and

shoots grown on +Pi and -Pi (Fig. 2-34). I observed an increase of almost all free amino acids in both shoot and roots of *pdr1* compared to the WT except His, methionine (Met), Arg, Trp, Val and Tyr irrespective of Pi status (Fig. 2-34). However, Pi challenged *pdr1* showed several fold accumulation of cysteine (Cys) and Thr in root in comparing to the +Pi grown mutant roots. The general response of *pdr1* to accumulate most of the free AA content more than the WT is perhaps due to the link of cross regulatory pathway as noted by Jones and Fink (1982); Hinnebusch (2005) and Ljungdahl and Daignan-Fornier (2012).

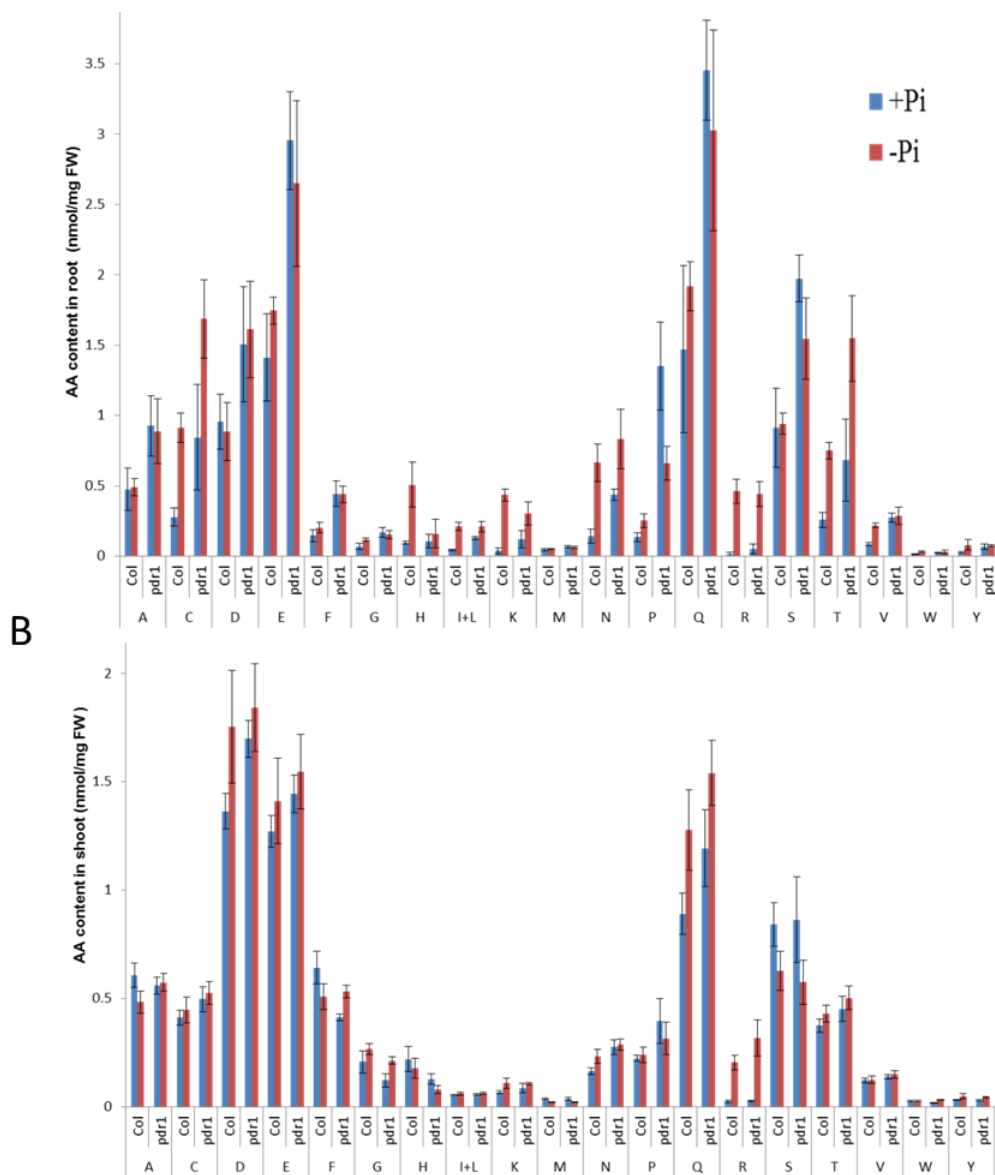


Figure 2-34. Free amino acid contents in shoots and roots of WT and *pdr1-1* seedlings. Plants were grown on +Pi agar for 5 days and then transferred to +Pi or -Pi medium. Two days after transfer, roots and shoots were separated, weighed, and processed for measuring the free amino acid contents of roots (A) and shoots (B). Values are the mean \pm SD of 4 independent measurements.

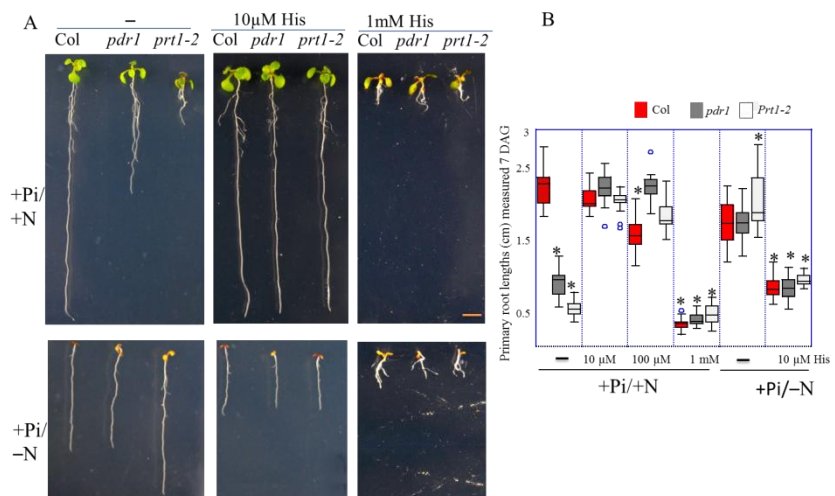
2.20 His supplement in N-deficient medium aggravate the growth

The overexpression of *PDR1/ATP-PRT1* in the *pdr1* and external supply of His in the growth media complement the *pdr1* root phenotype. As PDR1/PRT1 is the first committed enzyme for His biosynthesis and plays a major role in controlling the flux as suggested by Ingle (2015), the rescuing effect of His is very conceivable. However, I found that 10 μ M His supplementation in $-N$ deficient growth medium inhibits the PR growth of WT, *pdr1 prt1-2* (Fig. 2-35). The negative effect of His on the typical N-deficient medium responds of WT characterized by longer PR (Giehl et al., 2014) poses the question of the role of His. This result confirms that Arabidopsis is not using His as supplement of N, likely uses it to regulate the competent N sources for the proper growth and development.

2.21 High His supplement drastically restrict the Arabidopsis growth

The rescuing effect of *pdr1* by as low as 1 μ M His in the media has prompted us to interrogate the effect of a high concentration of His. Thus, WT *pdr1* and *prt1-2* were germinated and grown for 7 days on 10, 100 and 1000 μ M His supplemented complete media. Though low concentration found to promote the *pdr1* and *prt1-2* root growth and no remarkable effect on the WT, 1 mM His in the media found to restrict the growth of all the genotypes severely (Fig. 2-35A and 2-35B). Additionally, leaves phenocopied the N deficient symptom turning to yellow color while root barely grew beyond 0.5 cm (Fig. 2-35A). The responses of WT and the mutants to high His distinctly displayed the regulatory role of His.

Figure 2-35. Effect of external His on WT (Col-0), *pdr1-1* and *prt1-2* seedlings continuously grown for 7 days on +Pi+N or +Pi-N medium. (A) Shown are representative images of seedlings with no His supplementation (left panel), and with His supplementation as indicated



(middle and right panels). (B) Statistical analysis of PR length. Values are the mean \pm SD of 25-30 independent roots. *, difference between WT and *pdr1* mutant was significant by t-test ($P < 0.05$). Scale bar represents 2 mm.

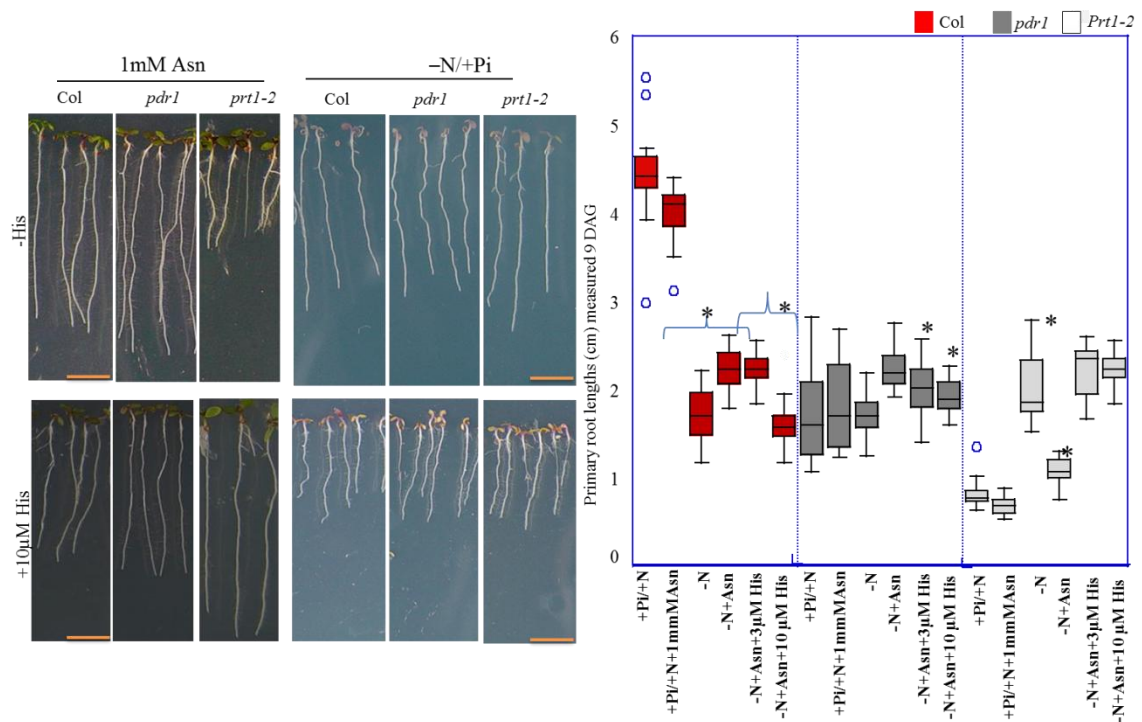


Figure 2-36. Effect of Asn with or without His on PR growth of WT (Col-0), *pdr1-1* and *prt1-2* seedlings after 7 days of growth on the respective media as indicated. (A) Representative images of the seedlings. (B) Statistical analysis of PR lengths. Values are the mean \pm SD of 25 independent roots. *, difference between WT and *pdr1* mutant was significant by t-test ($P < 0.05$). Scale bar represents 5 mm.

2.22 Effect of external amino acids on WT and *pdr1* root growth

In addition to His, I expanded these studies to obtain insight into the effect of other amino acids supplements at higher concentration (1 mM) (Fig. 2-36, Fig. 2-37). Similar to the severe inhibitory effect of 1 mM His, drastic root growth inhibition by Phe, Val, Trp, Arg, Asp, Glu, was also observed when applied the same concentration (1 mM) to the 7 mM NO_3^- containing complete growth medium or as a sole N sources on N-deficient medium (Fig. 2-37 and Fig. 2-38). By contrast, the equal concentration of Asp, Asn, Gly and Pro as a supplement in complete growth media showed no adverse effect on the WT while *pdr1* and *prt1-2* showed exactly the similar fashion of inhibition like NO_3^- . In N-deficient growth medium, substitution of those three AAs except Asn impinged the growth as did by all other tested amino acids (Fig. 2-36 and Fig 2-38). A drastic growth effect was found for threonine (Thr), tryptophan (Trp) and valine (Val) particularly on $-N$ medium. However, supplementation of 10 μM His to those tested AA on a complete or N-deficient medium showed no rescuing or adverse effect except Asn (Fig. 2-38). Interestingly, N substitution by 1 mM Asn substantially enhanced the

growth of all the three genotypes of WT, *pdr1* and *pri1-2* (Fig. 2-36). The equal root growth of *pdr1* compared to the WT and better improvement of the knock-down allele *pri1-2* under this condition (Fig. 2-36) is suggestive of the specificity of *pdr1* to N sensitivity. While the addition of His with Asn reversed the growth, including WT that phenocopied the N deficient condition (Fig. 2-36) suggesting the specificity of His.

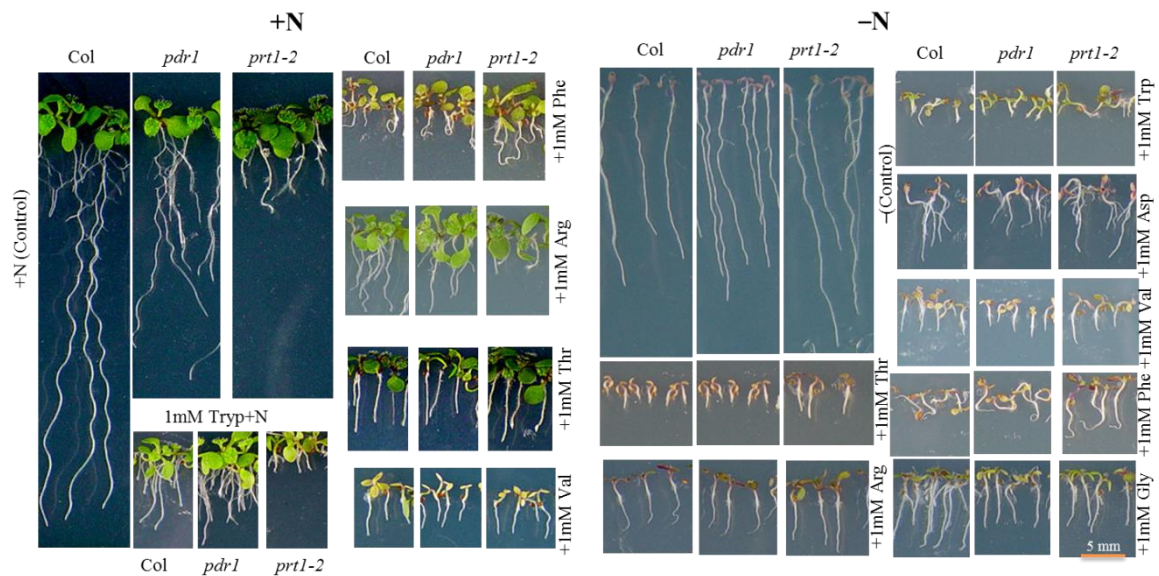


Figure 2-37. Effect of amino acid supplementation (1 mM each) on PR growth of WT, *pdr1-1* and *pri1-2* seedlings grown continuously for 7 days on vertically oriented agar plates of the indicated media. Representative seedlings are shown.

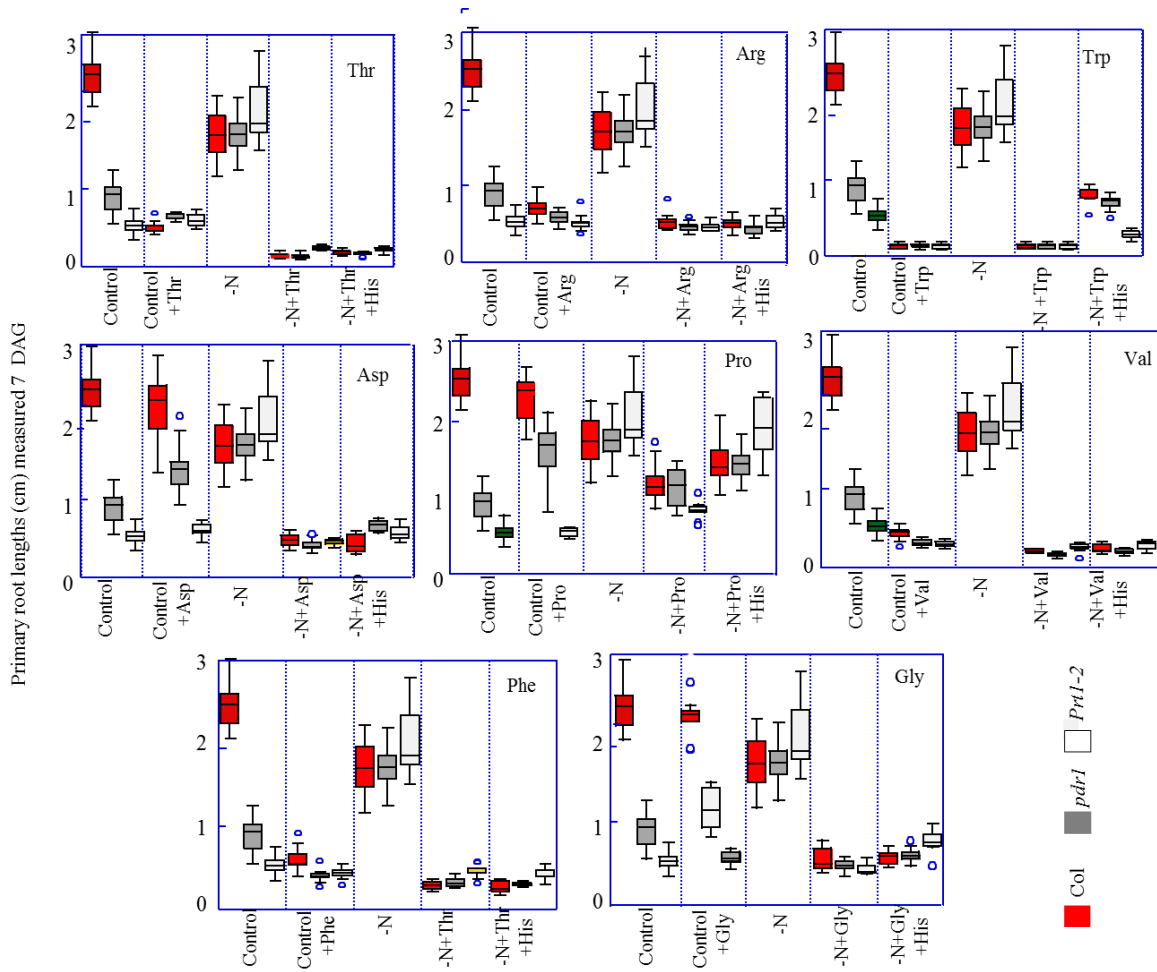


Figure 2-38. Effect of amino acid supplementation (1 mM each) on PR growth of WT, *pdr1-1* and *prt1-2* seedlings grown continuously for 7 days on vertically oriented agar plates of the indicated media (His was used at 10 μ M). Values are the mean \pm SD of 30-40 independent roots.

3. DISCUSSION

PDR1 encodes *ATP-PRT1* (*ATP-phosphoribosyl transferase 1*), the first enzyme for His biosynthesis in Arabidopsis. It has recently become apparent that histidine biosynthetic genes in Arabidopsis play an essential role for plant growth and development (Muralla et al., 2007; Bikard et al., 2009). A leaky mutant disrupted in His6a (*hpa*) responsible for catalyzing the sixth step of His synthesis exhibits a short root phenotype owing to serious defect on the meristems (Mo et al., 2006), and complete knockout of the gene is embryo lethal (Tzafrir et al., 2004). Paralleling the observation by Mo et al. (2006), the *pdr1* mutant also showed a short root phenotype compared to the WT (Fig. 2-1B). *pdr1-2* is the knock-down allele of *PDR1* that showed more severe root growth phenotype than *pdr1* (Fig. 2-12A). The soil grown *pdr1* phenotype was similar to the WT but, *pdr1-2* showed shorter growth (Fig. 2-1E). Like the earlier observation of Mo et al. (2006) for the *hpa* mutant, *pdr1* also showed no significant deviation of the aerial part biomass from that of the WT (Fig 2-22A) indicating the specificity of the effect of *pdr1* mutation on root growth. The comparatively short root of *pdr1* on a complete (+Pi) growth medium is not likely the consequence of global His starvation as it is plausible that the functionally active second isoform of *HisN1*, *ATP-PRT2* (Ohta et al., 2000) can sustain the His flux at the basal level. Indeed the free content of His in the mutant root is not significantly different from the WT seedlings grown on complete medium (Fig. 2-25A). The drastically reduced root phenotype of the *hpa1* mutant was also not because of global His starvation as the total His content of *hpa1* was not different from the WT (Mo et al., 2006). A similar observation of growth defects was also found in the *apg10* mutant that encodes BMII isomerase (HisN3) in spite of the elevated His content in the mutant (Noutoshi et al., 2005). Complete blockage of His biosynthesis by triazole herbicides results in an embryo-lethality of plants (Guyer et al., 1995; Mori et al., 1995). I also found seedling lethality of *pdr1-3* mutant carrying a T-DNA insertion in the fifth exon of *ATP-PRT1* (Fig. 16). Mind-bogglingly, I found 5×10^{-7} M His supplementation in the complete growth medium could partially rescue the *pdr1* short root phenotype (Fig. 2-12B). The optimum concentration for complete rescue of *pdr1* PR is 10^{-6} M while the corresponding concentration for *pdr1-2* is 3 μ M (Fig. 2-12B). Correspondingly, 10^{-5} M was used to rescue the *hpa1* mutant as reported by Mo et al., (2006). Thus, it appears that rescue of the phenotype by His is dose dependent depending on the demand of the mutant to reach a homeostatic condition. The requirement of His homeostasis in plant growth and development is also perspicuous from the pale green leaf and the dwarf phenotype of *apg10* mutant due to high His content (Noutoshi et al., 2005). Additionally, I also check the effect of D-Histidine in the growth media on the

pdr1 phenotype (Fig. 2-14). We hypothesized that if the physical binding of L-His with any particular molecule facilitates the rescuing of the *pdr1* phenotype, then the enantiomer D-His should also do the same. By contrast, if the rescuing effect of L-His is due to triggering biological response, D-His will be of no use in this case considering the non-recognition of this enantiomer by other catalytic enzymes (Murphy et al., 2011). The failure to rescue the short root phenotype of *pdr1* by D-His (Fig. 2-14) is eventually pointing to our alternative hypothesis. Furthermore, I also checked the imidazole and imidazole acrylic acid whether they could rescue the phenotype (Fig. 2-15). We used those because His has a positively charged imidazole functional group that facilitates it to participate in a common enzyme catalyzed reaction (Ingle, 2011) and imidazole acrylic acid is the metabolite of His. The growth assays showed that the requirement of His cannot be complemented by either of the molecules. Given that no obvious phenotypic effect on the aerial part (Fig. 2-22A), and the root rescuing effect of such a low concentration of His nods the hormone like specific regulatory role of His in regulating root meristem. Our further experimental data showed the altered short root phenotype of *pdr1* was associated with high NO_3^- (on complete growth medium) and Pi starvation (on $-\text{Pi}$ and $-\text{Pi}+\text{DNA}$ medium) (Fig. 2-2) which in turn mediated by His via unknown mechanisms.

3.1 PDR1 is required to maintain a low Pi response

The strong evidence of *pdr1* Pi specificity has been turned out from the root growth study on a DNA containing low Pi medium. The shorter PR length of *pdr1* mutant compared to WT under $-\text{Pi}$ condition, in spite of the presence of DNA (Fig. 2-1G), manifests its altered response to low Pi. Moreover, I have shown that altered PR growth of *pdr1* is a function of Pi concentration in the growth medium by keeping the NO_3^- concentration at 250 μM . Under this experimental condition, significantly shorter PR of *pdr1* than that of WT was observed on low Pi below the threshold level of 200 μM while above this concentration, there was no significant difference observed between *pdr1* and WT that indicated the tight link of *pdr1* phenotype to low Pi (Fig. 2-3). I further demonstrated that meristem activity of *pdr1* was conditionally Pi specific as the activity of *ProCycB1::GUS* expression in *pdr1* was similar to WT under $+\text{Pi}/+\text{N}$ condition and very less prominent on low Pi when transferred from the $+\text{Pi}$ (Fig. 2-23), that has imparted its distinct low Pi effect. PI staining of the root tip of *pdr1* grown under low Pi medium showed a disturbed cell patterning characterized by deformation of epidermal cell and early differentiation of meristematic cells (Fig. 2-24).

The RSA has been considered as a prominent marker for the study of nutritional stress in several studies (Krapp et al., 2011; Peret et al., 2014; Müller et al., 2015). Reduction of the PR and formation of more lateral roots are prominent features in response to limited Pi in the rhizosphere (Ticconi and Abel, 2004; Reymond et al., 2006; Svistoonoff et al., 2007; Giehl et al., 2014), the shorter PR and more lateral root emergence in *pdr1* in contrast to the WT control grown on the same low Pi containing medium suggests the altered response of *pdr1*. The increased lateral root under Pi deprivation condition could be the consequence of reduced meristematic activity (Sanchez-Calderon et al., 2005). The observed reduced meristem size and elongation zone and lower number of epidermal cell in the root meristem of *pdr1* in contrast to WT control (Fig. 2-24) indicated that higher lateral root formation in *pdr1* could be the consequence of the exhaustion of the meristem in response to low Pi. However, LR was inhibited by the low Pi, thus, more LR emergence per unit area than that of WT could not be compensated the total root length in *pdr1* (Fig. 2-21C). Adjustment of RSA by attenuating the PR and forming more lateral roots might be an attempt of *pdr1* to forage more available Pi from the top soil as the macronutrient becomes more limiting with increasing soil depth [reviewed in (Abel, 2011; Peret et al., 2011)].

No significant difference of free Pi content in the root, but lower free Pi content in the shoot of *pdr1* under both +Pi and -Pi condition (Fig. 2-5) could be due to the defect in the translocation of Pi from the root to shoot. However, the total Pi content in *pdr1* was not significantly different from the WT grown on -Pi medium (Delatorre, 2002). Thus, the shorter PR of *pdr1* under -Pi condition is unlikely the direct consequence of Pi deprivation. Instead, it could be the inability of *pdr1* to use organophosphate and/or might be altered setting of genetic program in *pdr1* that modulate the root growth upon Pi starvation. Consistently, the lower accumulation of free Pi and total phosphorus in shoots and roots of *pdr1* plants in nucleic acid-containing media were found by Delatorre (PhD thesis, 2002) reflected the inability of the mutant to activate the molecular machinery required to mine Pi from organophosphates. Conversely, the uptake rate of Pi by *pdr1* was found significantly higher than that of the WT counterpart grown on 10 μ M Pi provision while at 1 mM Pi, the rate was almost the same like WT (PhD thesis by Delatorre, 2002). This could be attributed to the higher Pi starvation of the mutant that induces a marked stimulation of nutrient uptake efficiency by the roots, which relies on the up-regulation of specific high-affinity ion transport systems as suggested the general response of mineral nutrient limitation (Clarkson and Lüttge, 1991; Gojon et al., 2009).

Moreover, biochemical responses like more starch and anthocyanin accumulation in *pdr1* and normalization of the accumulation of these pigments in *pdr1* seedlings by exogenous His supply to -Pi medium (Fig. 2-28) further cues the function of PDR1 for the conventional response to low Pi availability. A suite of studies has shown the accumulation of anthocyanin and starch as typical Pi starvation responses (Ticconi et al., 2001; Jiang et al., 2007), for example, the loss of function of a master regulator PHR1 reduces accumulation of anthocyanin in response to Pi limitation but not in response to N starvation or other stress-related treatments (Rubio et al., 2001).

3.2 Altered *PSI* gene expression in *pdr1*

The altered physiological and biochemical response of plants to Pi availability could be the consequence of changes in gene expression (Sanchez-Calderon et al., 2005; Pant et al., 2015). To determine whether the altered RSA and increased accumulation of starch and anthocyanin in *pdr1* is associated with the differential expression of *PSI* genes, I performed qRT-PCR analysis for *AtAT4*, *AtACP5*, *AtRNase2*, *AtPT2* for the WT and *pdr1* mutant grown on +Pi, -Pi and -Pi+His medium for 2 days after transferring 5 days old seedlings from the 250 μ M Pi medium (Fig. 2-29). The subjective selection of those genes was based on the hypothesis that *pdr1* is likely to be defective in systemic rather than local response based on earlier observation of its inability to grow on DNA containing only P source medium. *AT4* is a non-coding RNA induced upon Pi starvation possesses a conserved motif of 22- to 24-nucleotide-long sequence that is partially complementary to miR399 (Shin et al., 2006; Franco-Zorrilla et al., 2007). The overexpression of *AT4* counteracts miR399 by target mimicry that targets the *PHO2* and loss of function mutation in *AT4* facilitate more Pi accumulation under Pi deficit condition (Shin et al., 2006; Franco-Zorrilla et al., 2007). *ACP5* and *RNase2* are attested to be involved in solubilizing the organically bound Pi (Ticconi et al., 2001). Comparatively lower induction of those tested genes in the roots of *pdr1* in contrast to WT control (Fig. 2-29) confirms northern analysis based observation of Delatorre (2002). Furthermore, the lower *ProACP5::GUS* activity in the roots of homozygous transgenic *pdr1* plants than that of the WT under Pi starvation (Fig. 2-30) solidify our earlier observation. Supplementation of His in the -Pi containing media enriched the transcripts of those tested genes as well as normalization of the expression of *ProACP5::GUS* in *pdr1* roots to the WT level (Fig. 2-30). This suggests the possible regulatory role of His to trigger the activity of a number of key *PSI* genes, in a mechanism yet to be explored, to adopt upon the malnourishment of Pi. There is

no report of His biosynthetic genes in plants, including Arabidopsis known to play roles in the Pi regulatory pathway. However, in yeast it was known long before that *His1p* and *His4p* were linked with the phosphate pathway (PHO). For example, it has been shown in a number of studies that optimal expression of two yeast His biosynthetic genes *HIS4* and *HIS7* require the *Bas1p* and *Bas2p* (*PHO2*) transcription factor (Arndt et al., 1987; Ticebaldwin et al., 1989). Arndt et al., (1987) further demonstrated that HIS4p-lacZ activity of His4P is a function of cellular Pi concentration that requires the major transcription factor *PHO2* to activate. Northern analysis by Denis and coworkers (1998) showed the expression of *pdr1* homologue *His1P* in yeast was affected by the mutation of *PHO2* while other His biosynthetic genes were not affected. Furthermore, the expression of *PHO84*, the high affinity phosphate transporter (Secco et al., 2012b) in yeast was shown to be increased with the increasing concentration of AICAR, the metabolite of *HIS4p* (Pinson et al., 2009). The foregoing discussion tempts to speculate the existence of similar interaction of phosphate and His biosynthetic gene(s) in Arabidopsis, though such existence is hitherto unreported in plants. Characterization of the *pdr1* mutant support this notion and further work of Arabidopsis His biosynthetic genes in line of Pi starvation will bridge the gap.

3.3 PDR1 is required to use organophosphate

The impinged *pdr1* root growth under DNA containing low Pi medium explicitly indicated the inability of *pdr1* to use organophosphate as a sole source of Pi, which is often predominant in the soil solutions (Richardson, 2009). Plants including Arabidopsis evolutionarily developed the ability to forage Pi from a wide range of refractory organic P substrates in the rhizosphere (Ticconi and Abel, 2004; Richardson, 2009; Liang et al., 2010). The vibrant example is the Pi feeding plant like root growth of WT Arabidopsis plants on a DNA containing low Pi medium where the DNA serves as the only source of Pi (Fig. 2-1F and 2-1G). By contrast, the requirement of external Pi provision for the *pdr1* mutant to continue root growth and the failure to sustain the root development under the -Pi+DNA growth condition indicated its defect to induce the necessary hydrolases to scavenge the Pi. The facet of this was revealed by the experiment performed in hydroponic culture to test the use of DNA as a Pi source (Fig. 2-27). The experiment showed *pdr1* utilized less DNA compared to the WT grown over the 20 days as revealed by the gel electrophoresis of the sample collected from the media every five days. The visualization of DNA from the -Pi+DNA and -Pi+DNA+His medium displayed a gradual decrease of the DNA from the

media containing His confirm the utilization of DNA by *pdr1* only possible in the presence of exogenous His (Fig. 2-27A). The results of the qRT-PCR for the expression analysis of *AtACP5* and *AtRNase2*, and histochemical study of *ProACP5::GUS* are the additional support for its inability to trigger the secretion of necessary nucleoside hydrolyzing enzymes. For example, the induction of acid phosphatases (APase) upon low Pi availability is common in plants (Liu et al., 2012) that are capable of hydrolyzing orthophosphate monoesters into more mobile orthophosphate anions (Vincent et al., 1992), thus it could facilitate more Pi availability. Similarly, the requirement of RNases to scavenge Pi from soil-localized nucleic acids was testified by Ticconi and Abel (2004). In fact, this is corroborated with the findings of Tran and Plaxton (2008) who reported RNase 1 as the most abundant protein accumulating in the secretome of the Pi-starved Arabidopsis suspension cell. The exogenous application of His in the $-Pi+DNA$ medium reverted the short root of *pdr1* (Fig. 2-12A) likely by His mediated DNA hydrolysis (Fig. 2-27A) that could be supported by the His mediated induction of *RNase 2* and *ACP*. The necessity of His in DNA containing sole Pi source medium to restore the *pdr1* phenotype suggest the role of His to forage Pi from the orthophosphate. The 5-fold elevated His content in the root of WT grown on $-Pi$ in comparison to the Pi-sufficient grown roots (Fig. 2-25B) support the notion of its role under Pi starvation.

3.4 The short root phenotype of *pdr1* on a high Pi medium is linked to high NO_3^-

The comparatively short root phenotype of *pdr1* was found to be linked to the presence of high N in the growth medium as revealed by the equivalent growth of both *pdr1* mutant and WT control under $-N$ condition (Fig. 2-2). To confirm that this is not a general response in N deficient medium, I tested the mutant under different NO_3^- regimes (Fig. 2-2A and Fig. 2-2B). The observation showed the insensitivity of *pdr1* mutant at low concentrations, and enhanced with the increase of NO_3^- concentration in the growth medium. The similar inhibiting pattern of PR was also noticed in response to $(NH_4)_2SO_4$ and NH_4Cl , glutamine and glutamate in the growth medium (Fig. 2-2C and 2-2D). We have set up several alternative hypotheses to elucidate the possible cause of the altered root phenotype of *pdr1*, namely: i) the N sensing machinery of *pdr1* is defective; ii) acquisition of N from the external media is impaired; iii) the N assimilation pathway is disrupted; iv) *pdr1* is sensitive to high NO_3^- because of its toxicity; or v) the capacity of the mutant is debilitated to use the available N, also called 'N use efficiency'. The first hypothesis can be ruled out easily considering the promoting root

growth under low NO_3^- concentration and restricting PR growth on high NO_3^- medium. Moreover, prolific lateral root growth of *pdr1* on high N echoes the active sensory mechanism (Fig. 2-21A). This is also very unlikely that global starvation of N in *pdr1* causes the limited root growth as the mutant did not show any significant differences of NO_3^- and NH_4^+ content in contrast to the WT (Fig. 2-32A and Fig 2-32B). To inspect whether the downstream processes for the assimilation is impeded, I measured all the AAs in the shoot and root of *pdr1* and WT (Fig. 2-34). The results showed no decrease of any single AA content in the shoot or root of *pdr1* compared to the WT; rather some of the AA contents in *pdr1* increased significantly. More remarkably, the Gln, Glu, Asp, Asn content increased in *pdr1* root than in the WT. I also quantified the chlorophyll content (Chl a and Chl b) that showed no shift from the WT (Fig. 2-33) indicating no N or carbon starvation. Thus, the reckoning the AA and chlorophyll content of *pdr1* with respect to WT prompted us to null our third hypothesis. To determine if the excess NO_3^- toxicity is accounting for the short root phenotype of *pdr1*, I tested the WT and *pdr1-1*, *pdr1-2* growth on 1 mM to 100 mM KNO_3 concentration (Fig. 2-31A). The response of WT root showed progressively decreased at or above 25 mM NO_3^- and decreased dramatically to the almost equal level of *pdr1* at the 100 mM concentration (Fig. 2-31A). By contrast, the mutant lines *pdr1* and *pdr1-2* showed no further effect in response to this wide range of 1 to 100 mM NO_3^- in the growth media (Fig. 2-31A). If the mutants show similar NO_3^- toxicity, we would have expected the similar trend of inhibition with the increasing concentrations. This data clearly suggest the limited root growth of *pdr1* is not on account of toxicity, rather it refers to the last hypothesis of 'efficient use'. Given that no decrease in the turnover of N, as demonstrated by the AA level in *pdr1* (Fig. 2-34), the phrase 'efficient use' seems a vague. It is very inquisitive to reconnoiter why specifically root growth is sensitive to high NO_3^- . External His supplement and overexpression of *ATP-PRT1* in *pdr1* found to rescue the short root phenotype of *pdr1* (Fig. 2-10 and Fig. 2-11). There might be an argument if His is an alternative N source. However, the result presented here shows no rescuing effect of *pdr1* or even the WT by substituting His for N, rather His supplementation affects the normal N-deficient response by reducing the root growth of all the three genotypes (Fig. 2-35 A and Fig. 2-35B). Similarly, high concentration (1 mM) of exogenous His supplement in the complete growth medium also drastically restricted the growth of *pdr1* and WT (Fig. 2-35 A and Fig. 2-35B). Thus, considering that His is not a nutrient source for the Arabidopsis, including other plants (Polkinghorne and Hynes, 1975), and rescuing effect of a very low concentration (10^{-6} M), we can infer the role of His in coordinating the 'efficient use

of N⁺ sources by converting the nutritional signal to developmental signal as can be exemplified by the root development of *pdr1*.

According to the prediction by InterPro (protein sequence analysis and classification), ATP-PRT1 contains the PII protein domain at the end of the C-terminal, from the 310-394 AA. The superimposed AtATP-PRT1 on 2VD3, the structure of His inhibited Hisg from *Methanobacterium Thermoautotrophicum*, shows the similar match of C-terminal part with the PII domain (Fig. 2-8B). The presence of PII like domain in ATP-PRT1 (Fig. 2-8B), which is known to play a role in N sensing in several microorganisms (reviewed by Huergo et al., 2012) could also mediate the N sensing in Arabidopsis. Thus, it is palpable to infer that the defect in *pdr1* is not at metabolic level, rather at the signaling level that disrupts the transmission of the nutritional signal to a root specific developmental signal.

3.5 Effect of external amino acids on *pdr1* and WT, and specificity of His

The effect of His in *pdr1* root growth prompted us to check the response of the *pdr1* mutant to the high concentration (1 mM) of some other AA supplement in the N-sufficient and N-deficient growth medium. The results showed a variation of the specificity of *pdr1* sensitivity to different AA. A drastic inhibitory effect of Phe, Val, Trp, Arg, Asp and Glu on growth, including root was observed for all the three genotypes WT, *pdr1-1* and *pdr1-2* (Fig. 2-37 and Fig. 2-38). The deleterious effect of the tested AAs on the growth could be due to the disturbance of AA homeostasis by the external supply of feedback inhibited AA (Voll et al., 2004). There is an evidence from yeast that AA fluxes are inhibited by the exogenous supply of single AA because of end-product feedback inhibition of the biosynthetic pathway, resulting in the shortage of the AA (Voll et al., 2004). This might also be the result of a non-metabolic response such as alteration of membrane potentials or it might be the inhibition of NO₃⁻ uptake by free AA, as suggested by Muller and Touraine (1992). However, we are not ruling out the possibility of other metabolic perturbation that leads to the toxicity. In contrast to the extreme effect of the AA tested, 1 mM Gln and Asn supplements in the N-deficient medium showed substantial, but slower growth of WT compared to normal growth condition (Fig. 2-31B). This suggests Gln and Asn as an alternative of N sources for Arabidopsis, even though slower growth indicated not all nitrogen compounds support plant growth equally well. The response of *pdr1* to Gln was very similar to the NO₃⁻; showed impaired root growth while 3 μM His feeding rescued the root phenotype (Fig. 2-31B). The only exception was Asn, *pdr1* showed equivalent root growth like WT on medium with 1 mM Asn as a substitute

for N (Fig. 2-36). This manifests *pdr1* is not equally sensitive to all the N sources, in other words, it provides the evidence of the specificity of sensitivity of mutant is not to all N sources. Interestingly, the reduced PR growth of *pdr1* and WT on the Asn supplemented with 3 μ M His indicated the specificity of His in mediating the use of N for the growth and development of plants. The negative effect of His on the utilization of Asn with respect to growth is similar to the earlier report on the use of a number of AAs as N sources for *Aspergillus nidulans* (Polkinghorne and Hynes, 1975). However, the authors did not find any effect of His on NO_3^- , NH_4^+ , Glu, Gln use (Polkinghorne and Hynes, 1975). This could be due to the use of WT that barely enables to discriminate the specific molecular effect on a particular developmental process. This suggests that the role of His is imprinted at the genetic level to trigger the arrays of developmental responses towards the efficient use of N sources. Nevertheless, the question arises if His or a catabolite of His plays a role in this regard. Glu is one of the breakdown products of His and found to inhibit the root growth of WT when compared to the NO_3^- supported growth (Fig.2-31B). Similar inhibition of growth was also reported by several other publications. Likewise, another catabolite of His is NH_4^+ , the external application of this N source was also found not to rescue the *pdr1*, rather both Glu and NH_4^+ were found to be repressive (Fig. 2-2 B, Fig. 2-2C and Fig. 2-31B), indicating the repressive growth effect of the downstream degradation product of His. Furthermore, urocanate, one of the products of histidine ammonia-lyase (histidase or histidinase) activity, is not a sole N source and does not affect the utilization of any sources of N (Polkinghorne and Hynes, 1975). The failure of all other AA, including D-His, imidazole and imidazole acrylic acid supplementation with the high NO_3^- medium (+Pi/+N) in rescuing the short root phenotype of *pdr1* confirms the specificity of L-His (Fig. 2-14, ig. 2-15 and ig. 2-16). This further validates the role of His in using N sources for the plant not as a nutrient, but rather as cues for the development. The role of L-histidine in nitrogen balance in animals, including human has been reported in various studies (Wolf and Corley, 1939; Wissler et al., 1948). Lei et al. (2013) reported the positive correlation between the His application and yeast growth. They also found that His repressed the two nitrogen catabolite repression (NCR) sensitive genes GAP1 and MEP2 in yeast (Lei et al., 2013). NCR is the mechanism adopted by yeast for the preferential N source selection by preventing the uptake of poorer N sources when better N sources are available (Magasanik and Kaiser, 2002; Beltran et al., 2004). Recently, it was found that His completely inhibited the growth of flor yeast, a strain generally metabolized amino acids and dipeptides as the sole nitrogen source (Bou Zeidan et al., 2014).

A number of studies discussed the negative N balance in animals, including humans when His is omitted from the diet (Heger et al., 2007).

The results presented here also provide a new insight on the use of alternate sources of N for Arabidopsis. The result patently challenged the concept of using some free AA as a source of N nutrient as suggested in multiple reports (Chapin et al., 1993; Schmidt and Stewart, 1999; Nasholm et al., 2000; Kielland et al., 2006). The conflicting results with the present study could be because of the different research focus or species, as those studies were on uptake of free AA as N sources by different forest and agricultural species. Our results explicitly indicated the preferential choice of Arabidopsis as N sources are NO_3^- followed by Gln, Asn, NH_4^+ and Glu, respectively.

3.6 Functionally active PDR1/ATP-PRT1 and ATP-PRT2 most likely have distinct functionality *in planta*

ATP-PRT2 is a closely related to PDR1/ATP-PRT1 and both proteins share 74.6% amino acid identity. Both recombinant proteins are biochemically active as demonstrated by expression of Arabidopsis *ATP-PRT* cDNAs in the *his1 S. cerevisiae* mutant, which are able to suppress the His auxotrophy (Ohta et al., 2000). Overexpression of *ATP-PRT2* cDNA under the CaMV 35S promoter in *pdr1* showed complete rescue of the *pdr1* short root phenotype as did the overexpression of *ATP-PRT1* (Fig. 2-11C), which confirms the functionality of both isoforms in *planta* for the first time. In spite of the presence of *ATP-PRT2*, why does the EMS-induced leaky mutation of *pdr1* shows a severe root phenotype and its knock-down allele *pdr1-2* even showed more exacerbated root growth defect (Fig. 2-12A)? More interestingly, the knock-out allele *pdr1-3* was found to be seedling lethal and never reached maturity beyond the vegetative stage to flower (Fig. 2-17). The reason could be the distinct physiological role played by these redundant genes. No visible phenotype of the second redundant *atp-prt2* knockout allele from the study of Muralla et al., (2007) supports the notion of its distinct functionality. Furthermore, the authors also showed 10-fold less expression of *ATP-PRT2* than its sister isoform, *ATP-PRT1* in the root of Arabidopsis (Muralla et al., 2007). Thus, it could also likely be that the distinct expression patterns of both isoforms need to be investigated. The development of T2 homozygous *ProPRT2:GUS/GFP* is in progress to validate this notion.

3.7 The root, but not the shoot of *pdr1* is sensitive to high N and low Pi and the sensitivity is age dependent

The data displayed here showed no significant difference of the fresh weight of the aerial part between WT and *pdr1* (Fig 2-22A). By contrast, the fresh weight of *pdr1* root was found to be significantly less than that of WT in both high NO_3^- and low Pi growth conditions (Fig. 2-22B). An analogous situation with reference to the association of root, but not shoot developmental effect with His starvation was also revealed by Mo et al., (2006) in their study of *His6a* mutants (*hpa*). Conversely, 3 μM His feeding the media could equivalent the fresh weight of *pdr1* root to that of WT (Fig. 28B). Paralleling observation by Mo et al. (2006), the relative dependency of the *pdr1* root was also found to be age related (Fig. 2-1).

3.8 The effect of His is local

It is very inquisitive to reconnoiter why specifically root growth is sensitive to high NO_3^- . No global His starvation in *pdr1* compared to the WT under normal growth condition poses the question as to why it shows a short root phenotype. External His supplement or overexpression of *ATP-PRT1* in *pdr1* rescue the short root phenotype of *pdr1*. One hypothesis could be the mobility of His towards the root tip that could mediate the external NO_3^- use. This proposition was supported by our split-root experiments that have shown that the root tip of *pdr1* required to be in contact with His containing medium to continue the growth irrespective of the presence or absence of His contact with the other part of the seedlings (Fig. 2-26A). This means the effect is the local response of His for which the presence of His in the root tip is mandatory. The expression of *ProATP-PRT1::GUS/GFP* in the vascular tissues (Fig. 2-20) supports the mobility of His but the absence of GUS staining in the PR tips (Fig. 2-20) contradicts the results of local effect, even though we cannot rule out the possibility of the movement of His to the root tip. Of note, the expression was tested only for the *ATP-PRT1* not for the His, that cannot support us to conclude its absence in the root tip. Additional support is the presence of His in the sap and xylem indicating it as a mobile component (Frommer et al., 1995; Lohaus and Moellers, 2000). His content in the roots and leaves of *pdr1* under normal growth condition showed no significant difference from the WT while under a Pi starvation condition only *pdr1* root had five-fold less His than that of WT. This

could suggest the predominant site of His synthesis is the leaf from where it moves towards the root and thus, mediate the root growth in response to high N and low Pi.

3.9 Crosstalk between Pi and N

Three important observations came out from the study of *pdr1* mutant; it is hypersensitive to high N, hypersensitive to low Pi (obvious under low NO_3^- condition) or DNA containing low Pi medium, and external His is required to restore the N- and Pi-related root growth phenotype. This indicates the existence of complex layers of interplay between Pi and N, His and N, and His and Pi. However, such phenomenon has not been studied extensively. Recently, Kant et al. (2011) proposed a model based on their results that NO_3^- inhibits the Pi uptake by the roots, thus more Pi is taken up under low external NO_3^- condition. However, two other nutrient components, S and Fe that are also known to alter the root architecture in Arabidopsis (Giehl et al., 2014; Müller et al., 2015) have shown to have no additional deficient effect on *pdr1* as found by Delatorre (PhD thesis, 2002).

3.10 Does His act as a “hormone”?

A very low concentration of His in the growth medium makes a huge difference in the root growth of *pdr1* that could elicit the question whether it is a signaling molecule. The response of plants to 5×10^{-7} M of exogenous His application is indeed a mind-blowing (Fig. 2-12A). In addition to roots, the development of callus formation is also inhibited in the *hisn2-1* mutant and His supplements rescued the growth of callus (Muralla et al., 2007). Low concentration stimulates the growth, while high concentration causes extreme developmental aberration mirroring the typical hormone response. The complete knockout of His biosynthetic genes resulted in embryo or seedling lethal (Mo et al., 2006; Fig. 34), while the knock-down allele, *prt1-2*, of the biosynthetic genes showed a dwarf phenotype in the soil. The complete blockage of His causes embryo lethal as demonstrated by herbicide triazole application and blocking the key biosynthetic enzymes (Guyer et al., 1995; Mori et al., 1995). This is also evident from the seedling-lethality of the *prt1-3* knock-out allele (Salk_152420) as shown in Figure 2-17, indicating His is vital for the plant survival. The early requirement of His is more important than the later part of the plant life as displayed by the *pdr1* mutant. Mo et al., (2006) also concluded the age dependent requirement of His for the *hpa*, a weak mutant allele of His6a. Our results clearly showed that His modulate the cell division and cell elongation (Fig. 2-24) and elicited wide arrays of responds to low Pi and high N in the growth medium. His is a mobile component as found in the sap and xylem (Frommer et al., 1995; Lohaus and

Moellers, 2000) that can be transported to various organs. The activation *ProATP-PRTI::GUS/GFP* in the vascular tissues of root and shoot of our experiment also support it. Like other hormone functions to increase the tolerance of metal stress, His also does the same (Ingle et al., 2005). All those characteristics resemble the typical plant growth hormone functions. Moreover, the evidences have been mounted over the years regarding the multiple roles of His in the life science that support the same notion of hormone like activity. For instance, Parkash and Asotra (2011) demonstrated the modulation of glucose-induced insulin secretion by histidine-induced activation of calcium sensing receptor (CaR) through an increased spatial interaction between CaR and VDCC in β -cells. The regulatory role of His has also recently been reported in the work of Sun et al., (2014) revealing the alleviation of inflammation in the adipose tissue of high-fat diet-induced obese rats by L-His via the NF- κ B- and PPAR γ -involved pathways. The physiological study of Sasahara et al., (2015) revealed more fascinating result of His mediated mental fatigue and cognitive performance in human as found the daily ingestion improved the clear thinking and attentiveness and ameliorates the exhaustion of the subjects. The study of Natarajan et al., (2001) revealed that most of the His starvation affected genes in the yeast are known to be mediated by DNA-binding factor Gcn4p. The foregoing results and discussion supports the notion of the regulatory function of His, it may be possible to contemplate that Histidine is a novel plant hormone vital for the growth and development.

CHAPTER 3

A pdr2 Suppressor Screen Identifies LOW PHOSPHATE ROOT 1 (LPR1) and ALUMINUM-ACTIVATED MALATE TRANSPORTER 1 (ALMT1)

ABSTRACT

The *phosphate deficiency response 2* (*pdr2*) mutant, which is hypersensitive to low Pi, was subjected to further chemical mutagenesis to identify the potential extragenic suppressor mutations. The screens resulted in the isolation of 11 suppressors of which 5 were found to be allelic to *LPR1* (*LOW PHOSPHATE ROOT 1*) and one, called R01A1, to *ALMT1* (*ALUMINUM-ACTIVATED MALATE TRANSPORTER 1*). The second-site mutation of *pdr2* in the *ALMT1* locus reverts the Pi-conditional short root phenotype of *pdr2* likely via restoring of root cell elongation. A T-DNA insertion knock-out mutant of *ALMT1* confers insensitivity of root growth inhibition to low Pi conditions. Further characterization of the R01A1 suppressor and the T-DNA knock-out line of *ALMT1* provided evidence Fe-dependent root growth inhibition in low Pi. Identification of *ALMT1*, a major Al⁺³ tolerance gene in plants, reveals a novel link between Pi starvation responses and metal homeostasis in plants.

1. INTRODUCTION

Plant development from germination to maturity in a nutritionally challenged environment is a major challenge, which is met by the plasticity of the root system architecture (RSA) to efficiently explore the soil and exploit its mineral nutrients. Thus, RSA modification has been considered as a typical indicator of plant acclimatization and nutritional stress (Forde and Lorenzo, 2001; Lopez-Bucio et al., 2003; Malamy, 2005; Osmont et al., 2007) and its underlying genetic control is of high interest to dissect the adaptive mechanisms at the molecular level (Abel, 2011; Giehl et al., 2014). Several studies showed nutrient availability in the soil as a cue for their RSA adaptation by inducing molecular and morphological changes that modify root cell division and differentiation for distinct physiological functions (Ticconi et al., 2004; Svistoonoff et al., 2007; Ticconi et al., 2009; Müller et al., 2015). The split-root experiments by exposing half of PR roots to high Pi and other half to low Pi revealed attenuation of primary root (PR) and enhanced phosphatase activity as soon as they come in contact with the low Pi concentration containing compartment (Linkohr et al., 2002; Zhang et al., 2014). It was shown that physical contact of the root with the low Pi is necessary to activate the response machinery in plants, even though the shoot and the upper part of the root remains in contact with high Pi. This indicates that the possible Pi sensing site is located in the root tip. Despite of numerous studies on RSA modulation by external phosphate supply independent of internal Pi concentration (Bates and Lynch, 1996; Lopez-Bucio et al., 2003), how does the root tip sense the external Pi remained a paradox until the pioneering molecular insight into the Pi sensing by the root tip has been revealed by the isolation of *PHOSPHATE DEFICIENCY RESPONSE 2 (PDR2)*. Indeed, the major breakthrough in local Pi sensing was the identification of *PDR2* and its interactor *LPR1* and *LPR2 (LOW PHOSPHATE ROOT 1/2)* (Ticconi et al., 2004; Svistoonoff et al., 2007; Ticconi et al., 2009). The *PDR2* gene encodes the single P5-type ATPase (AtP5A) in Arabidopsis and the *pdr2* mutant is hypersensitive to low Pi showing a very short PR growth, which is conditionally low Pi specific because under +Pi or +Phi (phosphite, a reduced, non-metabolized analog of Pi) it shows normal root growth like WT.

The fate of PR root growth relies on the quiescent center (QC) which is required to maintain stem cell status of its adjoining undifferentiated cells (initials) and descendent of these initials that ultimately determine the length of the root by undergoing cell division, elongation and

differentiation. *PDR2* is required for the maintenance of stem cells as demonstrated by the rapid loss of QC (using QC25 and QC184 marker), decrease of *ProCycB1;1::GUS* expression (a marker for cell division), enhanced activity of *ProACP5::GUS* (a marker for Pi starvation and cell differentiation) and formation of amyloplast in the layer of columella initials of *pdr2* mutant under Pi starvation (Ticconi et al., 2009). Furthermore, it was shown by the same authors that *PDR2* is required for the post-translational expression of SCARECROW (*SCR*) a key regulator of root patterning, and for stem-cell maintenance in Pi-deprived roots. This provides an evidence of its function as to maintain and fine-tune meristematic activity by monitoring the external Pi status and finally shaping RSA (Ticconi et al., 2004; Ticconi et al., 2009).

In contrast to the *pdr2* mutant phenotype, disruption of the function of *LPR1* displays an insensitive root growth phenotype on low Pi, which was identified from a recombinant inbred lines of accessions, Bay and Sha accession of Arabidopsis (Svistoonoff et al., 2007). *LPR1* and its paralogue *LPR2* encode multicopper oxidases (Svistoonoff et al., 2007; Ticconi et al., 2009). A further study showed the localization of *PDR2* and *LPR1* in the endoplasmic reticulum (ER) and the expression domain of them overlap in the root meristematic region (Ticconi et al., 2009). The authors also showed the suppression of hypersensitive *pdr2* root phenotype by insensitive *lpr* mutant by demonstrating the longer PR growth of triple mutants *pdr2lpr1lpr2* than that of WT under Pi-deficient conditions that provides an evidence of a strong genetic interaction between them. The recent study of Muller et al. (2015) elucidated the mechanism of such interaction between *LPR1* and *PDR2*. The authors showed that the *LPR1-PDR2* module mediates cell-specific Fe deposition in cell walls of the root apical meristem and elongation zone during Pi limitation by displaying the contrasting pattern of Fe accumulation in WT, *pdr2* and *pdr2lpr1lpr2* triple mutants. It was shown earlier that external Fe availability in the growth medium modified the Pi-dependent root growth responses (Svistoonoff et al., 2007; Ward et al., 2008; Ticconi et al., 2009). Fe overloading in the Pi deficient roots trigger the accumulation of callose that overlaps the site of Fe accumulation which block the plasmodesmata based cell-to-cell communication and SCN maintenance as revealed by the restricted SHORT-ROOT (*SHR*) movement in *pdr2* in contrast to double mutant *lpr1lpr2* and WT (Müller et al., 2015). *SHR* is a transcription factor and moves from the stele into the QC and endodermis to determine cell fate, partly by interacting with *SCR* (Nakajima et al., 2001; Sabatini et al., 2003; Cui, 2007). Thus, the authors (Müller et al., 2015) displayed the close interconnection of two key transcription factors *SHR* and *SCR*

required to maintain the root meristem organization both of which are disturbed in *pdr2* mutant due to overaccumulation of Fe that was shown to be relieved by the *lpr1* mutation in the *pdr2* background. In addition to the LPR1/LPR2 and PDR2 interaction, a number of additional genes might also be involved in the upstream or downstream of PDR2 in regulating the adaptive responses via local signaling upon Pi starvation.

To identify and characterize the unknown gene(s), if any, in the PDR2 signaling pathway, we initiated *pdr2* suppressor screening. I confirmed 11 suppressor lines of which one was found to affect the *ALMT1* gene that encodes *ALUMINUM-ACTIVATED MALATE TRANSPORTER 1*. The mutation substituted the Gly by Arg at position 71 of the gene. Five of the suppressor lines were found to be allelic to *LPR1* as would have been expected, while the rest of the five remains to be identified. The *ALMT1* is the new gene in the phosphate field which was well characterized previously for Al^{3+} tolerance (Sasaki et al., 2004; Hoekenga et al., 2006). In Arabidopsis, 14 *ALMT* genes were identified while *ALMT1* plays the dominant role in Al^{3+} tolerance (Delhaize et al., 2007). The proteins of the ALMT family are predicted to have 7-8 transmembrane domains (Delhaize et al., 2007). ALMT enhanced the Al tolerance by secreting the organic anions that protect the roots by chelating the Al^{3+} (Delhaize et al., 2007; Gruber et al., 2010). All the ALMT family members in plants have not been implicated only for Al^{3+} tolerance, for example, the protein of ZmALMT1 from wheat (*Triticum aestivum*) expressed in *Xenopus laevis* oocytes found to be more permeable to inorganic anions such as sulphate and nitrate than to malate or citrate (Pineros et al., 2008). Thus, the authors proposed it to play a role in mineral nutrition. *AtALMT9* was shown to play no role in tolerance of Al^{3+} rather it internally mobilizes the malate from the cytoplasm to the vacuole (Kovermann et al., 2007). In Arabidopsis, other than the ALMT family, MULTI-DRUG AND TOXIN EXTRUSION (MATE) genes also plays role in Al^{3+} tolerance and resistance (Delhaize et al., 2007). *AtMATE*, a homologue of sorghum and barley Al^{3+} -tolerance genes was identified in Arabidopsis encode an Al-ACTIVATED CITRATE TRANSPORTER (Liu et al., 2009). It is expressed primarily in roots and is induced by Al, the knock-down line found to abolish Al-activated root citrate exudation (Liu et al., 2009). The authors also showed the double mutant of *AtALMT1* and *AtMATE* lacked both Al-activated root malate and citrate exudation. *FRD3* (*FERRIC REDUCTASE DEFECTIVE3*) belongs to MATE family also confer Al^{3+} resistance if ectopically overexpressed in Arabidopsis roots (Durrett et al., 2007) which is originally known to play a role in Fe homeostasis (Delhaize and Randall, 1995; Rogers and Guerinot, 2002; Green and Rogers, 2004). *AtALS3* (*Al-SENSITIVE-3*), the loss of function of which

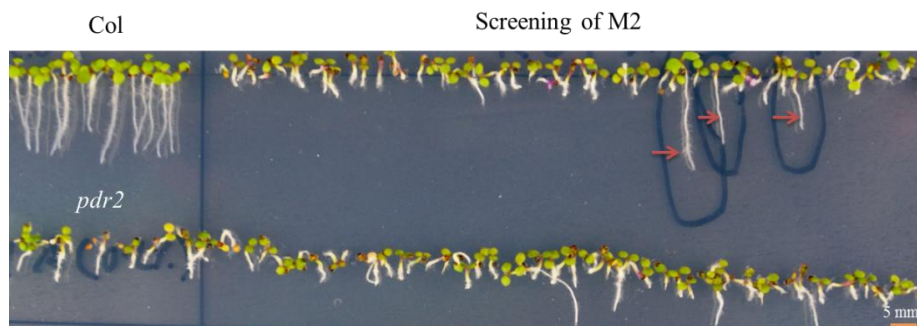
(*als3*) is Al^{3+} -sensitive encodes a plasma membrane-localized ABC transporter expressed primarily in the root cortex, the leaf hydathodes, and the phloem throughout the plant (Larsen et al., 2005). *ALS3* has recently been implicated in playing a role under Pi starvation, the mutant of which showed a severe root growth inhibition and developed more root hairs under phosphate starvation in a sugar dependent manner (Belal et al., 2015). Here I present the novel role of *AtALMT1* in Pi starvation the mutation of which in *pdr2* mutant showed restoration of the PR growth on low Pi. The knock-out allele, *almt1*, surpassed the WT PR length under Pi starvation resembling the *lpr1* mutant growth.

2. RESULTS

2.1 Screening for *pdr2* suppressors

The *pdr2* mutant isolated previously from ethyl methyl sulfonate (EMS) induced mutant population is hypersensitive to low Pi showing very short PR growth (Chen et al., 2000). Identification of the suppressors would have a huge implication in dissecting the pathway of the *pdr2* functioning. Hence, the suppressor screening was carried out by treating *pdr2* seeds with EMS of 0.2% and 0.4% concentration (detailed described in methods). Approximately 30 EMS treated seeds that termed as M1 were sown in each 11x11 cm sized pot and seeds from each pot called one parental group. I screened 200-250 M2 seeds (progeny of M1) of each of the 500 parental groups of 0.2% concentration on $-Pi$ to identify the putative suppressors (Fig. 3-1). The initial screening of M2 resulted in the identification of 136 individual candidates belonging to 92 parental groups and transferred those to the soil for the generation of M3 seeds. Subsequently, genotyping was performed for homozygosity of the mutation of *pdr2* locus to avoid any unexpected contamination. Many of the candidate lines showed false positive in the M3 generation under the $-Pi$ scrutiny, some died in the seedling stage, or did not reach the matured stage to flower when transferred to the soil. Subsequent growth analysis in M3 under $-Pi$ resulted in the identification of 11 confirmed suppressors that were also validated in M4 (Fig. 3-2) and one suppressor R13L2 was dropped from the list due to inconsistent phenotype. The PR growth assays of the 11 suppressors enabled to group them into 2 distinct classes of *lpr1* like or WT like root growth phenotype (Fig 3-2). Suppressor lines R014F4, R017F4, R19J4, R29A1 and R30I2 fell into the former category, while R01A1, R13L3, R23i2, R31A5, and R31J2 fell into the latter category.

Figure 3-1. Screening of EMS mutagenized *pdr2* seeds to identify putative suppressor mutants that develop a long PR on low Pi medium. Shown is the



representative image of an original M2 screen on vertically oriented agar plates containing $-Pi$ medium. Around 200-250 M2 seeds were plated on $-Pi$ agar and after 6 days of germination the putative candidates (shown by red arrows) were transferred to soil. The resulting M3 progeny was tested again for heritability of the revertant root phenotype.

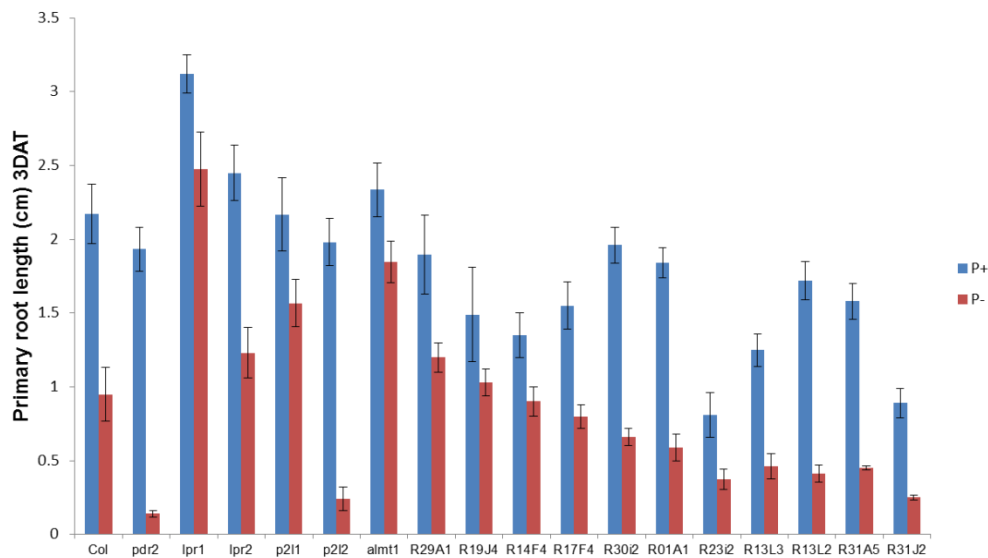


Figure 3-2. The M4 progeny of 12 confirmed suppressors lines (M3) were validated on high and low Pi media. Plants were germinated and grown on +Pi agar for 4 days and were then transferred to -Pi medium. PR growth was determined 3 days after transfer (DAT). Values are the mean \pm SD of 20-30 independent roots.

2.2 Five of the *pdr2* suppressor mutations are allelic to *LPR1*

The loss of *LPR1* function causes insensitivity to low Pi as revealed by longer PR, late differentiation of the meristematic cells, and integrity of QC and SCN on prolonged Pi-starvation condition compared to the WT (Svistoonoff et al., 2007; Ticconi et al., 2009; Müller et al., 2015). The cell wall staining by propodium iodide (PI) of five suppressors, R014F4, R017F4, R19J4, R29A1 and R30I2 under -Pi showed a similar meristem pattern like *lpr1* (Fig 3-2A). Thus, the *LPR1* gene including the promoter from each suppressor line was PCR amplified and compared with the amplified *LPR1* from the *pdr2* mutant. All *LPR1* genes from the suppressors were new *LPR1* alleles (Fig 3-2B). R29A1 and R30I2 were found affecting *LPR1* at exactly the same position 319, substituting Gly to Arg. Two lines, R014F4 and R19J4, induced mutations that caused premature stop codons at amino acid positions 77 and 282, respectively. The remaining suppressor line, R17F4, substituted Ala by Val at position 282. The result is not surprising as the mutant of *LPR1* is known to show contrasting phenotype of *pdr2* and interacts genetically to mediate the RSA in low Pi condition (Svistoonoff et al., 2007; Ticconi et al., 2009; Müller et al., 2015). Thus, the identification of several alleles of *LPR1* validates the genetic interaction of *LPR1* and *PDR2* under Pi starvation.

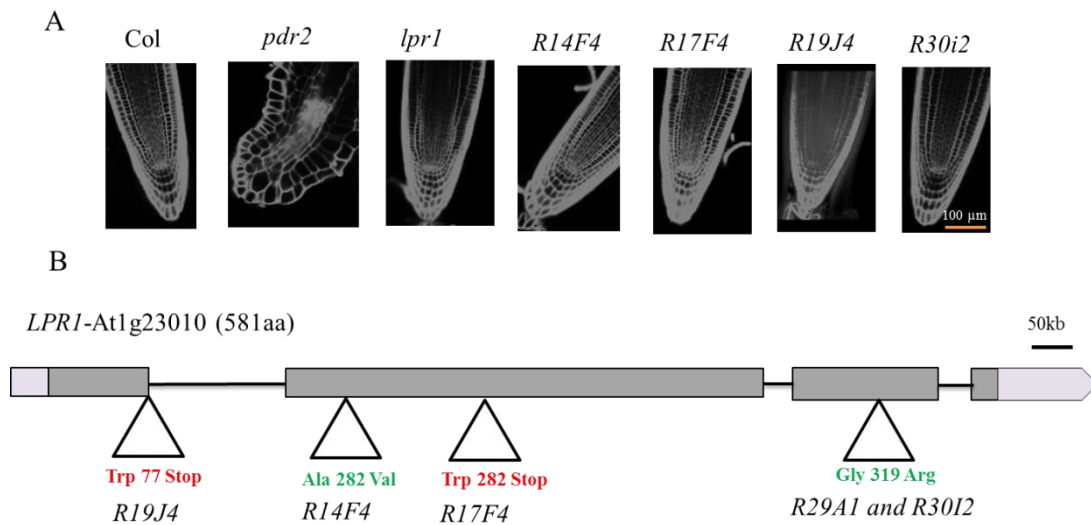


Figure 3-3. Five *pdr2* suppressor lines are allelic to *LPR1*. (A) Propidium iodide (PI) staining of the root meristem of 4 suppressor lines in comparison with WT (Col-0), *lpr1* and *pdr2* roots. Seedlings were grown on a vertically oriented agar plate for 4 days after germination and then transferred to – Pi. Three days after transfer, Pi-starved roots were stained with PI. (B) Schematic representation of the *AtLPR1* gene structure. White boxes represent 5' UTR (left) and 3' UTR (right), gray boxes and black lines represent exon and introns or intergenic regions, respectively. Triangles show the position of the EMS-induced mutations in the five *pdr2* suppressor lines.

2.3 Suppressor line R01A1 carries a mutation in *AtALMT1*

The suppressor line R01A1 was further characterized for root growth by cell biological and histochemical assays. PR growth assays clearly showed the WT-like root growth restoration of the *pdr2* short-root phenotype (Fig. 3-4). However, the PR showed absence or very less lateral roots (LR) and root hair formation even though it possesses numerous root hair bulges (Fig. 3-4D). The mutation in R01A1 was not found to affect any of the *LPR1* or *LPR2* loci. Then, I checked the *AtALMT1* gene considering it as a putative candidate based on the information from Dr. Thierry Desnos (personal communication, CEA Cadarache, DSV DEVM Laboratoire de Biologie du Développement des Plantes, UMR 6191 CNRS-CEA, Aix-Marseille II, F-13108, France) who identified the *almt1* mutant from an EMS population screened in –Pi condition for a *lpr1*-like PR phenotype (unpublished). Sequencing of the PCR amplified *AtALMT1* from line R01A1 revealed a point mutation at the end of the first exon, in AA position 71, which changes the Gly to Arg (Fig. 3-5A). This point mutation was further confirmed by genotyping with dCAPS markers. Aluminum sensitivity tests were done because the *almt1* mutant is known to be hypersensitive to Al^{+3} (Hoekenga et al., 2006). The

results revealed a similar sensitivity of R01A1 and no discernable development of the root after germination was observed like *almt1* (Fig. 3-5B). Furthermore, allelism tests were done by crossing the R01A1 line with the *almt1* knocked-out line (Salk_009629), which revealed that both mutations are allelic (Fig. 3-6). Thus, the *pdr2* suppressor mutation of line R01A1 resides in *AtALMT1* and reverts the *pdr2* root phenotype under Pi-deficient condition.

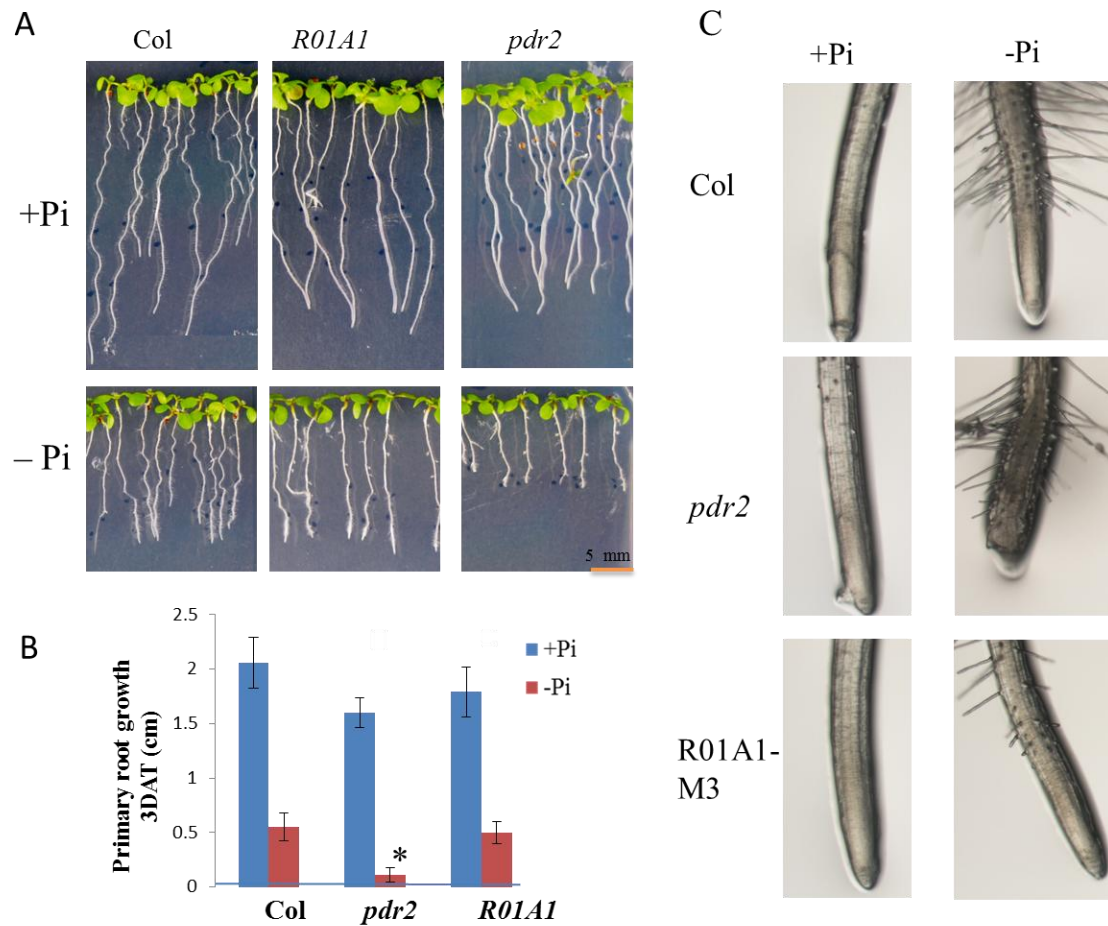


Figure 3-4. The phenotype of the suppressor line R01A1 (M3 generation) on -Pi medium. Shown are (A) representative image of the seedlings grown on +Pi and -Pi. (B) PR growth statistics. (D) Root tip images showing the reduced root hair formation of line R01A1 under -Pi growth conditions. The seeds were germinated and grown on the vertically oriented agar plates containing +Pi for 4 days and transferred to +Pi and -Pi medium for growing another 3 days for growth assays and 2 days for taking the images of root tips under stereo microscope. Values are the mean \pm SD of 20 independent roots. *, difference of *pdr2* and R01A1 from the WT was significant by t-test ($P < 0.05$).

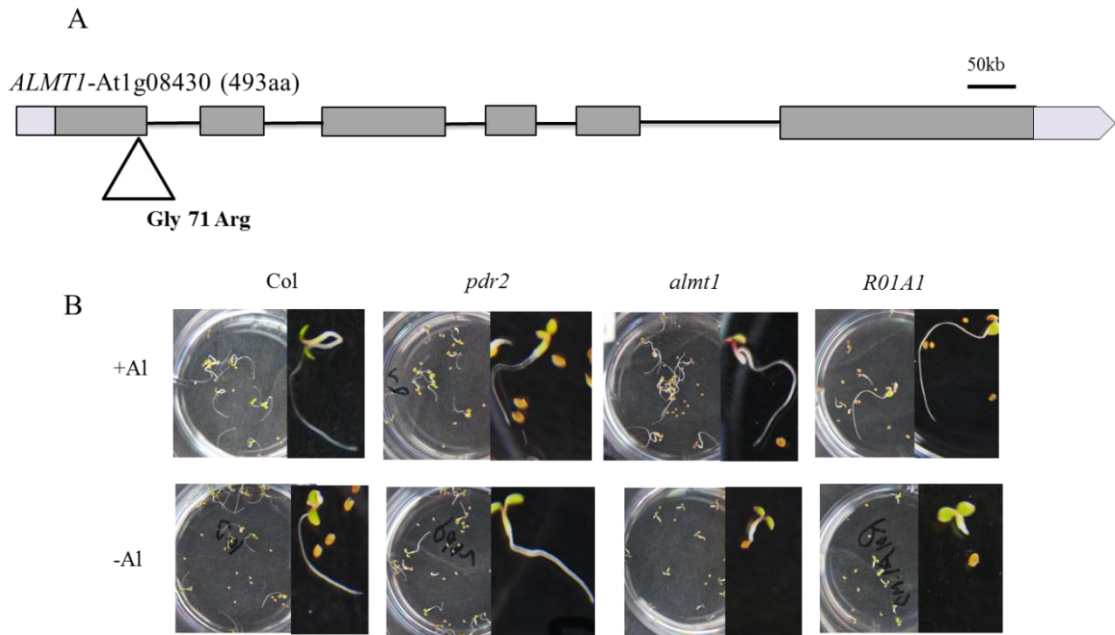
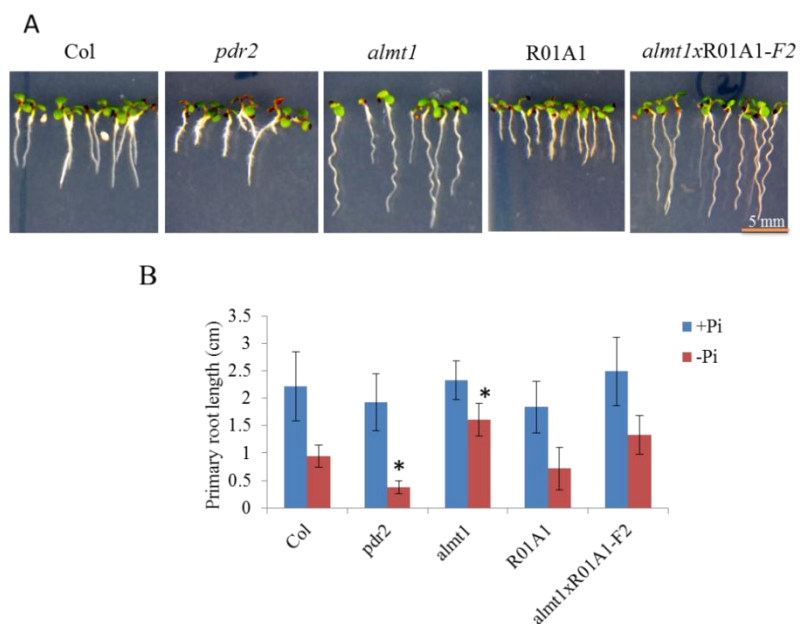


Figure 3-5. The *pdr2* suppressor mutation in line R01A1 is allelic to *AtALMT1*. (A) Schematic representation of the *AtALMT1* gene structure (white boxes represent 5'UTR and 3'UTR, gray boxes and black lines represent exon and introns regions respectively). The triangular mark shows the position of the EMS induced mutation that replaced Gly for Arg at position 71 of the ALMT1 protein (B) Al^{+3} sensitivity test of WT, R01A1, *pdr2* and *almt1* seedlings grown on 10 μM $AlCl_3$ supplemented liquid culture for 4 days after germination.

Figure 3-6. Allelism test to verify that the mutation of the *pdr2* suppressor line R01A1 is in *ALMT1*. The R01A1 line was crossed with the *almt1* mutant plant and F2 seeds were germinated and grown on +Pi and -Pi medium along with WT (Col-0), *pdr2*, and *almt1*. Shown are (A) representative images of the seedlings and (B) root



growth statistics. Values are the mean \pm SD of 15 independent roots. *, difference between the WT and other genotypes was significant by t-test ($P < 0.05$).

2.4 Genetic analysis confirmed the *almt1* mutation in R01A1 as recessive

R01A1 was back crossed with *pdr2* to determine the mode of inheritance. All the resultant F1 progeny under Pi-deficient medium showed the short root phenotype, because both of the genotypes carry the homozygous *pdr2* mutation. The subsequent inbred F2 progenies were tested on –Pi and the phenotype was scored for the long and sort root (Fig. 3-7). Of the total 227F2 plants, 169 showed *pdr2* like phenotype and 58 showed a long root phenotype (Fig. 3-7B) that represents the segregation ratio of 2.9:1 ~3:1. The chi square statistics showed the ratio of segregation was not statistically deviant from the Mendelian trait of inheritance, 3:1 (χ^2 value 0.378, P value 0.53<0.05) suggested the mutation is a single recessive allele.

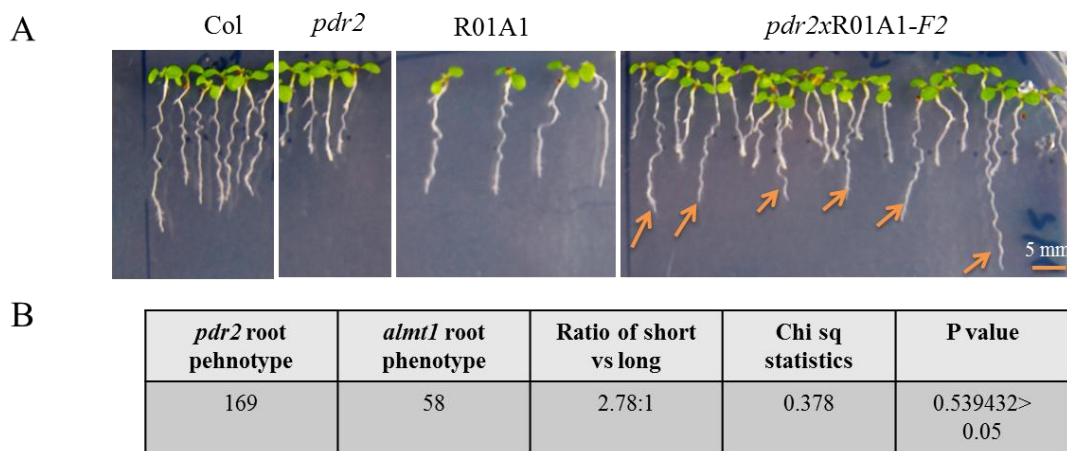


Figure 3-7. The mutation in R01A1 segregates as a single recessive allele. Line R01A1 was back crossed with *pdr2* to determine the mode of inheritance. (A) Representative images of seedlings of the crosses (F2) along with WT (Col-0), *pdr2*, and R01A1 grown for 4 days on +Pi and then transferred to –Pi medium. Following 3 days of starvation, the phenotype was scored; the analysis is shown in (B). The arrows indicate the long roots due to the mutation in the suppressor locus (*AtALMT1*). The chi square value shows the ratio of segregation is not statistically deviant from the Mendelian trait of inheritance.

2.5 The mutation in *AtALMT1* in *pdr2* restores the meristematic function of *pdr2*

The shorter PR length of *pdr2* is restored in R01A1 under Pi limiting growth conditions (Fig. 3-4). Given that root elongation rates are controlled through cell division and cell expansion (Beemster and Baskin, 1998; Petricka et al., 2012b; De Vos et al., 2014; Müller et al., 2015), I interrogate how the suppressor *almt1* affects this growth in *pdr2* and which cell growth process serves as the primary target. Therefore, I measured the length of meristem size and

elongation zone as well as count the number of those cells of a single trichoblast cell-file of the 3 days Pi-starved roots that were transferred from the +Pi after 4 days of germination (Fig. 3-8). I observed the second mutation of *pdr2* in the *almt1* locus prevent the impeded growth of *pdr2* and conferred the increased meristematic activity (Fig. 3-8A). The meristem size of *pdr2* which was five-fold shorter (50 μm) than that of the WT (250 μm) was found to be restored in the R01A1 line under Pi starvation. Likewise, the reduced length of the elongation zone (85%) in *pdr2* compared to the WT was also increased significantly in R01A1, but compared to WT, it was significantly shorter (Fig. 3-8). Comparatively shorter elongation zone and less number of elongated cells in R01A1 in contrast to WT as well as equivalent length and number of meristem size and cells suggest the target of the suppressor *almt1* is the restoration of meristem activity. To validate it, meristematic activity was then evaluated by histochemical staining of *ProCycB1::GUS*. The GUS staining of the R01A1 seedlings grown on -Pi condition after transfer of 3 days from the +Pi grown plate showed exactly similar pattern of staining like WT roots suggesting the rescue of the cell division of *pdr2* (Fig. 3-9). The meristematic activity of *pdr2* was reported to be completely blocked after 2-3 days of Pi starvation as documented by the *ProCycB1::GUS* activity and the expression of QC25 (Ticconi et al., 2004) which is very consistent with the present study of *ProCycB1::GUS* in *pdr2* in my experimental condition (Fig. 3-9). To further look into the meristem organization, I stained 1-3 days Pi-starved roots of Col-0, *pdr2* and R01A1 with PI after transfer 4 days old seedlings from the +Pi. Consistent with the earlier argument, the complete disturbances of the root meristem evident from the early differentiation after 1 day (visible from root hair bulges indicated by white arrow) and disturbance of the QC (highlighted by the red circle) after 2 days of transfer to -Pi was also observed in the *pdr2* root in my experiment (Fig. 3-10). In contrast to *pdr2*, the PI staining of R01A1 PR showed opposite pattern, characterized by late differentiation, however, compared to WT, the QC region in the mutant showed higher staining (Fig. 3-10). This poses a question whether the meristem of R01A1 is fully restored or not.

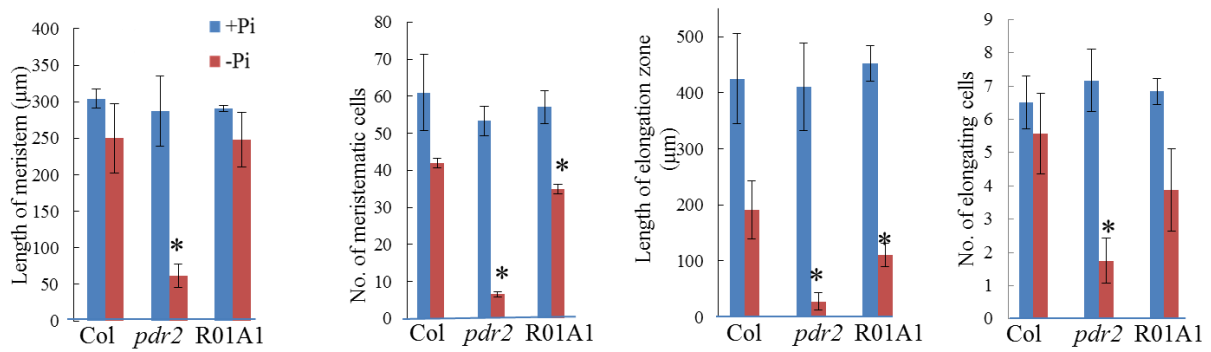


Figure 3-8. Cell biological characterization of WT, *pdr2* and R01A1 PR tip. The number and length of meristematic and elongating cells were counted and measured, respectively from a single trichoblast-cell file of the 3 days Pi-starved roots that were transferred from +Pi after 4 days of germination. Values are the mean \pm SD of 7 independent roots. *, difference of *pdr2* and R01A1 from the WT was significant by t-test ($P < 0.05$).

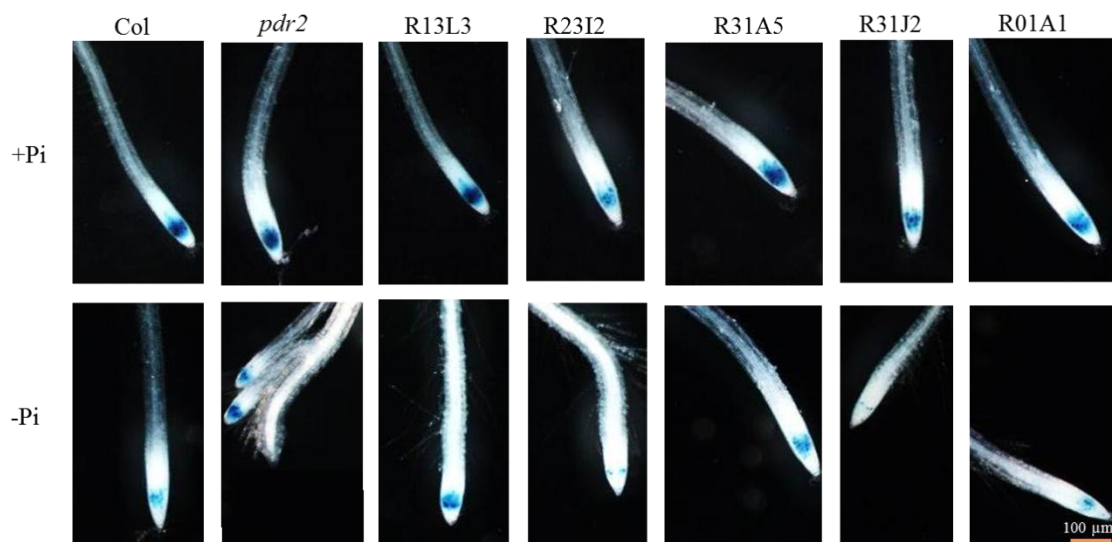


Figure 3-9. The *ProCycB1::GUS* expression in the PR of the five suppressor lines. Plants were grown on the vertically oriented agar plate containing +Pi for 4 days after germination and then transferred to -Pi. GUS staining was performed 3 days after transfer to -Pi.

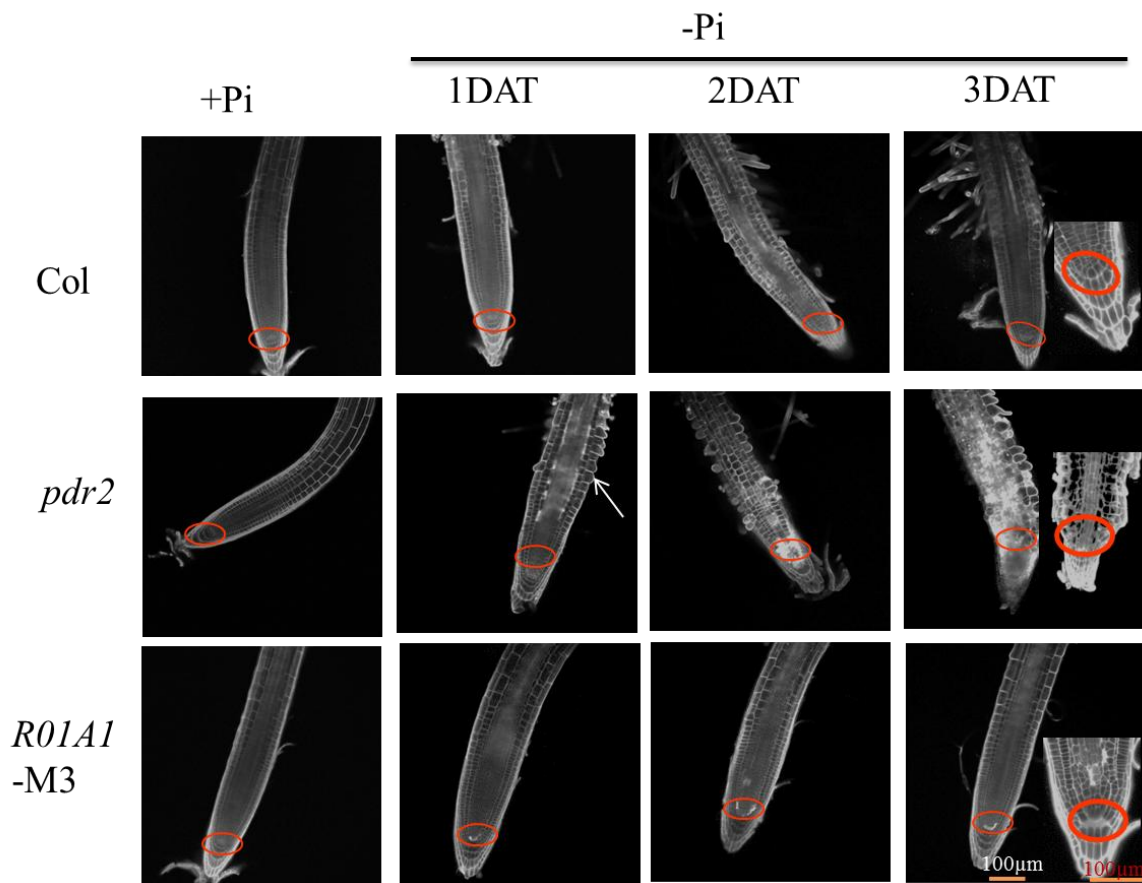


Figure 3-10. Cell viability test of line R01A1 by propidium iodide (PI) staining. Seedlings of WT (Col-0), *pdr2* and R01A1 were grown on +Pi 4 days after germination and then transferred to +Pi or – Pi medium. 1-3 days of Pi-starved and +Pi roots were stained with PI staining solution as described in the method section, red circles show the site of QC along with stem-cell niche (SCN) and white arrow indicates the root hair bulges.

2.6 The mutation in *AtALMT1* in *pdr2* drives away iron accumulation of *pdr2*

The antagonistic interactions of Pi and Fe availability in the growth medium were proposed to control the root growth under Pi starvation (Abel, 2011; Müller et al., 2015). Thus, it was intriguing to see the effect of the second mutation of *pdr2* in *AtALMT1* could prevent the *pdr2*

from overloading of Fe. For this, I stained the roots following 1, 2 and 3 days of Pi starvation that were transferred from +Pi after 4 days of germination by Perls/diaminobenzidine (DAB) staining solution according to the method described by Müller et al., (2015). The Perls/DAB histochemical solutions are able to stain the labile (non-heme) Fe^{3+} and some Fe^{2+} (Meguro et al., 2007; Roschztardt et al., 2009). For +Pi grown seedlings, no accumulation of Fe was observed for any of the three genotypes (Fig. 3-11). As was earlier reported for *pdr2* (Müller et al., 2015), I also found the similar staining pattern of *pdr2* that extended from the root tip to the whole matured part of the Pi-starved root (Fig. 3-11). Intensity of staining was several magnitudes higher in *pdr2* than the WT control and it increased with the increasing of the day of starvation as can be visualized from images over the three days of starvation (Fig. 3-11). By contrast, the suppressor line *ROI1A1* showed complete opposite intensity and pattern of Fe distribution in the root, only observed in the root tip including QC region and in the differentiation zone after 3 days of starvation. Though the intensity of Fe accumulation found to be less in *ROI1A1* than the Col-0, the presence of staining at the root tip including the QC even at the earlier starvation time point necessitate the closer look of the QC. It could be that QC of *pdr2* is not rescued fully in the suppressor line, rather the longer root resulted from the elongation of the previously dividing cells or the meristematic cell division remained active for some days upon exposed to low Pi .

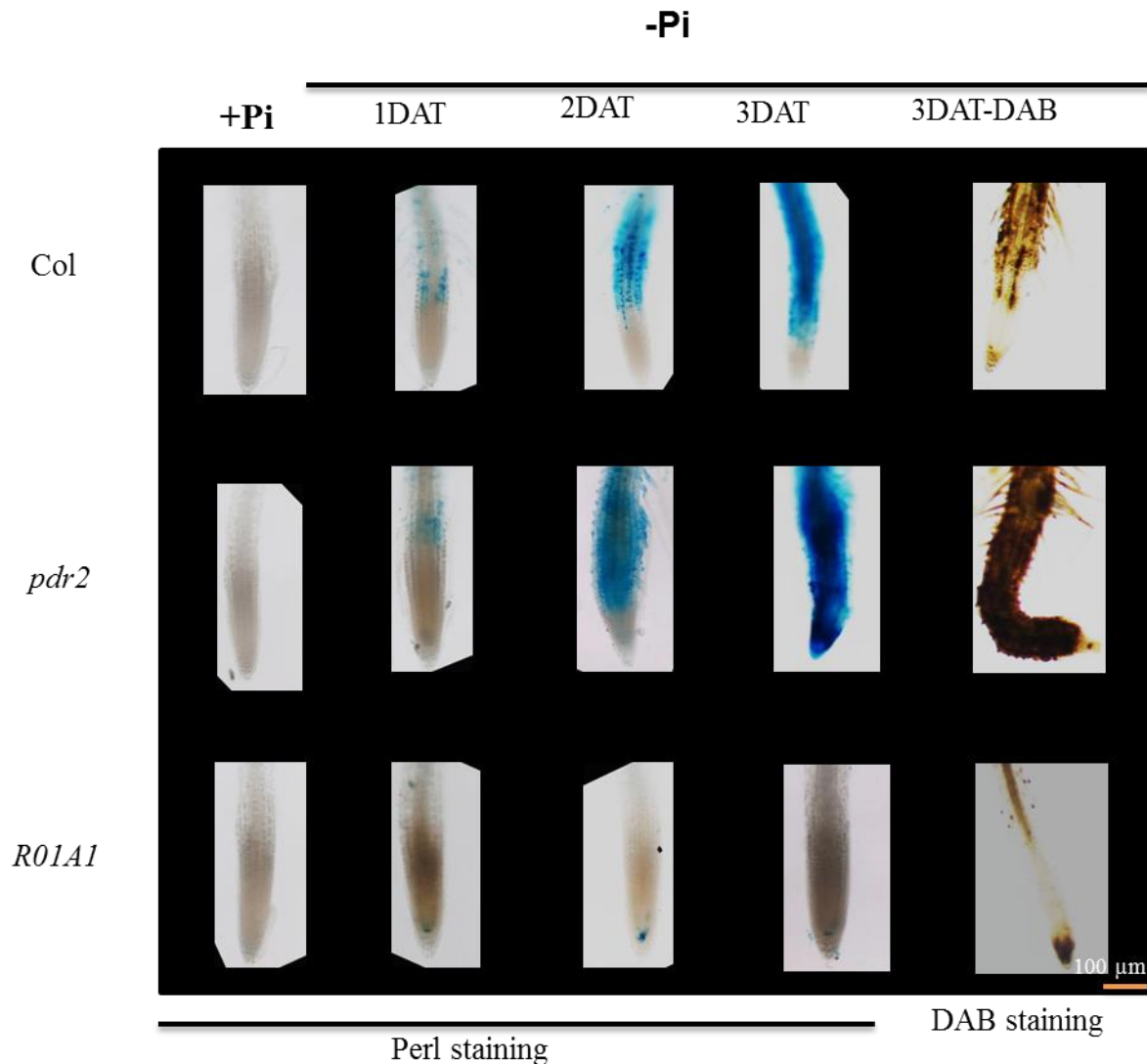


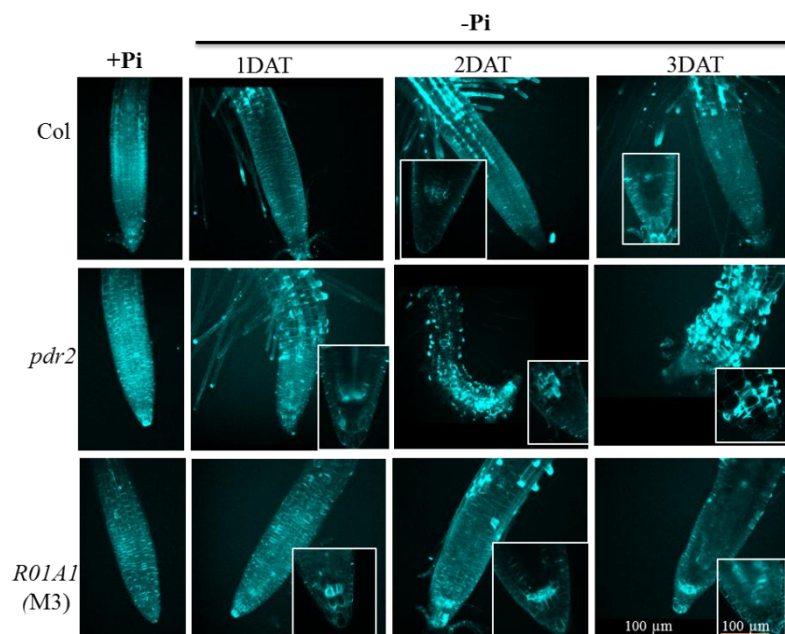
Figure 3-11. Iron accumulation and distribution in line R01A1 as visualized by Perl and DAB staining. Seedlings of WT (Col-0), *pdr2* and line R01A1 were germinated and grown for 4 days on +Pi medium and were then transferred to +Pi or -Pi medium. After transfer for 1-3 days, roots were stained with an iron staining solution.

2.7 The mutation in *AtALMT1* of *pdr2* prevents root callose accumulation

The implication of callose (β -1,3 glucan) in regulating the root growth and development has been investigated recently (Zavaliev et al., 2011; Benitez-Alfonso et al., 2013). The severe disturbance of *pdr2* meristem under Pi starvation is the consequence of the overloading of Fe in the meristematic zone that triggers the accumulation of callose as demonstrated by Müller et al. (2015). The authors also demonstrated the site of Fe accumulation overlapped the callose accumulation in *pdr2* that interfere the cell-to-cell communication as found reduced

movement of a reporter *GFP* gene under control of the companion cell-specific gene promoter *SUCROSE-H⁺ SYMPORTER 2 (ProSUC2)*. Thus, I also checked if the pattern and distribution of callose shifts in the R01A1 compared to the *pdr2* and Col-0. Histochemical staining of the Pi starved roots by aniline blue showed the mutation in *ALMT1* of *pdr2* indeed drove the callose accumulation from the meristematic zone resembling the Col-0 control root (Fig. 3-12). However, the accumulation of callose in the SCN of the suppressor line was not found to be the exception from the *pdr2* mutant (Fig. 3-12). In the same SCN, Fe was also accumulated that raise the question if the QC of the suppressor is viable or not. Further research using the QC marker is necessary to confirm this notion.

Figure 3-12. Accumulation and distribution of callose in line R01A1 was tested by aniline blue staining. Seedlings of WT (Col-0), *pdr2* and line R01A1 were germinated and grown four days on +Pi since germination and were then transferred to +Pi and -Pi. After 1-3 days, roots were stained with callose staining solution as described in the method section. The closer look of callose accumulation is shown in the inset.



2.8 The *almt1* mutant is insensitive to low Pi

The T-DNA insertion knock-out allele of *ALMT1* was further tested for PR growth assay, cell wall viability as well as Fe and callose accumulation in the root tip of +Pi and -Pi grown seedlings. The PR growth of *almt1* mutant on +Pi condition showed no difference with the WT, however, it excelled the PR length more than twofold than the WT under Pi limiting growth conditions (Fig. 3-13). PI staining of the root tip showed the similar staining pattern like the WT in the QC and SCN region, which was sharply in contrast to the *pdr2* mutant under -Pi condition (Fig. 3-13). A similar observation was also found for the Fe and callose

accumulation in the root tip of the *almt1* mutant. Moreover, absence of Fe staining in the transition zone in *almt1* and less Fe in the matured part of the root compared to the WT (Fig. 3-13) could be the explanation of its insensitivity under –Pi growth condition.

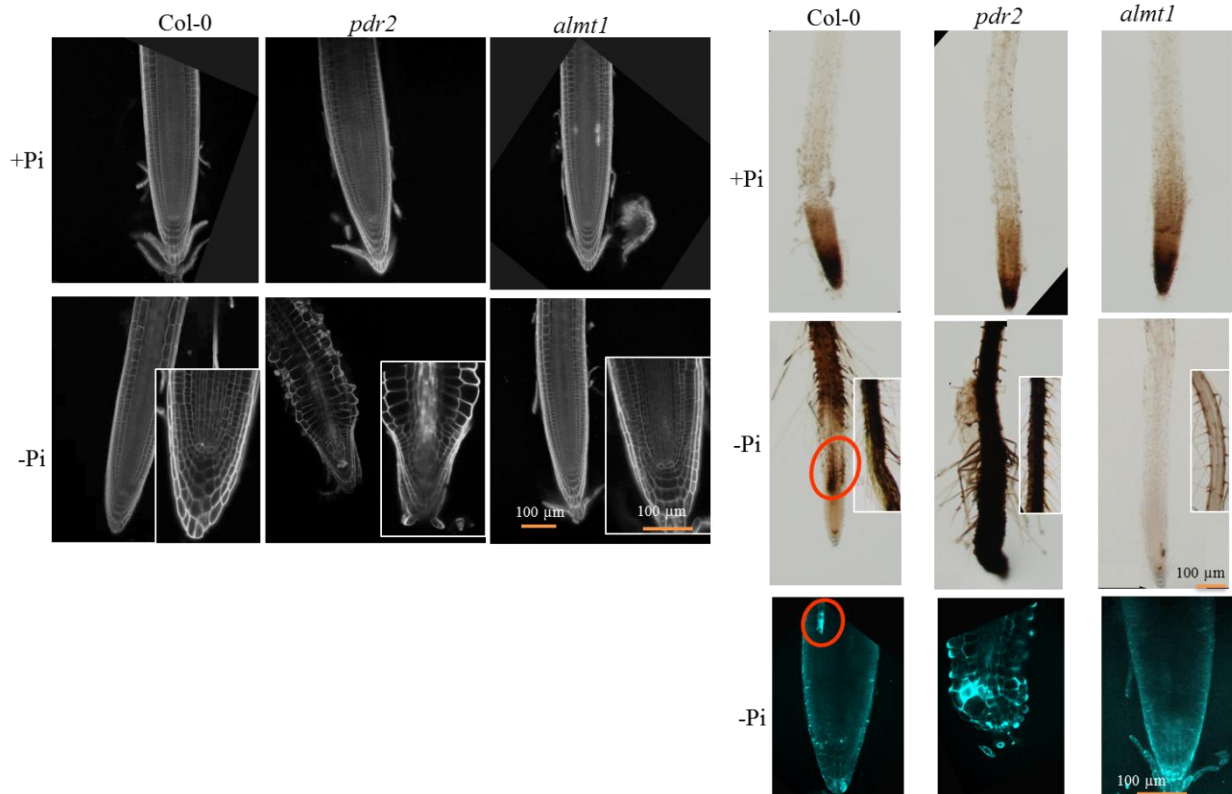


Figure 3-13. Root meristem characterization of the *almt1* knock-out allele compared with WT (Col-0) and *pdr2* under Pi starvation. Plants were grown 4 days on +Pi medium prior to transfer +Pi and –Pi medium. Three days after transfer root tips were stained with PI for cell viability (A), with Perl and DAB for Fe accumulation (B), and with aniline blue for callose accumulation and distribution (C). Red circle indicates the transition zone of WT with accumulation of Fe and callose. The corresponding zone in *almt1* is marked by the absence of Fe and callose.

2.9 The loci of the four suppressor lines are yet to be identified

The four suppressors R13L3, R23I2, R31A5, and R31J2 were further characterized for physiological and histochemical assay under Pi starvation condition compared to the *Col-0* and *pdr2*. The PR growth assays after transfer to the low Pi from +Pi showed R13L3 and R31A5 were mostly like WT while the other two lines R23I2 and R31J2 showed shorter than the WT, but longer than the *pdr2* (Fig. 3-2). The *ProCycB1::GUS* activity of R13L3 and R31A5 under 3 days of Pi starvation condition was found to be WT like (Fig. 3-9). On the contrary, R23I2 and R31J2 showed very less GUS activity following the 3 days of Pi

starvation compared to the WT (Fig. 3-9). The *pdr2* mutant on the identical starvation condition after 3 days lost the GUS staining completely (Fig. 3-9). However, Cell wall staining of the PR meristem by PI showed all the four suppressor lines were disturbed (Fig. 3-14A). The accumulation of Fe and callose in the PR tips also showed similar in R23I2 and R31J2 and lower in R13L3 and R31A5 compared to the *pdr2* (Fig. 3-14A).

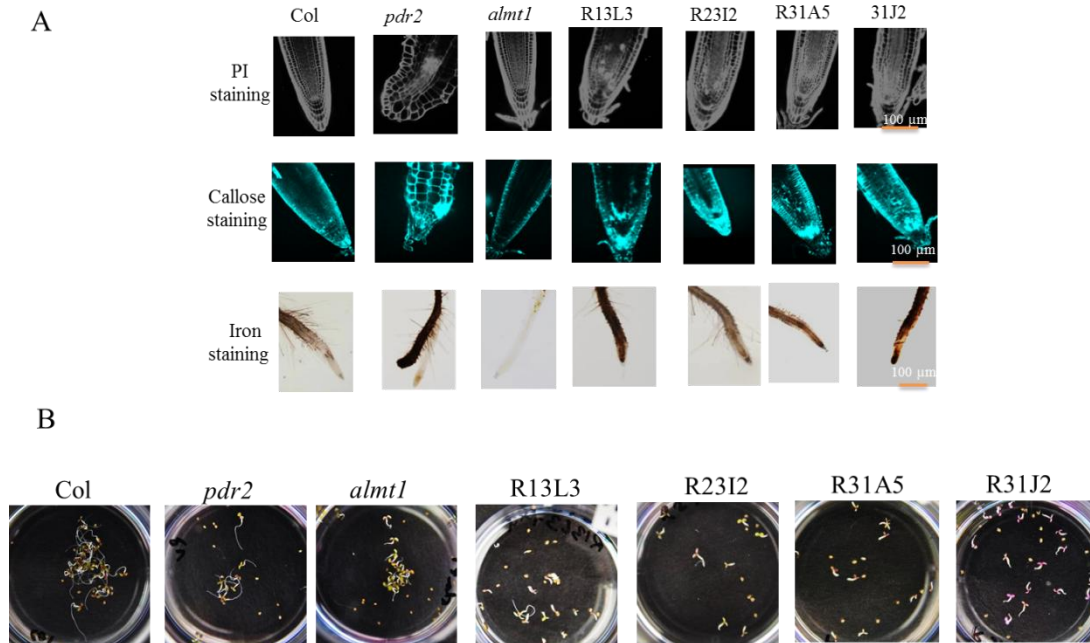


Figure 3-14. Characteristics of four suppressor lines (M3) the loci of whose remain to be deciphered. The images show PI staining (upper panel), Callose staining (middle panel) and Iron staining (bottom panel) in (A) and Al^{+3} sensitivity in (B). For staining, seedlings were grown on +Pi four days after germination and then transferred to -Pi. 3 days after transfer, Pi-starved roots were stained with a respective staining solution as described in the method section. For Al^{+3} sensitivity test, the seeds were germinated and grown for 4 days in the hydroponic culture containing 10 μM $AlCl_3$.

Furthermore, I also tested the sensitivity of those mutants in 10 μM Al^{+3} in the hydroponic culture that showed the hypersensitivity of all the four lines resembling the sensitiveness of *almt1* mutant (Fig. 3-14B). *ALMT1* sequence remained to be analyzed to see whether mutation of those lines affect this locus. However, they are not allelic to *LPR1* as confirmed by the sequencing of the genes and analyzing the F2 generation of the crosses with *LPR1*. *LPR2* locus was also PCR amplified and sequenced, but no mutation was found in this locus for any of the lines.

3. DISCUSSION

The *pdr2* suppressor screening resulted in the identification of 11 lines which were confirmed in the M4 generation based on the PR growth assay on –Pi (Fig. 3-2). All the suppressor lines did not equally restore the short-root phenotype of *pdr2* under Pi limiting condition, some showed insensitivity, some were either WT-like or shorter than WT but longer than the *pdr2*. Subsequent studies showed that 5 suppressors were allelic to *LPR1* and one to *ALMT1*. The genetic interaction of *LPR1* and *PDR2* was discussed earlier (Ticconi et al., 2009; Müller et al., 2015), thus identifying *LPR1* allele in *pdr2* suppressor screening was not a surprise. Rather identification of multiple alleles of this gene validates the functional interaction of the two encoded proteins in fine-tuning the meristem activity under Pi starvation.

The longer root of the R01A1 line when compared to that of *pdr2* on –Pi condition prompted me to study in more detail the rescue effect of R01A1, which is caused by the mutation in *ALMT1*. Therefore, I studied the cellular pattern of root tips of the suppressor line R01A1 by counting the cell number and measuring the length of meristem and elongation zone of trichoblast cell-file to determine which cell growth processes served as the primary target. The equivalent meristem size of the R01A1 PR compared to WT indicated the restoration of meristematic activity of *pdr2* mutant. This is very consistent with the WT-like activity of *ProCycB1::GUS* in the Pi-starved roots of R01A1. Conversely, comparatively shorter length of elongating cells of R01A1 compared to the WT indicated the target of rescue might not be the elongation zone. This result was in contrast to the intense PI staining in the presumed QC of the root tip of R01A1 (Fig. 3-10). The QC is the determinant of stem-cell mitotic activity to generate the daughter cells, which in turn determine the PR length. However, if the mutation in *ALMT1* of *pdr2* mutant failed to restore the QC viability, how could the root be longer than the *pdr2* on Pi-deplete condition is a question. The ultimate fate of the root length depends on the rate of cell division and differentiation and the extent of expansion and elongation of cells (Scheres et al., 2002). Several publications indicate the elongation of the cell is an earlier event to be affected upon Pi starvation while the meristem reduction is late event (Sánchez-Calderón et al., 2005; Svistoonof et al., 2007; Ticconi et al., 2004). Thus, based on the observation of PI staining in the QC region and *ProCycB1::GUS* activity, I can infer that longer root of the suppressor R01A1 could be the restoration of cell elongation and delaying effect of early differentiation while maintaining the previously generated meristematic cell divisions. This is consistent with the Fe and callose accumulation of the suppressor (Fig. 3-11 & 3-12). Because, I did not see the accumulation of Fe and callose in the elongation zone of

the suppressor, however intense accumulation of both Fe and callose was found in the root tip indicating the disturbance of QC. However, it is important to perform further studies to find out if meristematic or elongating cells or both are the primary target of the mutation in R01A1.

3.1 ALMT1 mediates the PDR2 responses under Pi starvation

The novel finding was the PR growth rescuing effect of *pdr2* by the second mutation in the *ALMT1* locus, the role of which (*ALMT1*) in Pi starvation was not known previously. *ALMT1* is the major Al^{+3} tolerance gene in Arabidopsis expressed in the roots under Al^{+3} treatment, and the encoded transporter secretes malate (Sasaki et al., 2004; Hoekenga et al., 2006; Delhaize et al., 2007; Gruber et al., 2010). The release of such organic acids into the rhizosphere is important for Pi acquisition, because they mobilize not only inorganic Pi, but also organic P, which can be a major fraction of soil P, especially when P availability is low (Turner et al., 2013). If the secretion of malate which are known to facilitate the Pi uptake is blocked due to the mutation in *ALMT1*, how could the plant promote the root growth under Pi limiting condition is intriguing. Thus, I have hypothesized here three possible propositions, namely, i) excluding the Fe uptake; ii) remobilizing the over-loaded Fe from the root tip and meristems to the less sensitive tissues; and iii) remodeling the membrane lipid composition.

3.1.1 Excluding the Fe uptake

Most of the phosphates both organic and inorganic forms are bound to the Al and Fe in acidic soil and to Ca and Mg in alkaline soil (Brady and Weil, 1996). Under low Pi availability, plants secrete carboxylates like citrate and malate from root cells into the rhizosphere in order to mobilize organic and inorganic phosphate from humic/metal bound complexes (Vance et al., 2003; Ticconi and Abel, 2004; Fang et al., 2009; Richardson, 2009; Plaxton and Tran, 2011). Concomitantly, the organic acids also chelate Fe (Santi and Schmidt, 2009) and the chelated complex is mobilized to the root surface (Lambers et al., 2015) where FERRIC REDUCTASE OXIDASE2 (FRO2) reduces it (Robinson et al., 1999) for the uptake by metal transporter IRON REGULATED TRANSPORTER1 (IRT1) (Eide et al., 1996; Henriques et al., 2002; Varotto et al., 2002; Vert et al., 2002). Complex antagonistic interaction between external Pi and Fe bioavailability was highlighted by Abel (2011) and Müller et al., (2015) demonstrated the overloading of Fe in the roots of Pi challenged Arabidopsis WT and *pdr2*

mutants that restricts the root growth. Same authors displayed the less Fe accumulation of two low Pi insensitive double mutants *lpr1lpr2* in contrast to a hyper accumulation of Fe in the root of Pi hypersensitive *pdr2* mutant under Pi limiting growth condition. I also observed the similar results of Fe over-accumulation in *pdr2* while R01A1 root showed less accumulation under -Pi (Fig. 46). One striking difference of R01A1 from the WT is the absence of Fe accumulation in the elongation zone and more Fe in the root tip. This hints the target to rescue the *pdr2* mutant by the suppressor is the elongation zone. The *almt1* mutant showed opposite pattern of Fe distribution in the root tip compared to the WT (Fig. 3-13). It could be the malate secreted by *ALMT1* binds with the Fe and mobilizes the complex for the further uptake that likely causes the overloading of Fe in the cell. Thus, the loss of function of the *ALMT1* resulted in the reduced secretion of malate, perhaps caused less chelation of Fe to mobilize to the root surface area for further uptake. The root cell specific accumulation of callose deposition likely triggered by the accumulation of Fe was reported to regulate symplastic signaling in the SCN and RAM activity as demonstrated by SHORT-ROOT movement (Müller et al., 2015). The authors showed impaired SHORT-ROOT movement in *pdr2* while low Pi insensitive double mutants *lpr1lpr2* showed normal movement of SHORT-ROOT under Pi starvation conditions. I also observed the pattern of callose accumulation exactly matches the site of Fe accumulation, more in the root tip of R01A1 and was absent in the elongating zone of the root (Fig. 3-12). Thus, avoiding the excessive Fe uploading in the root could be one of the possible ways to rescue the root growth of *pdr2* by the second mutation in *ALMT1*. The insensitive PR growth and contrasting pattern of Fe and callose in the *almt1* T-DNA knock-out line compared to the WT under Pi starvation supports the Fe mediated low Pi sensitivity in regulating the root growth as also reported earlier (Ticcono et al., 2009; Müller et al., 2015).

3.1.2 Remobilization of internal iron

One hypothesis could also be the translocation of Fe from the meristematic zone once it is taken up. *FRD3* belongs to *MATE* gene family likely plays a role in this regards. *FRD3* mobilize the iron from the sensitive root meristem region to the other less sensitive part of the tissue as an Fe: citrate complex (Green and Rogers, 2004; Durrett et al., 2007). It is not clear how *ALMT1* is involved in this respect, but the observed pattern of Fe staining could be the redistribution of Fe in both lines of R01A1 suppressor and *almt1* mutant if not excluded the uptake to facilitate the root growth under Pi starvation. The measurement of Fe content or

monitoring the uptake by tracing the isotop labeled Fe in both R01A1 and *almt1* mutant plants would answer the notion if it is mobilized from the root to other less sensitive parts.

3.1.3 Remodeling membrane Lipid composition

Multiple lines of evidence suggest the differences in lipid composition and in lipid biosynthesis pathway affect the Al^{+3} tolerance of plants (Zhang et al., 1996; Wagatsuma et al., 2015). This phenomenon is associated with the strong induction of electrically neutral lipids, such as galactolipid and sulfolipid synthesis genes and repression of the genes for *de novo* synthesis of phospholipids which create a negative charge at the surface of the plasma membrane (Hammond et al., 2003; Misson et al., 2005; Morcuende et al., 2007; Lan et al., 2012; Woo et al., 2012). The recent study of Wagatsuma et al. (2014) showed CYP51 mediated higher sterol content and a simultaneous decrease of phospholipid content in the membranes as a strategy to the Al^{+3} tolerance of several species. Likewise, the Pi starvation also trigger the lipid remodeling, hydrolyzing the phospholipid that comprises around 30% of total cellular Pi in plant to recycle the Pi and replace it by galactolipids and sulfolipids (Nakamura et al., 2009). This suggests the interconnection of Pi adoptive and Al^{+3} tolerance responses in plants. It can be speculated that plants trigger the other molecular responses to change the lipid composition to confer more Al^{+3} resistance in absence of *ALMT1* which could be an added advantage to cope with the low Pi challenge.

Evidence from the other Al^{+3} tolerance gene *ALS3* in Pi starvation responses are completely opposite to the *ALMT1* driven response in *pdr2*. The T-DNA knock-out mutant of *ALS3* showed hypersensitive to root growth under Pi starvation in a sugar dependent manner (Belal et al., 2015). *ALS3* was originally identified from the mutant screening as a hypersensitive mutant to Al^{+3} that restricts the growth of shoot and root (Larsen et al., 1997) which encodes a phloem-localized ABC transporter-like protein, a homologue to the putative bacterial metal resistance protein ybbM (Larsen et al., 2005). It is expressed in leaf hydathodes and phloem and root cortex under Al^{+3} treatments (Larsen et al., 2005). This poses a question why two Al^{+3} sensitive mutants respond oppositely to the Pi starvation, *almt1* knock-out allele is significantly longer than the WT (Fig. 3-2) while *als3* is hypersensitive under Pi starvation as found by Belal et al., (2015). The function might be due to the distinct physiological role of the two proteins as *ALMT1* is secreting malate to protect the root tip from the Al^{+3} toxicity while the *ALS3* enhanced the Al^{+3} tolerance likely via trans-locating Al^{+3} from sensitive

tissues such as growing roots to tissues less sensitive to the toxic effects of Al^{+3} as proposed by Larsen et al. (2005).

Alike the altered Pi starvation phenotype of Al^{+3} sensitive mutants, the Pi sensitive mutants also show the altered Al^{+3} phenotype in a Pi dependent manner. *PHOSPHATIDATE PHOSPHOHYDROLASE 1 AND 2* (*AtPAH1* and *AtPAH2*) are the example in this context, both of which encodes PAPHs involved in galactolipid biosynthesis and double mutants are defective in replacing the phospholipids by non-phosphorus galactolipids and sulfolipid likely to recycle the Pi under deficient conditions (Härtel et al., 2000; Andersson et al., 2003; Jouhet et al., 2004; Nakamura et al., 2009). Hence, the defect in lipid remodeling in the double mutant resulted in the failure to cope with the Pi starvation showing the short root phenotype as well as retarded shoot growth (Nakamura et al., 2009). In addition to the hypersensitivity of this double mutant (*pah1pah2*), sensitivity to Al^{+3} was also documented by the same authors showing higher sensitivity under Pi stress than under the Pi-replete condition (Kobayashi et al., 2013) that further implicate the interplay of Pi and Al^{+3} . The common strategy of Arabidopsis to secrete the organic acid under Al^{+3} stress (Delhaize et al., 1993; Ma, 2000; Ryan et al., 2001) and Pi stress (Vance et al., 2003; Ticconi and Abel, 2004; Fang et al., 2009; Richardson, 2009; Plaxton and Tran, 2011) suggests plants have evolved the common molecular mechanism to deal with the Al^{+3} toxicity and Pi starvation and *ALMT1* could be in the central of this network.

The direct link of malate secretion and Pi starvation was further confirmed by a metabolic study in our research group. Jörg Ziggler showed higher content of malate in the root of WT while the *almt1* mutant showed significantly less content under Pi starvation (unpublished data). Further study of Jens Müller showed the exogenous application of malate in the growth medium of -Pi reduced the PR growth of WT (unpublished) which was associated with the intense Fe accumulation in the root. These data clearly showed the interplay of malate and Pi, and *ALMT1* is an ideal candidate to explore the underlying molecular mechanism. Thus, it can be inferred from the above result and discussion that *ALMT1* mediate the fine tuning of root growth under Pi starvation via Fe dependent manner that may trigger the downstream signaling cascade yet to decipher.

3.2. Concluding remarks

The concern for P has been deeply rooted to the rapidly declining the parental rock stock (Cooper and Carliell-Marquet, 2013) and increasing environmental hazards due to the huge wastage of the applied P-fertilizer that accounts for 70% or more (Lopez-Arredondo et al., 2014). It has been estimated in 2011 that the present stock could serve at least 50 more years and at best 235 years based on the present demand, population size and agricultural practices (Rosemarin et al., 2011). Considering the increasing global demand that would expected be peaked in 2030 (Cordell et al., 2009) with a concomitant price shooting, the major challenge in the agriculture would be feeding the millions of hungry mouths. The only alternative has been suggested to be to reuse and recycle P efficiently both within the environment (Elser and Bennett, 2011) and within the plant (Veneklaas et al., 2012). Genetic manipulation of the crops to develop the tolerant crops on low Pi has also been suggested (Lopez-Arredondo et al., 2014; Ruan et al., 2015). Richardson et al., (2011) suggested the adoption of microbial strategies to improve the plant P use efficiency. However, most of the discussion was centered on the typical plant responds to explore available Pi in the rhizosphere or associated role of mycorrhiza. Provided that many plants are non-michorrhizal associated and Pi in soil solution is very low, how plant could have survived in Pi challenged environment? The answer remained in the capacity of the plant not only to look for the available usable Pi in the soil but also to make the stock adequate from the recalcitrant sources for example the organophosphate for further uptake. Abel and colleagues demonstrated the ability of WT Arabidopsis to use nucleic acids as sole sources of Pi that unveiled the facet of this intrinsic ability of plants (Chen et al., 2000). In search of the same direction, *pdr1* is a followed up research to better understand the genetic and molecular mechanism of how does PDR1 use the organic phosphate. In such context, identification of *pdr1* locus and revelation of the use of external DNA facilitation by the end product (His) of the corresponding enzyme has a huge practical implication. It has opened up the opportunity for the further research to decipher the complex network at the molecular level for the efficient use of organic sources of Pi that accounts for 50%. Thus, the results presented here would be a benchmark in future research and expected to contribute to minimize the challenge of Pi limitation in natural ecosystem including agriculture.

In equal magnitude, *pdr1* is important for its magnificent role to ensure the 'efficient use' of N. A higher sensitivity of the mutant to high N sources and rescuing effect by His or promoting effect on the root length on low N containing medium compared to the WT control strongly support the implication of PDR1 in N use. We can infer the role of His in

coordinating the ‘efficient use of N’ sources by converting the nutritional signal to developmental signal as can be exemplified by the root development of *pdr1*. Future research should also be driven towards the decryption of the underlying molecular mechanism of its functionality in N use. Additionally, isolation, identification and characterization of a set of important *pdr2* suppressor mutants have laid a foundation for the future research in this direction. Importantly, the identification of *ALMT1* locus that is known to confer Al^{+3} tolerances has revealed a novel link to the Pi signaling pathway.

4 EXPERIMENTAL PROCEDURE

4.1. Plant Material

Wild type *Arabidopsis thaliana* (L.) Heynh. accessions Columbia-0 and *Landsberg erecta* were obtained from the Arabidopsis Biological Resource Center (Ohio State University, Columbus, USA). The *pdr1* mutant was derived from ethyl methanesulfonate (EMS)-mutagenized populations of *A. thaliana* (Columbia) and was previously referred as *p18* line (Chen et al., 2000). Seeds of all the T-DNA lines used in this experiment were obtained from the European Arabidopsis Stock Center (NASC). Seeds of transgenic *ProCycB1::GUS* plants (Columbia) were obtained from A. Colón-Carmona (Colón-Carmona et al., 1999) and double-homozygous F3 progeny of crosses with *pdr1* were used for analysis of root cell division. The seeds of *pdr2* mutants harboring the *ProCycB1::GUS* were used from our lab stock for the suppressor mutagenesis. The *almt1* knock-out mutant seeds (SALK_009629) were kindly reved from Dr. Thierry Desnos (CEA Cadarache, DSV DEVM Laboratoire de Biologie du Développement des Plantes, UMR 6191 CNRS-CEA, Aix-Marseille II, F-13108, France).

4.2. Growth Conditions

Seeds were surface sterilized and germinated on autoclaved 0.8% P (w/v) phytagar (Duchefa) medium containing 5 mM KNO_3 , 2.5 mM KH_2PO_4 (adjusted to pH 5.5 with KOH), 2 mM $MgSO_4$, 2 mM $Ca(NO_3)_2$, 50M Fe-EDTA, 70 μM H_3BO_3 , 14 μM $MnCl_2$, 0.5 μM $CuSO_4$, 1 μM $ZnSO_4$, 0.2 μM $NaMoO_4$, 10 μM NaCl, and 0.01 μM $CoCl_2$ and 0.5% (w/v) sucrose. 2.5 mM MES [2-(N-morpholino)-ethanesulfonic acid]-KOH (pH 5.5) was used to adjust the pH of the growth medium to 5.6. This medium is referred to as high Pi/+N or +Pi medium. For low Pi (-Pi) medium, KH_2PO_4 was omitted from the above nutrient solution. For DNA-

containing low Pi (-Pi /+DNA) medium filter-sterilized purified DNA was substituted for KH_2PO_4 and added to the autoclaved medium to a final concentration of 0.4 mg mL^{-1} , equaling about 1.5 mM total phosphorus (Chen et al., 2000). For iron-free medium (-Fe), Fe-EDTA was omitted from the nutrient solution. Nitrogen-free medium (-N) was prepared by substituting CaCl_2 for $\text{Ca}(\text{NO}_3)_2$, and omitting KNO_3 . For nitrate and phosphate free medium (-N/-Pi) 3 mM KCl was substituted for KNO_3 and KH_2PO_4 , respectively. Amino acids were used for chemical complementation or as nitrogen sources, they were filter sterilized and added to the autoclaved medium. The agar was routinely purified and contributed 8–10 μM P and 3–6 μM Fe to the growth medium (Ticconi et al., 2009). After stratification at 4°C for 2 days, the seeds were germinated in a controlled environmental chamber at 25°C under 16h daily light. To facilitate analysis of roots, plants were grown on vertically oriented square agar plate.

4.3. EMS Mutagenesis

EMS (Ethyl Methyl Sulfonate) was purchased from the Sigma Aldrich, Germany for inducing the mutation on *pdr2* mutant that carries *ProCycB1::GUS* marker gene. The *pdr2* mutant was isolated and characterized previously (Chen et al., 2000; Ticconi et al., 2004; Ticconi et al., 2009). Two different final concentrations, 0.2% and 0.4% of EMS was used for the screening while 1% used as a negative control for only 1000 seeds. Phosphate buffer was used to dilute the EMS to reach a final concentration of the solution. The volume of the solution was 25 times the volume of the seeds. On an average, each 1 mg seeds contained 35 seeds and we used 15000 seeds for the treatment of each of the 0.2% or 0.4% concentration that corresponds to 428.6 mg seeds with an equivalent volume of 0.6-0.7 ml. Accordingly, a total of 17.5 ml of EMS solution was prepared for each concentration (0.2% or 0.4%) and 1ml for the 1% EMS concentration. Seeds were soaked in the EMS solution in the 50 mL tube and kept in the table shaker with 500 rpm at room temperature for 15 hours (overnight). Followed by 30 times washing with water, seeds were mixed up with 0.1% agar solution (5 L for agar solution for each concentration) of which 10 mL contained approximately 30 seeds that were sown in each 11x11 cm sized pot by using the 10ml pipette and transferred to the greenhouse. The immediate EMS treated seeds was termed M1 and the progeny from it called M2. After harvesting the seeds from each pot that called as one parental group (altogether I had 500 parental group for each treatment), seeds were sterilized and approximately 200-250 seeds of each parental groups were sown on the vertically oriented agar plate containing the -Pi

medium. For comparison, Col-0 and *pdr2* were used in each plate as control and 4 putative candidates that restored the short root phenotype of *pdr2* to WT like was rescued, transferred to +Pi for 5 more days before transferred to the soil for the generation of M3 seeds. M3 generation was further validated for the inheritance of the phenotype and the confirmed suppressors were isolated for the identification and characterization of the corresponding loci.

4.4. Purification of herring sperm DNA

Free-acid crude oligo-nucleotides from herring sperm purchased from Sigma (Reidstr. 2, D-89555 Steinheim, Germany), were used as organic phosphorus supplements in plant growth media and purified as described in Chen et al., (2000). Briefly, 5 g of the nucleic acids was dissolved in 50 ml 1 M Tris-HCl (pH 9). The suspension was diluted to 100 ml with 10 mM Tris-HCl (pH 8), 1 mM EDTA and cleared by centrifugation (10,000 x g for 15 min). The crude nucleic acid solution was extracted six to eight times with 50 ml of buffer-saturated phenol/chloroform (1 vol/1 vol) until the aqueous-organic interface became transparent. After precipitation with 70% ethanol, the nucleic acid pellet was dissolved in 30 ml 10 mM Tris-HCl (pH 8), 1 mM EDTA and desalted by gel permeation chromatography on a Sephadex G-25 column (superdex 200 prep grade 16/60). The column was developed with buffer (10 mM Tris-HCl, 1 mM EDTA, 50 mM NaCl, pH 8) and connected to ÄKTA pure chromatography systems at a flow rate of 40 ml h⁻¹, and 50 ml fractions were collected. Fractions containing high-molecular-weight nucleic acids were combined. After ethanol precipitation, nucleic acids were dissolved in 10 mM Tris-HCl (pH 8), 1 mM EDTA, and the concentration was determined spectrophotometrically, assuming that one A260 unit equals 33 µg ml⁻¹ DNA.

4.5. Genetic Mapping and identification of the *PDR1* locus

The *pdr1* mutant was back crossed with the WT Col-0 three times prior to any genetic analysis. To obtain a chromosomal map position for the mutation in *pdr1*, homozygous *pdr1* plants were outcrossed with polymorphic mapping ecotype of accession Landsberg *erecta* (Ler-0). The resulting F1 progeny of this cross was subsequently selfed to establish a F2 generation and subsequently in F2, short root phenotype of *pdr1* was scored on -Pi. Based on the score, 50 individual plants were selected and transferred to the soil for bulk genomic DNA isolation. F3 population from each of the parental group of 50 individual F2 plants were evaluated again for short root phenotype on -Pi and +Pi/+N to confirm that causal mutation was homozygous in the sequencing pool and 10 F3 plants from each of 50 F2 parental plants

were used for fine mapping. All the 50 F2 leaf tissues were pooled to isolate the bulk DNA. After quantifying the extracted DNA and checking the integrity in gel, total 76 µg DNA was sent to BGI, Hongkong for the Whole Genome Resequencing by Illumina Hiseq2000 sequencing platform with 60X coverage.

The sequencing reads (79.87 Million) were aligned onto the public data of the reference Col-0 genome (Tair 10) using SOAP2 (<http://soap.genomics.org.cn/soapaligner.html>). The SNPs variation of the sequenced genome of *pdr1* pooled DNA was detected by using SOAPsnp (<http://soap.genomics.org.cn/soapsnp.html>). Fine mapping was done using around 500 F3 plants generated from the 50 F2 mother plants (10 from each). Taking the advantage of the Ler-0 alleles in the mapping population that serve as a genetic marker, I used the TAIR website to map the insertion/deletion (INDEL) between Col-0 and Ler-0 at different chromosomal positions within the candidate region of the chromosomal segment for genotyping the simple sequence length polymorphism (SSLP). The presence of the SNP was confirmed by sequencing the corresponding locus of PCR amplicon and by Cleaved-amplified polymorphic sequences (CAPS).

4.6. Hydroponic culture for DNA utilization experiment

The nutrient constituents used in hydroponic culture were exactly similar to the agar plates mentioned in section 4.2. Purified filter sterilized DNA (0.6 mg L^{-1}) and 3 µM His were supplemented in the respective growth media. Sterilized WT and *pdr1* seeds were grown on 6 well plates containing liquid media for 20 days. The 6 well plates were incubated for 20 days on an orbital shaker (110 rpm) at the room temperature for 16 hours daily light. Every 5 d, 10 µL aliquots of the liquid media were collected from the cultures and diluted to 1:4 for gel electrophoresis on 0.8% agarose gel.

4.7. Split-root experiments

WT and *pdr1* plants were grown on +Pi for 6 days after germination on vertically oriented square agar plates. Subsequently, the seedlings were transferred to agar-splitting round plates in such a way that the shoot and most part of the primary root were placed on the upper and just the primary root tips (~1 mm) on the lower compartment. The media composition of each compartment (i.e., +Pi, -Pi, +Pi+His, or -Pi+His). For simplicity, +Pi on upper and -Pi on

lower compartments referred as +Pi/-Pi. . Filter-sterilized 3 μM L-His was supplemented in the respective autoclaved medium. PR lengths were determined after 3 days of transfer.

4.8. Quantitative analysis of cellular free Pi content

Plants were grown on + Pi and transferred to +Pi and -Pi after 5 days of germination. After 3 days of transfer, root and shoots were harvested and biomass (fresh weight) was determined separately before grounded using a 5 mm steel bead in a bead mill at 25 s^{-1} for 50 s in liquid N. The resulting powder was extracted by vigorous shaking for 20 min with 50 μl of 70 % (v/v) of methanol containing 2 nmol norvaline and 5 nmol each [2,2,4,4- ^2H]-citric acid, [2,3,3- ^2H]-malic acid, and [2,2,3,3- ^2H]- succinic acid as internal standards. After two centrifugations at 10,000 rpm for 5 min, the resulting supernatant was stored at -80 $^{\circ}\text{C}$ until further processing.

10 μl of the root extract was evaporated to dryness, methoxylated with 20 mg ml^{-1} methoxyamine in pyridine for 1.5 hrs at room temperature and silylated for 30 min at 37 $^{\circ}\text{C}$ using Silyl 991. GC-MS/MS analysis was performed using an Agilent 7890 GC system equipped with an Agilent 7000B triple quadrupole mass spectrometer operated in the positive chemical ionization mode (reagent gas: methane, gas flow: 20 %; ion source temperature: 230 $^{\circ}\text{C}$). One μl was injected (pulsed [25 psi] splitless injection, 220 $^{\circ}\text{C}$) and separations were performed on an Rxi@-5ms column (15 m x 0.25 mm, 0.25 μm ; Restek GmbH, Bad Homburg, Germany) using helium as a carrier gas (2.39 ml min^{-1}). The initial temperature of 70 $^{\circ}\text{C}$ was hold for 1 min, followed by increases with 9 $^{\circ}\text{C min}^{-1}$ to 150 $^{\circ}\text{C}$ and 30 $^{\circ}\text{C min}^{-1}$ to 300 $^{\circ}\text{C}$. The final hold at 300 $^{\circ}\text{C}$ was 5 min. The transfer line was set to a temperature of 250 $^{\circ}\text{C}$ and N₂ and He were used a collision and quench gasses, respectively (1.5 and 2.25 ml min^{-1}). Data were acquired by multiple reaction monitoring using compound specific parameters. Peak areas were automatically integrated using the Agile algorithm of the MassHunter Quantitative Analysis software (version B.06.00) and manually adjusted if necessary. All subsequent calculations were performed with Excel (Microsoft Office Professional Plus 2010), using the peak areas of the respective internal standards for quantification.

4.9. Amino acid measurements

Plants were grown on +Pi for 5 days and then transferred to +Pi and -Pi. After transfer of two days, roots and shoots were separated, weighed, and processed for measuring the free amino acid contents according to the method described by Ziegler and Abel (2014).

4.10. Root growth analysis

For root growth measurements, at least 20 sterilized seeds were sown in a single row on square plates containing solid media with different nutrient or amino acid sources. The plates were oriented vertically to allow for root growth along the agar surface. Root length and lateral root number were scored for respective transfer or continuous growth experiment. Images of the roots were captured with a COHU high-performance CCD camera and quantitative analysis was done by Image J.

4.11. Root meristem size and cell elongation

Cell biological assay was done under the confocal laser scanning microscopy (LSM-7100, Carl Zeiss). Roots were mounted on the glass slide then stained with propidium iodide and covered with the glass cover slip. Images were captured using different objectives under reflector AF488, 2D and/or 3D projections were generated, and anatomical parameters were calculated as described previously (Berger et al., 1998). Root meristem size was determined as the number of cells in a single trichoblast cell file, starting from the QC to the first elongating cell. The average number of elongating cells in the same cell file was calculated from the first elongating to the first differentiating cell, as determined by the appearance of a root hair bulge.

4.12. Starch staining

6 days old seedlings grown on +Pi, -Pi+His, -Pi, -Pi+His, -Pi+DNA and -Pi+DNA+His containing media were incubated overnight in 96% ethanol to remove the pigments. After washing with water, the samples were then incubated in 1.5% KI and 0.3% I₂ for 30 minutes. Images were then captured under the stereo microscope after extensive washing with water.

4.13. Anthocyanin quantification

Accumulation of anthocyanin of seedlings grown on +Pi, +Pi+His, -Pi, -Pi+His for 3 days after transferring 5 days old seedlings from +Pi were determined according to a slight modification of Schmidt and Mohr (1981). Filter-sterilized 3 μM L - His was supplemented in the respective media. Shoots were dissected from the roots, weighed and frozen immediately before preceding the next step. The pigment was extracted from the tissues incubated in a heat block at 100°C for 3 minutes in 1 mL of propanol: HCl: water (18:1:81) and then kept at room temperature overnight. After centrifugation at 1000xg to clean the extracts, absorption at 535 and 650nm was measured spectrophotometrically and anthocyanins was calculated as $\Delta A_{(535-650)}/\text{g FW}$. Four replicates were measured for each treatment.

4.14. Measurement of NO_3^- and NH_4^+ content

NO_3^- was measured according to Cataldo et al. (1975). Plants were grown vertically on agar plates for 8 days after germination on +Pi, +Pi+H and -N containing growth medium before harvesting the shoot and root separately. The sample weight was determined and immediately frozen in liquid nitrogen. The tissues were homogenized using a 5 mm steel bead in a bead mill at 30s⁻¹ for 1 minute. Phosphate buffer (PH 7.2) was then added to the resulting powder in a ratio of 1:6 (w/v), briefly mixed and centrifuged at 15,000xg for 15 minutes. 200 μL supernatant were pipetted into a 50 mL tube and mixed thoroughly with 0.8 mL of 5% salicylic acid in concentrated H_2SO_4 (SA- H_2SO_4) and kept for 20 minutes at room temperature. 19 mL of 2N NaOH was then added to raise the pH above 12. Samples were cooled to room temperature before measuring the absorption. The blank used in this experiment was the 0.8 mL concentrated H_2SO_4 without salicylic acid in 19 mL of 2N NaOH. 500 μL aliquot was used to read the absorption at 410 nm in TECAN Infinite® PRO M1000 microplate reader connected with a UV silicon photodiode detector. -N grown plants were used as negative control. NH_4^+ was determined according to Baethgen and Alley (1989). Briefly, root and shoot were harvested as described above. $(\text{NH}_4)_2\text{SO}_4$ was used as a standard stock solution and reading of absorbance at 650 nm was recorded for the determination of NH_4^+ .

4.15. Analysis of photosynthetic pigments (chlorophyll a and b)

WT, *pdrl* and *prt1-2* mutants were grown on +Pi for 5 days and then transferred to +Pi, -Pi, +Pi+H, -Pi+H for growing another 3 days before harvesting the leaf. The chlorophyll

extraction and concentration was calculated according to the method described by Ni et al., (2009) modified from Mochizuki et al., (2001). Reading for absorption was taken at 663 and 645 in the TECAN Infinite® PRO M1000 microplate reader connected with a UV silicon photodiode detector.

4.16. RT- and qRT-PCR analysis

Total RNAs from various tissues were isolated using Trizol reagent (Invitrogen) according to the protocol, and first-strand cDNA was synthesized from 5 µg RNA using an oligo(dT)18 primer and reverse transcriptase using the SuperScript II Reverse Transcriptase (RT) kit (Life technology). As an internal control, Actin (F: 5'-CAAAGACCAGCTCTTCCATC-3', R: 5'-CTGTGAACGATTCCTGGACCT-3') was used for RT-PCR and PP2A (F: 5'-AGCCAACTAGGACGGATCTGGT-3', R: 5'-CTATCCGAACTTCTGCCTCATTA-3' for qRT-PCR analyses. Quantitative RT-PCR analysis was performed using a Fast SYBR® green master mix (Applied biosystem). The fluorescence detection of the sample was quantified in ABI 7500 fast real time PCR system. The PSI genes including primers tested are ATPT2 (AT2G38940 F: 5'-CTAGGAGAAGAAGAATGGCAAGGG-3'; R: AGAATCCCATTCGGCGATTATG-3') RNS2 AT2G39780 (F:5'-TCATCATGCAATGGTGGGAAAGGG-3'; R:5'-AAGTCCCATGTTTCTCCCACTCG-3'), AT3G17790 ATACP5 (F:5'-GTCTCTCGTTGCTTATCAGATGGG-3'; R: 5'-TCTCCCGTAGACACCACGAAATC-3') and AT4 AT5G03545.1 (F: 5'-GCGATGAAGATTGCATGAAGGTTG-3'; R: 5'-GGATCGAAGTTGCCCAAACGAG-3'). Data were normalized with respect to the PP2A to calculate the relative expression of *AtACP5*, *AtAt4*, *AtPT2*, *AtRNase2* and *AtSPX3*. Three biological replications with two technical replications for each sample were analysed, significant difference from the WT was determined by two-sample t-test (P<0.05).

4.17. Construction of transgenic plant (overexpression and promoter GUS/GFP lines)

To create *CaMV Pro35S::PDR1/ATP-PRT1::GFP*, Gateway® Technology with Clonase™ II was used. The full length cDNA of PDR1/ATP-PRT1 was amplified By PCR using gene specific primer. The forward primers (5'-ATGTCTCTCCTTCTCCC-3') and reverse primer (5'-ATCCCGAGGTTTCTCAGG-3') were attached with the 3'-end of ATTB1 (5'-

GGGGACAAGTTTGTACAAAAAAGCAGGCTTC-3') and ATTB2 (5'-GGGGACCACTTTGTACAAGAAAGCTGGGTCA-3') site respectively. Entry clone was then generated by BP recombination reaction with the amplified ATTB-PCR product by mixing 1-3µl PCR product of 150 ng/µl with 1µl pDONR221 of 150ng/µl and 1µL BP Clonase™ II enzyme. Total 5µl volume was adjusted with double distilled (ddest) water and incubated the reaction at 25°C for 1 hour. To stop the reaction, 1 µl of the Proteinase K solution was added and incubated at 37°C for 10 minutes. The BP reaction was then transformed to 50 µl TOP10 competent *E. coli* cells by incubating on ice for 30 minutes followed by heat shock at 42°C for 30 seconds returned to the ice for 2 minutes respectively. The cells were then incubated with 250 µL SOC media at 37°C with 150 rpm for 1 hour before plating to the LB agar containing selective antibiotics growth medium which was incubated overnight at 37°C. The positive colonies was then confirmed by PCR amplification with M13 primers (For. 5'-GTAAAACGACGGCCAG-3'; Rev. 5'-CAGGAAACAGCTATGAC-3') to make sure the fidelity of the construct before further generating the destination clone.

To create *CaMV35SPro::ATP-PRT2::GFP*, pENTR™ Directional TOPO® Cloning Kits from Invitrogen was used. The full length cDNA was amplified using gene specific forward primer with four additional CACC bases (5'-caccATGCCAATCTCAATTCCCC-3') and reverse primer (5'-AAGGCCGAGGTTACTCAGAAG-3'). The pENTR™/D-TOPO vector allows rapid directional TOPO® cloning of the blunt PCR products for entry into the Gateway® system without any ligase or restriction enzyme. The protocol according to the manufacturer's instruction was followed throughout the cloning procedure. In brief, the gel purified PCR products of 10-15 ng/µl was incubated with 15ng/µl pENTR™ D-TOPO® vector for 30 minutes followed by transformation into TOP10 chemically competent *E. coli* cells as described above.

For the promoter GUS/GFP construct of *ATP-PRT1* and *ATP-PRT2*, Gateway® Technology with Clonase™ II was used. Forward primer (5'-GAGGTTCAAGAAGTCGGCTG-3') and reverse primer (5'-TGTTGTGTGGCTTTTCGAGA-3') for *ATP-PRT1* and forward 5'-CGATTTTGATGGTGAAGTGCT-3' and reverse- 5'-TGTAGAGTGGCGTTAAGGGG-3' for *ATP-PRT2* were generated with proper ATTB site (ATTB1 and ATTB2 as mentioned above). The *ATP-PRT1* primer amplified 2355bp promoter of the gene, while *ATP-PRT2* primer amplified 1324 bp including the full length (993 bp except ATG) of the neighbouring upstream gene (AT1G09794, COX 19 family protein, no expression according to EST data

base). I included the neighboring gene because the promoter of *ATP PRT2* is only 279 bp long.

After subsequent plasmid isolation from the positive colony, the construct was PCR amplified with M13 primers (For. 5'-GTAAAACGACGGCCAG-3'; Rev. 5'-CAGGAAACAGCTATGAC-3') and sequenced to check the fidelity of the insert with respect to the WT copy using 'Clone Manager Professional 9' before generating the destination clone.

The entry plasmids for over expression and promoter activity study of *ATP-PRT1* and *ATP-PRT2* were then subjected to LR clonase reactions with the Gateway-compatible binary destination vectors pB7WGF2 to generate *CaMV Pro35S::PDR1/ATP-PRT1::GFP*, *CaMV Pro35S::ATP-PRT2::GFP* and pBGWFS7 vector for generating the promoter GUS/GFP line of *ATP-PRT1* and *ATP-PRT2*. LR reaction was then done with 1-3 µl entry clone isolated and purified plasmid of 150 ng/µl with 1 µl destination vector plasmid of 150ng/µl and 1 µL LR Clonase™ II enzyme and the volume was adjusted to 5 µl. Transformation to competent TOP10 *E. coli* cell and subsequent plating on the LB plate were done in the same way as described above for entry clone. The positive colonies were analyzed by restriction analysis to confirm the presence and correct orientation of the cassette.

For transforming to the *Agrobacterium tumefaciens* cell, 5 µl of the purified positive plasmid from destination clone was added with thawed 50 µl *A. tumefaciens* cells by cold shock (30 minutes on ice followed by freezing in liquid nitrogen for 5 minutes and at 37°C for 5 minutes respectively) which was then mixed with 250 µl SOC media to incubate 2 hours at 37°C. The cells were then plated to LB plate with the right antibiotics and cultured for 48 hours at 30°C in an incubating shaker with 180rpm.

For transient transformation, p19 cells, a viral-encoded suppressor of post-transcriptional gene silencing protein (Voinnet et al., 2003) were grown in parallel to the *A. tumefaciens* colonies carrying the plasmid constructs in the selective liquid media at 30°C for two days. The cells were then harvested by centrifugation (10000 rpm, 5 min) and washed twice by infiltration buffer and mixed with the P19 cells in a ratio of 1:1 after determining the optical density (0.6-0.8). The mixture was infiltrated to the abaxial surface of *Nicotiana benthamiana* leaves after incubation of 1 hour at room temperature and subsequently after three days, the GFP tagged fusion proteins were analyzed under Confocal Laser Scanning Microscopy (CLSM). For stable transformation, the constructs were transformed according to the protocol of Clough and Bent (1998). In brief, *Agrobacterium tumefaciens* strain harboring the gene of interest on

a binary vector was grown in LB agar plate with antibiotics at 28°C. The cells were collected from the surface, resuspended in 5% freshly made sucrose solution to OD600 = 0.8. Before dipping, Silwet L-77 added to a concentration of 0.05% (500 ul/L) and mixed well. The healthy flowering plants were dipped (above-ground parts) in *Agrobacterium* solution for 15 seconds with gentle agitation. Dipped plants were then kept horizontally in the tray under a white thin polythene sheet cover for the overnight to maintain high humidity. The following day plants were exposed to the normal greenhouse condition till harvesting the T1 seeds.

4.18. Subcellular localization study

The subcellular localization the GFP tagged ATP-PRT1 and ATP-PRT2 proteins transiently transformed to tobacco leaves (*Nicotiana benthamiana*) and stable transformed to *Arabidopsis* via *Agrobacterium* were conducted under confocal laser scanning microscope. The samples were collected after 3 days of infiltration in tobacco leaves and the 5 days old T2 homozygous overexpression lines grown vertically on agar plates and GFP fluorescence was visualized on a Zeiss LSM 710 confocal laser scanning microscope. All images were obtained using a 40× water-immersion objective. The excitation wavelength was 488 nm; emission was detected between 493 and 580 nm. For All images were obtained using the sequential mode to prevent false positive signals. Transgenic *Arabidopsis* plants were generated by *Agrobacterium*-mediated transformation. T2 lines showing a segregation ratio of 3:1 for resistance to Basta® were selected for subsequent microscopic analysis.

4.19. Promoter GUS/GFP study

The T2 generation of *Agrobacterium*-mediated transformed ATP-PRT1 promoter in WT *Arabidopsis* was tested in the vertically oriented agar plate containing the complete growth medium supplemented with Basta®. The lines showing segregation ratio of 3:1 for resistance to Basta® were selected for subsequent microscopic analysis. The GUS was detected in the 5 days old seedlings grown on +Pi/+N under stereo microscope.

4.20. Histochemical staining

Propodium iodide (PI), Fe and callose staining were done as described in Müller et al., (2015). Plants were grown on vertically oriented agar plates containing the complete Pi medium as described in the respective results section. Likewise, GUS staining for the *ProCycB1* was done after 3 days of transfer.

4.21. Al⁺³ sensitivity test

The test was carried out in hydroponic culture containing the growth medium of 2.1mM NH₄NO₃, 1.9 mM KNO₃, 0.4 mM CaCl₂, 0.15 mM MgSO₄, 2mM HomoPipes (pH 4.4) and 0.5% sucrose. 10 μM AlCl₃ was supplemented in the autoclaved growth medium for the sensitivity test while the medium without AlCl₃ supplement used as a control. The sterile seeds (20 approximately for each genotype) of WT (Col-0), *RO1A1* suppressor, *almt1* mutant were germinated and grown for 4 days for the assay in 3 ml cultured media in the six well plate. Of note, No EDTA, vitamins, Pi, Fe or microelements were used in the growth media.

Identification of ALMT1

4.22. Genotyping of *pdr1* and *almt1* mutants

The derived Cleaved-amplified polymorphic sequences (dCAPS) markers were developed using web based tool *dCAPS Finder 2.0* (helix.wustl.edu/dcaps/dcaps.html) to genotype the mutation in *pdr1* and *almt1*. For *pdr1*, SNP was genotyped by amplifying PCR product with forward 5'-ATATCTTTTGGCCGTTGAAACCA-3' and reverse primer 5'-ATGTGAAGTGTTGTTTGCCTTTG-3' followed by the restriction digestion of the PCR product with DdeI restriction enzyme. While for *almt1*, PCR product was amplified by forward 5'-GTTGTCTTTGAATTCTCCGTG-3' and reverse primer 5'-GCACCCGACAATCTTGCTAG-3' followed by digestion the PCR amplicon with BsaJ1 restriction enzyme that cut the WT version.

5. REFERENCES

- Abel, S.** (2011). Phosphate sensing in root development. *Current opinion in plant biology* **14**, 303-309.
- Alifano, P., Fani, R., Lio, P., Lazcano, A., Bazzicalupo, M., Carlomagno, M.S., and Bruni, C.B.** (1996). Histidine biosynthetic pathway and genes: structure, regulation, and evolution. *Microbiological reviews* **60**, 44-69.
- Andersson, M.X., Stridh, M.H., Larsson, K.E., Liljenberg, C., and Sandelius, A.S.** (2003). Phosphate-deficient oat replaces a major portion of the plasma membrane phospholipids with the galactolipid digalactosyldiacylglycerol. *FEBS letters* **537**, 128-132.
- Arndt, K.T., Styles, C., and Fink, G.R.** (1987). Multiple global regulators control HIS4 transcription in yeast. *Science* **237**, 874-880.
- Aung, K., Lin, S.-I., Wu, C.-C., Huang, Y.-T., Su, C.-I., and Chiou, T.-J.** (2006). *pho2*, a phosphate overaccumulator, is caused by a nonsense mutation in a microRNA399 target gene. *Plant Physiology* **141**, 1000-1011.
- Baethgen, W.E., and Alley, M.M.** (1989). A manual colorimetric procedure for measuring ammonium nitrogen in soil and plant Kjeldahl digests. *Commun. Soil Sci. Plant Anal.* **20** (9&10),961-969.
- Bari, R., Pant, B.D., Stitt, M., and Scheible, W.R.** (2006). PHO2, microRNA399, and PHR1 define a phosphate-signaling pathway in plants. *Plant Physiology* **141**, 988-999.
- Bariola, P.A., MacIntosh, G.C., and Green, P.J.** (1999). Regulation of S-like ribonuclease levels in Arabidopsis. Antisense inhibition of RNS1 or RNS2 elevates anthocyanin accumulation. *Plant Physiology* **119**, 331-342.
- Bates, T., and Lynch, J.** (1996). Stimulation of root hair elongation in Arabidopsis thaliana by low phosphorus availability. *Plant, Cell & Environment* **19**, 529-538.
- Beemster, G.T., and Baskin, T.I.** (1998). Analysis of cell division and elongation underlying the developmental acceleration of root growth in Arabidopsis thaliana. *Plant Physiol* **116**, 1515-1526.
- Belal, R., Tang, R., Li, Y., Mabrouk, Y., Badr, E., and Luan, S.** (2015). An ABC transporter complex encoded by Aluminum Sensitive 3 and NAP3 is required for phosphate deficiency responses in Arabidopsis. *Biochemical and biophysical research communications*.
- Beltran, G., Novo, M., Rozes, N., Mas, A., and Guillamón, J.M.** (2004). Nitrogen catabolite repression in Saccharomyces cerevisiae during wine fermentations. *FEMS yeast research* **4**, 625-632.
- Benitez-Alfonso, Y., Faulkner, C., Pendle, A., Miyashima, S., Helariutta, Y., and Maule, A.** (2013). Symplastic intercellular connectivity regulates lateral root patterning. *Developmental cell* **26**, 136-147.
- Bikard, D., Patel, D., Le Mette, C., Giorgi, V., Camilleri, C., Bennett, M.J., and Loudet, O.** (2009). Divergent Evolution of Duplicate Genes Leads to Genetic Incompatibilities Within A-thaliana. *Science* **323**, 623-626.
- Bojović, B., and Marković, A.** (2009). Correlation between nitrogen and chlorophyll content in wheat (Triticum aestivum L.). *Kragujevac Journal of Science* **31**, 69-74.
- Bonneau, L., Huguet, S., Wipf, D., Pauly, N., and Truong, H.N.** (2013). Combined phosphate and nitrogen limitation generates a nutrient stress transcriptome favorable for arbuscular mycorrhizal symbiosis in Medicago truncatula. *New Phytologist* **199**, 188-202.
- Borders, C., Broadwater, J.A., Bekeny, P.A., Salmon, J.E., Lee, A.S., Eldridge, A.M., and Pett, V.B.** (1994). A structural role for arginine in proteins: multiple hydrogen bonds to backbone carbonyl oxygens. *Protein Science* **3**, 541-548.

- Bou Zeidan, M., Zara, G., Viti, C., Decorosi, F., Mannazzu, I., Budroni, M., Giovannetti, L., and Zara, S.** (2014). L-histidine inhibits biofilm formation and FLO11-associated phenotypes in *Saccharomyces cerevisiae* flor yeasts. *PLoS one* **9**, e112141.
- Brady, N.C., and Weil, R.R.** (1996). *The nature and properties of soils.* (Prentice-Hall Inc.).
- Branscheid, A., Sieh, D., Pant, B.D., May, P., Devers, E.A., Elkrog, A., Schauser, L., Scheible, W.R., and Krajinski, F.** (2010). Expression Pattern Suggests a Role of MiR399 in the Regulation of the Cellular Response to Local Pi Increase During Arbuscular Mycorrhizal Symbiosis. *Molecular Plant-Microbe Interactions* **23**, 915-926.
- Briat, J.-F., Rouached, H., Tissot, N., Gaymard, F., and Dubos, C.** (2015). Integration of P, S, Fe, and Zn nutrition signals in *Arabidopsis thaliana*: potential involvement of PHOSPHATE STARVATION RESPONSE 1 (PHR1). *Frontiers in plant science* **6**.
- Bustos, R., Castrillo, G., Linhares, F., Puga, M.I., Rubio, V., Pérez-Pérez, J., Solano, R., Leyva, A., and Paz-Ares, J.** (2010). A central regulatory system largely controls transcriptional activation and repression responses to phosphate starvation in *Arabidopsis*. *PLoS genet* **6**, e1001102.
- Cataldo, D.A., Maroon, M., Schrader, L.E., and Youngs, V.L.** (1975). Rapid colorimetric determination of nitrate in plant tissues by nitration of salicylic acid. *Commun. Soil Science and Plant Analysis*, **6**(1),71-80.
- Carthew, R.W., and Sontheimer, E.J.** (2009). Origins and mechanisms of miRNAs and siRNAs. *Cell* **136**, 642-655.
- Catarecha, P., Segura, M.D., Franco-Zorrilla, J.M., García-Ponce, B., Lanza, M., Solano, R., Paz-Ares, J., and Leyva, A.** (2007). A mutant of the *Arabidopsis* phosphate transporter PHT1; 1 displays enhanced arsenic accumulation. *The Plant Cell* **19**, 1123-1133.
- Chapin, F.S., Moilanen, L., and Kielland, K.** (1993). Preferential use of organic nitrogen for growth by a non-mycorrhizal arctic sedge.
- Chen, D.L., Delatorre, C.A., Bakker, A., and Abel, S.** (2000). Conditional identification of phosphate-starvation-response mutants in *Arabidopsis thaliana*. *Planta* **211**, 13-22.
- Chen, Y.-F., Li, L.-Q., Xu, Q., Kong, Y.-H., Wang, H., and Wu, W.-H.** (2009). The WRKY6 transcription factor modulates PHOSPHATE1 expression in response to low Pi stress in *Arabidopsis*. *The Plant Cell* **21**, 3554-3566.
- Chen, Z., Nimmo, G., Jenkins, G., and Nimmo, H.** (2007). BHLH32 modulates several biochemical and morphological processes that respond to Pi starvation in *Arabidopsis*. *Biochem. J* **405**, 191-198.
- Chevalier, F., Pata, M., Nacry, P., Doumas, P., and Rossignol, M.** (2003). Effects of phosphate availability on the root system architecture: large-scale analysis of the natural variation between *Arabidopsis* accessions. *Plant, Cell & Environment* **26**, 1839-1850.
- Chiou, T.J. and Lin, S.I.** (2011). Signaling Network in Sensing Phosphate Availability in Plants. *Annual Review Plant Biology* **62**,185–206.
- Chiou, T.-J., Aung, K., Lin, S.-I., Wu, C.-C., Chiang, S.-F., and Su, C.-I.** (2006). Regulation of phosphate homeostasis by microRNA in *Arabidopsis*. *The Plant Cell* **18**, 412-421.
- Clarkson, D.T., and Lüttge, U.** (1991). Mineral nutrition: inducible and repressible nutrient transport systems. In *Progress in botany* (Springer), pp. 61-83.
- Colón-Carmona, A., You, R., Haimovitch-Gal, T., and Doerner, P.** (1999). Spatio-temporal analysis of mitotic activity with a labile cyclin-GUS fusion protein. *Plant Journal* **20**, 503-508.
- Cooper, J., and Carliell-Marquet, C.** (2013). A substance flow analysis of phosphorus in the UK food production and consumption system. *Resour Conserv Recy* **74**, 82-100.

- Cordell, D., Drangert, J.-O., and White, S.** (2009). The story of phosphorus: global food security and food for thought. *Global environmental change* **19**, 292-305.
- Cui, H.** (2007). An evolutionarily conserved mechanism delimiting SHR movement defines a single layer of endodermis in plants (vol 316, pg 421, 2007). *Science* **318**, 1866-1866.
- Czarnecki, O., Yang, J., Weston, D.J., Tuskan, G.A., and Chen, J.-G.** (2013). A dual role of strigolactones in phosphate acquisition and utilization in plants. *International journal of molecular sciences* **14**, 7681-7701.
- Danova-Alt, R., Dijkema, C., De Waard, P., and Koeck, M.** (2008). Transport and compartmentation of phosphite in higher plant cells—kinetic and ³¹P nuclear magnetic resonance studies. *Plant, Cell & Environment* **31**, 1510-1521.
- Daram, P., Brunner, S., Rausch, C., Steiner, C., Amrhein, N., and Bucher, M.** (1999). Pht2; 1 encodes a low-affinity phosphate transporter from Arabidopsis. *The Plant Cell* **11**, 2153-2166.
- Delatorre, C.A.** (2002). Phosphate deficiency response: Understanding the signaling pathway. PhD thesis submitted to the University of California, Davis. Pp158.
- De Vos, D., Vissenberg, K., Broeckhove, J., and Beemster, G.T.S.** (2014). Putting Theory to the Test: Which Regulatory Mechanisms Can Drive Realistic Growth of a Root? *Plos Comput Biol* **10**.
- Del Pozo, J.C., Allona, I., Rubio, V., Leyva, A., De La Peña, A., Aragoncillo, C., and Paz-Ares, J.** (1999). A type 5 acid phosphatase gene from Arabidopsis thaliana is induced by phosphate starvation and by some other types of phosphate mobilising/oxidative stress conditions. *The plant journal* **19**, 579-589.
- Delhaize, E., and Randall, P.J.** (1995). Characterization of a phosphate-accumulator mutant of Arabidopsis thaliana. *Plant Physiology* **107**, 207-213.
- Delhaize, E., Ryan, P.R., and Randall, P.J.** (1993). Aluminum tolerance in wheat (*Triticum aestivum* L.)(II. Aluminum-stimulated excretion of malic acid from root apices). *Plant Physiology* **103**, 695-702.
- Delhaize, E., Gruber, B.D., and Ryan, P.R.** (2007). The roles of organic anion permeases in aluminium resistance and mineral nutrition. *FEBS letters* **581**, 2255-2262.
- Denis, V., Boucherie, H., Monribot, C., and Daignan-Fornier, B.** (1998). Role of the myb-like protein bas1p in *Saccharomyces cerevisiae*: a proteome analysis. *Molecular microbiology* **30**, 557-566.
- Devaiah, B.N., and Raghothama, K.G.** (2007). Transcriptional regulation of Pi starvation responses by WRKY75. *Plant signaling & behavior* **2**, 424-425.
- Devaiah, B.N., Karthikeyan, A.S., and Raghothama, K.G.** (2007). WRKY75 transcription factor is a modulator of phosphate acquisition and root development in Arabidopsis. *Plant Physiology* **143**, 1789-1801.
- Devaiah, B.N., Madhuvanthi, R., Karthikeyan, A.S., and Raghothama, K.G.** (2009). Phosphate starvation responses and gibberellic acid biosynthesis are regulated by the MYB62 transcription factor in Arabidopsis. *Molecular Plant* **2**, 43-58.
- Donald, J.E., Kulp, D.W., and DeGrado, W.F.** (2011). Salt bridges: Geometrically specific, designable interactions. *Proteins: Structure, Function, and Bioinformatics* **79**, 898-915.
- Duan, K., Yi, K., Dang, L., Huang, H., Wu, W., and Wu, P.** (2008). Characterization of a sub-family of Arabidopsis genes with the SPX domain reveals their diverse functions in plant tolerance to phosphorus starvation. *The plant journal* **54**, 965-975.
- Durrett, T.P., Gassmann, W., and Rogers, E.E.** (2007). The FRD3-mediated efflux of citrate into the root vasculature is necessary for efficient iron translocation. *Plant Physiology* **144**, 197-205.
- Eide, D., Broderius, M., Fett, J., and Guerinot, M.L.** (1996). A novel iron-regulated metal transporter from plants identified by functional expression in yeast. *Proceedings of the National Academy of Sciences* **93**, 5624-5628.

- Elser, J., and Bennett, E.** (2011). Phosphorus cycle: A broken biogeochemical cycle. *Nature* **478**, 29-31.
- Fang, Z., Shao, C., Meng, Y., Wu, P., and Chen, M.** (2009). Phosphate signaling in *Arabidopsis* and *Oryza sativa*. *Plant Science* **176**, 170-180.
- Forde, B., and Lorenzo, H.** (2001). The nutritional control of root development. *Plant Soil* **232**, 51-68.
- Franco-Zorrilla, J.M., Valli, A., Todesco, M., Mateos, I., Puga, M.I., Rubio-Somoza, I., Leyva, A., Weigel, D., Garcia, J.A., and Paz-Ares, J.** (2007). Target mimicry provides a new mechanism for regulation of microRNA activity. *Nature genetics* **39**, 1033-1037.
- Frink, C.R., Waggoner, P.E., and Ausubel, J.H.** (1999). Nitrogen fertilizer: Retrospect and prospect. *Proceedings of the National Academy of Sciences of the United States of America* **96**, 1175-1180.
- Frommer, W.B., Hummel, S., Unsel, M., and Ninnemann, O.** (1995). Seed and vascular expression of a high-affinity transporter for cationic amino acids in *Arabidopsis*. *Proceedings of the National Academy of Sciences of the United States of America* **92**, 12036-12040.
- Fujii, H., Chiou, T.J., Lin, S.I., Aung, K., and Zhu, J.K.** (2005). A miRNA involved in phosphate-starvation response in *Arabidopsis*. *Current biology : CB* **15**, 2038-2043.
- Giehl, R.F., Gruber, B.D., and von Wiren, N.** (2014). It's time to make changes: modulation of root system architecture by nutrient signals. *Journal of experimental botany* **65**, 769-778.
- Gojon, A., Nacry, P., and Davidian, J.C.** (2009). Root uptake regulation: a central process for NPS homeostasis in plants. *Current opinion in plant biology* **12**, 328-338.
- Goldstein, A.H., Baertlein, D.A., and McDaniel, R.G.** (1988). Phosphate Starvation Inducible Metabolism in *Lycopersicon esculentum*: I. Excretion of Acid Phosphatase by Tomato Plants and Suspension-Cultured Cells. *Plant Physiol* **87**, 711-715.
- Green, L.S., and Rogers, E.E.** (2004). FRD3 controls iron localization in *Arabidopsis*. *Plant Physiol* **136**, 2523-2531.
- Gruber, B.D., Giehl, R.F., Friedel, S., and von Wiren, N.** (2013). Plasticity of the *Arabidopsis* root system under nutrient deficiencies. *Plant Physiol* **163**, 161-179.
- Gruber, B.D., Ryan, P.R., Richardson, A.E., Tyerman, S.D., Ramesh, S., Hebb, D.M., Howitt, S.M., and Delhaize, E.** (2010). HvALMT1 from barley is involved in the transport of organic anions. *Journal of experimental botany* **61**, 1455-1467.
- Guo, B., Jin, Y., Wussler, C., Blancaflor, E.B., Motes, C.M., and Versaw, W.K.** (2008). Functional analysis of the *Arabidopsis* PHT4 family of intracellular phosphate transporters. *The New phytologist* **177**, 889-898.
- Guyer, D., Patton, D., and Ward, E.** (1995). Evidence for cross-pathway regulation of metabolic gene expression in plants. *Proceedings of the National Academy of Sciences of the United States of America* **92**, 4997-5000.
- Hackenberg, M., Shi, B.J., Gustafson, P., and Langridge, P.** (2013). Characterization of phosphorus-regulated miR399 and miR827 and their isomiRs in barley under phosphorus-sufficient and phosphorus-deficient conditions. *BMC plant biology* **13**, 214.
- Hageman, R.H., and Lambert, R.J.** (1988). The use of physiological traits for corn improvement. In GF Sprague, JW Dudley, eds, *Corn and corn improvement*, Ed 3. American Society of Agronomy and Soil Society of America, Madison, pp. 21431-461.
- Hamburger, D., Rezzonico, E., MacDonald-Comber Petetot, J., Somerville, C., and Poirier, Y.** (2002). Identification and characterization of the *Arabidopsis* PHO1 gene involved in phosphate loading to the xylem. *Plant Cell* **14**, 889-902.

- Hammond, J.P., and White, P.J.** (2011). Sugar signaling in root responses to low phosphorus availability. *Plant Physiol* **156**, 1033-1040.
- Hammond, J.P., Bennett, M.J., Bowen, H.C., Broadley, M.R., Eastwood, D.C., May, S.T., Rahn, C., Swarup, R., Woolaway, K.E., and White, P.J.** (2003). Changes in gene expression in *Arabidopsis* shoots during phosphate starvation and the potential for developing smart plants. *Plant Physiol* **132**, 578-596.
- Haran, S., Logendra, S., Seskar, M., Bratanova, M., and Raskin, I.** (2000). Characterization of *Arabidopsis* acid phosphatase promoter and regulation of acid phosphatase expression. *Plant Physiol* **124**, 615-626.
- Härtel, H., Dörmann, P., and Benning, C.** (2000). DGD1-independent biosynthesis of extraplastidic galactolipids after phosphate deprivation in *Arabidopsis*. *Proceedings of the National Academy of Sciences* **97**, 10649-10654.
- Heger, J., Patras, P., Nitrayova, S., Dolesova, P., and Sommer, A.** (2007). Histidine maintenance requirement and efficiency of its utilization in young pigs. *Archives of animal nutrition* **61**, 179-188.
- Helariutta, Y., Fukaki, H., Wysocka-Diller, J., Nakajima, K., Jung, J., Sena, G., Hauser, M.T., and Benfey, P.N.** (2000). The SHORT-ROOT gene controls radial patterning of the *Arabidopsis* root through radial signaling. *Cell* **101**, 555-567.
- Henriques, R., Jasik, J., Klein, M., Martinoia, E., Feller, U., Schell, J., Pais, M.S., and Koncz, C.** (2002). Knock-out of *Arabidopsis* metal transporter gene IRT1 results in iron deficiency accompanied by cell differentiation defects. *Plant molecular biology* **50**, 587-597.
- Hinnebusch, A.G.**, (2005) Translational regulation of GCN4 and the general amino acid control of yeast. *Annu. Rev. Microbiol.* **59**, 407-450.
- Hinsinger, P.** (2001). Bioavailability of soil inorganic P in the rhizosphere as affected by root-induced chemical changes: a review. *Plant Soil* **237**, 173-195.
- Hoekenga, O.A., Maron, L.G., Pineros, M.A., Cancado, G.M.A., Shaff, J., Kobayashi, Y., Ryan, P.R., Dong, B., Delhaize, E., Sasaki, T., Matsumoto, H., Yamamoto, Y., Koyama, H., and Kochian, L.V.** (2006). AtALMT1, which encodes a malate transporter, is identified as one of several genes critical for aluminum tolerance in *Arabidopsis*. *Proceedings of the National Academy of Sciences of the United States of America* **103**, 9738-9743.
- Hurlimann, H.C., Pinson, B., Stadler-Waibel, M., Zeeman, S.C., and Freimoser, F.M.** (2009). The SPX domain of the yeast low-affinity phosphate transporter Pho90 regulates transport activity. *Embo Rep* **10**, 1003-1008.
- Ingle, R.A.** (2015). Histidine. In *Amino Acids in Higher Plants* (Ed. J D'Mello), CABI International, Wallingford, UK, p. 251-261.
- Ingle, R.A.** (2011). Histidine Biosynthetic. *Arabidopsis Book*, 2011; 9: e0141.(doi: 10.1199/tab.0141).
- Jain, A., Poling, M.D., Smith, A.P., Nagarajan, V.K., Lahner, B., Meagher, R.B., and Raghothama, K.G.** (2009). Variations in the composition of gelling agents affect morphophysiological and molecular responses to deficiencies of phosphate and other nutrients. *Plant Physiol* **150**, 1033-1049.
- Jiang, C., Gao, X., Liao, L., Harberd, N.P., and Fu, X.** (2007). Phosphate starvation root architecture and anthocyanin accumulation responses are modulated by the gibberellin-DELLA signaling pathway in *Arabidopsis*. *Plant Physiol* **145**, 1460-1470.
- Jones, E.W., and Fink, G.R.** (1982). Regulation of amino acid and nucleotide biosynthetic in yeast, pp. 181-299 in *The Molecular Biology of the Yeast Saccharomyces: Metabolism and Gene Expression*, edited by J. N. Strathern, E. W. Jones, and J. R. Broach. Cold Spring Harbor Laboratory Press, Cold Spring Harbor, NY.

- Jouhet, J., Maréchal, E., Baldan, B., Bligny, R., Joyard, J., and Block, M.A.** (2004). Phosphate deprivation induces transfer of DGDG galactolipid from chloroplast to mitochondria. *The Journal of cell biology* **167**, 863-874.
- Kant, S., Peng, M.S., and Rothstein, S.J.** (2011). Genetic Regulation by NLA and MicroRNA827 for Maintaining Nitrate-Dependent Phosphate Homeostasis in Arabidopsis. *Plos Genetics* **7**.
- Kielland, K., McFarland, J., and Olson, K.** (2006). Amino acid uptake in deciduous and coniferous taiga ecosystems. *Plant Soil* **288**, 297-307.
- Kisko, M., Bouain, N., Rouached, A., Choudhary, S.P., and Rouached, H.** (2015). Molecular mechanisms of phosphate and zinc signalling crosstalk in plants: Phosphate and zinc loading into root xylem in Arabidopsis. *Environ Exp Bot* **114**, 57-64.
- Knappe, S., Flugge, U.I., and Fischer, K.** (2003). Analysis of the plastidic phosphate translocator gene family in Arabidopsis and identification of new phosphate translocator-homologous transporters, classified by their putative substrate-binding site. *Plant Physiology* **131**, 1178-1190.
- Kobayashi, Y., Kobayashi, Y., Watanabe, T., Shaff, J.E., Ohta, H., Kochian, L.V., Wagatsuma, T., Kinraide, T.B., and Koyama, H.** (2013). Molecular and physiological analysis of Al³⁺ and H⁺ rhizotoxicities at moderately acidic conditions. *Plant Physiology* **163**, 180-192.
- Kock, M., Theierl, K., Stenzel, I., and Glund, K.** (1998). Extracellular administration of phosphate-sequestering metabolites induces ribonucleases in cultured tomato cells. *Planta* **204**, 404-407.
- Krapp, A., Berthome, R., Orsel, M., Mercey-Boutet, S., Yu, A., Castaings, L., Elftieh, S., Major, H., Renou, J.P., and Daniel-Vedele, F.** (2011). Arabidopsis Roots and Shoots Show Distinct Temporal Adaptation Patterns toward Nitrogen Starvation. *Plant Physiology* **157**, 1255-1282.
- Kuwabara, A., and Gruissem, W.** (2014). Arabidopsis RETINOBLASTOMA-RELATED and Polycomb group proteins: cooperation during plant cell differentiation and development. *Journal of experimental botany* **65**, 2667-2676.
- Lambers, H., Hayes, P.E., Laliberte, E., Oliveira, R.S., and Turner, B.L.** (2015). Leaf manganese accumulation and phosphorus-acquisition efficiency. *Trends in plant science* **20**, 83-90.
- Lan, P., Li, W., and Schmidt, W.** (2012). Complementary proteome and transcriptome profiling in phosphate-deficient Arabidopsis roots reveals multiple levels of gene regulation. *Molecular & cellular proteomics : MCP* **11**, 1156-1166.
- Larsen, P.B., Kochian, L.V., and Howell, S.H.** (1997). Al inhibits both shoot development and root growth in als3, an Al-sensitive Arabidopsis mutant. *Plant Physiology* **114**, 1207-1214.
- Larsen, P.B., Geisler, M.J.B., Jones, C.A., Williams, K.M., and Cancel, J.D.** (2005). ALS3 encodes a phloem-localized ABC transporter-like protein that is required for aluminum tolerance in Arabidopsis. *Plant Journal* **41**, 353-363.
- Lastdrager, J., Hanson, J., and Smeekens, S.** (2014). Sugar signals and the control of plant growth and development. *Journal of experimental botany* **65**, 799-807.
- Lea, P.J.** (1993). Nitrogen Metabolism. In Lea, P.J., Leegood, R.C. eds, *Plant biochemistry and Molecular Biology*. John Wiley & sons, New York, pp. 21155-180.
- LeBlanc, M.S., McKinney, E.C., Meagher, R.B., and Smith, A.P.** (2013). Hijacking membrane transporters for arsenic phytoextraction. *J Biotechnol* **163**, 1-9.
- Lei, H.J., Li, H.P., Mo, F., Zheng, L.Y., Zhao, H.F., and Zhao, M.M.** (2013). Effects of Lys and His supplementations on the regulation of nitrogen metabolism in lager yeast. *Applied microbiology and biotechnology* **97**, 8913-8921.

- Li, B.H., Li, G.J., Kronzucker, H.J., Baluska, F., and Shi, W.M.** (2014). Ammonium stress in Arabidopsis: signaling, genetic loci, and physiological targets. *Trends in plant science* **19**, 107-114.
- Li, D., Zhu, H., Liu, K., Liu, X., Leggewie, G., Udvardi, M., and Wang, D.** (2002). Purple acid phosphatases of Arabidopsis thaliana. Comparative analysis and differential regulation by phosphate deprivation. *The Journal of biological chemistry* **277**, 27772-27781.
- Liang, C.Y., Tian, J., Lam, H.M., Lim, B.L., Yan, X.L., and Liao, H.** (2010). Biochemical and Molecular Characterization of PvPAP3, a Novel Purple Acid Phosphatase Isolated from Common Bean Enhancing Extracellular ATP Utilization. *Plant Physiology* **152**, 854-865.
- Lin, S.I., and Chiou, T.J.** (2008). Long-distance movement and differential targeting of microRNA399s. *Plant Signal Behav* **3**, 730-732.
- Lin, W.Y., Huang, T.K., and Chiou, T.J.** (2013). NITROGEN LIMITATION ADAPTATION, a Target of MicroRNA827, Mediates Degradation of Plasma Membrane-Localized Phosphate Transporters to Maintain Phosphate Homeostasis in Arabidopsis. *Plant Cell* **25**, 4061-4074.
- Linkohr, B.I., Williamson, L.C., Fitter, A.H., and Leyser, H.M.O.** (2002). Nitrate and phosphate availability and distribution have different effects on root system architecture of Arabidopsis. *Plant Journal* **29**, 751-760.
- Liu, J.P., Magalhaes, J.V., Shaff, J., and Kochian, L.V.** (2009). Aluminum-activated citrate and malate transporters from the MATE and ALMT families function independently to confer Arabidopsis aluminum tolerance. *Plant Journal* **57**, 389-399.
- Liu, J.Q., Allan, D.L., and Vance, C.P.** (2010). Systemic Signaling and Local Sensing of Phosphate in Common Bean: Cross-Talk between Photosynthate and MicroRNA399. *Molecular Plant* **3**, 428-437.
- Liu, Y., LI, X.-H., SUN, X., and ZHANG, C.-Y.** (2012). The change of acid phosphatase activity and analysis of genotypic variation in P efficiency of soybean under phosphorus stress. *Journal of Plant Genetic Resources* **13**, 521-528.
- Ljungdahl, P.O. and Daignan-Fornier, B.** (2012). Regulation of Amino Acid, Nucleotide, and Phosphate Metabolism in *Saccharomyces cerevisiae*. *Genetics*, Vol. 190, 885-929.
- Lohaus, G., and Moellers, C.** (2000). Phloem transport of amino acids in two Brassica napus L. genotypes and one B-carinata genotype in relation to their seed protein content. *Planta* **211**, 833-840.
- Lopez-Arredondo, D.L., Leyva-Gonzalez, M.A., Gonzalez-Morales, S.I., Lopez-Bucio, J., and Herrera-Estrella, L.** (2014). Phosphate Nutrition: Improving Low-Phosphate Tolerance in Crops. *Annu Rev Plant Biol* **65**, 95-123.
- Lopez-Bucio, J., Cruz-Ramirez, A., and Herrera-Estrella, L.** (2003). The role of nutrient availability in regulating root architecture. *Current opinion in plant biology* **6**, 280-287.
- Ma, J.F.** (2000). Role of organic acids in detoxification of aluminum in higher plants. *Plant Cell Physiol* **41**, 383-390.
- Magasanik, B., and Kaiser, C.A.** (2002). Nitrogen regulation in *Saccharomyces cerevisiae*. *Gene* **290**, 1-18.
- Malamy, J.E.** (2005). Intrinsic and environmental response pathways that regulate root system architecture. *Plant Cell Environ* **28**, 67-77.
- Malboobi, M.A., Zamani, K., Lohrasebi, T., Sarikhani, M.R., Samaian, A., and Sabet, M.S.** (2014). Phosphate: the silent challenge. *Progress in Biological Sciences* **4**, 1-32.

- Martinez, P., and Persson, B.L.** (1998). Identification, cloning and characterization of a derepressible Na⁺-coupled phosphate transporter in *Saccharomyces cerevisiae*. *Molecular and General Genetics* **258**, 628-638.
- Maruta, T., Otori, K., Tabuchi, T., Tanabe, N., Tamoi, M., and Shigeoka, S.** (2010). New insights into the regulation of greening and carbon-nitrogen balance by sugar metabolism through a plastidic invertase. *Plant Signal Behav* **5**, 1131-1133.
- McDonald, A.E., Niere, J.O., and Plaxton, W.C.** (2001). Phosphite disrupts the acclimation of *Saccharomyces cerevisiae* to phosphate starvation. *Canadian journal of microbiology* **47**, 969-978.
- Medici, A., Marshall-Colon, A., Ronzier, E., Szponarski, W., Wang, R.C., Gojon, A., Crawford, N.M., Ruffel, S., Coruzzi, G.M., and Krouk, G.** (2015). AtNIGT1/HRS1 integrates nitrate and phosphate signals at the Arabidopsis root tip. *Nat Commun* **6**.
- Meguro, R., Asano, Y., Odagiri, S., Li, C., Iwatsuki, H., and Shoumura, K.** (2007). Nonheme-iron histochemistry for light and electron microscopy: a historical, theoretical and technical review. *Archives of histology and cytology* **70**, 1-19.
- Miflin, B.J., and Lea, P.J.** (1980) Ammonia assimilation. In Miflin BJ, ed, *The Biochemistry of Plants. Vol c5. Amino Acids and Their Derivatives*. Academic Press, New York, pp 169–202.
- Miller, M.J., Barrett-Wilt, G.A., Hua, Z., and Vierstra, R.D.** (2010). Proteomic analyses identify a diverse array of nuclear processes affected by small ubiquitin-like modifier conjugation in Arabidopsis. *Proceedings of the National Academy of Sciences of the United States of America* **107**, 16512-16517.
- Misson, J., Raghothama, K.G., Jain, A., Jouhet, J., Block, M.A., Bligny, R., Ortet, P., Creff, A., Somerville, S., Rolland, N., Doumas, P., Nacry, P., Herrerra-Estrella, L., Nussaume, L., and Thibaud, M.C.** (2005). A genome-wide transcriptional analysis using Arabidopsis thaliana Affymetrix gene chips determined plant responses to phosphate deprivation. *Proceedings of the National Academy of Sciences of the United States of America* **102**, 11934-11939.
- Miura, K., Rus, A., Sharkhuu, A., Yokoi, S., Karthikeyan, A.S., Raghothama, K.G., Back, D., Koo, Y.D., Jin, J.B., Bressan, R.A., Yun, D.J., and Hasegawa, P.M.** (2005). The Arabidopsis SUMO E3 ligase SIZ1 controls phosphate deficiency responses (vol 102, pg 7760, 2005). *Proceedings of the National Academy of Sciences of the United States of America* **102**, 9734-9734.
- Mo, X.R., Zhu, Q.Y., Li, X., Li, J., Zeng, Q.N., Rong, H.L., Zhang, H.M., and Wu, P.** (2006). The hpa1 mutant of Arabidopsis reveals a crucial role of histidine homeostasis in root meristem maintenance. *Plant Physiology* **141**, 1425-1435.
- Morcuende, R., Bari, R., Gibon, Y., Zheng, W.M., Pant, B.D., Blasing, O., Usadel, B., Czechowski, T., Udvardi, M.K., Stitt, M., and Scheible, W.R.** (2007). Genome-wide reprogramming of metabolism and regulatory networks of Arabidopsis in response to phosphorus. *Plant Cell Environ* **30**, 85-112.
- Mori, I., Fonnepfister, R., Matsunaga, S., Tada, S., Kimura, Y., Iwasaki, G., Mano, J., Hatano, M., Nakano, T., Koizumi, S., Scheidegger, A., Hayakawa, K., and Ohta, D.** (1995). A Novel Class of Herbicides - Specific Inhibitors of Imidazoleglycerol Phosphate Dehydratase. *Plant Physiology* **107**, 719-723.
- Muchhal, U.S., Pardo, J.M., and Raghothama, K.G.** (1996). Phosphate transporters from the higher plant Arabidopsis thaliana. *Proceedings of the National Academy of Sciences of the United States of America* **93**, 10519-10523.
- Muller, B., and Touraine, B.** (1992). Inhibition of NO₃ uptake by various phloem-translocated amino acids in soybean seedling. *Journal of Experimental Botany* **43**, 617-23.

- Müller, J., Toev, T., Heisters, M., Teller, J., Moore, K.L., Hause, G., Dinesh, D.C., Burstenbinder, K., and Abel, S.** (2015). Iron-dependent callose deposition adjusts root meristem maintenance to phosphate availability. *Dev Cell* **33**, 216-230.
- Parkash, J., and Asotra, K.** (2011). L-histidine sensing by calcium sensing receptor inhibits voltage-dependent calcium channel activity and insulin secretion in β -cells. *Life Sci.*, **88**(9-10),440-406.
- Muralla, R., Sweeney, C., Stepansky, A., Leustek, T., and Meinke, D.** (2007). Genetic dissection of histidine biosynthesis in Arabidopsis. *Plant Physiology* **144**, 890-903.
- Murphy, J.T., Bruinsma, J.J., Schneider, D.L., Collier, S., Guthrie, J., Chinwalla, A., Robertson, J.D., Mardis, E.R., and Kornfeld, K.** (2011). Histidine Protects Against Zinc and Nickel Toxicity in *Caenorhabditis elegans*. *Plos Genetics* **7**.
- Nagarajan, V.K., Jain, A., Poling, M.D., Lewis, A.J., Raghothama, K.G., and Smith, A.P.** (2011). Arabidopsis Pht1;5 Mobilizes Phosphate between Source and Sink Organs and Influences the Interaction between Phosphate Homeostasis and Ethylene Signaling. *Plant Physiology* **156**, 1149-1163.
- Nakajima, K., Sena, G., Nawy, T., and Benfey, P.N.** (2001). Intercellular movement of the putative transcription factor SHR in root patterning. *Nature* **413**, 307-311.
- Nakamura, Y., Koizumi, R., Shui, G.H., Shimojima, M., Wenk, M.R., Ito, T., and Ohta, H.** (2009). Arabidopsis lipins mediate eukaryotic pathway of lipid metabolism and cope critically with phosphate starvation. *Proceedings of the National Academy of Sciences of the United States of America* **106**, 20978-20983.
- Nasholm, T., Huss-Danell, K., and Hogberg, P.** (2000). Uptake of organic nitrogen in the field by four agriculturally important plant species. *Ecology* **81**, 1155-1161.
- Natarajan, K., Meyer, M.R., Jackson, B.M., Meyer, M.R., Slade, D., Roberts, C., Hinnebusch, A.G., and Marton, M.J.** (2001). Transcriptional Profiling Shows that Gcn4p Is a Master Regulator of Gene Expression during Amino Acid Starvation in Yeast. *Molecular and Cellular Biology* **21**(13),4347-4368.
- Nürnberg, T., Abel, S., Wolfgang J. and Glund K.** (1990). Induction of an Extracellular Ribonuclease in Cultured Tomato Cells upon Phosphate Starvation. *Plant Physiol.* **92**, 970-976.
- Noutoshi, Y., Ito, T., and Shinozaki, K.** (2005). ALBINO AND PALE GREEN 10 encodes BBMII isomerase involved in histidine biosynthesis in Arabidopsis thaliana. *Plant Cell Physiol* **46**, 1165-1172.
- Nussaume, L., Kanno, S., Javot, H., Marin, E., Pochon, N., Ayadi, A., Nakanishi, T.M., and Thibaud, M.C.** (2011). Phosphate import in plants: focus on the PHT1 transporters. *Frontiers in plant science* **2**.
- Ohta, D., Fujimori, K., Mizutani, M., Nakayama, Y., Kunpaisal-Hashimoto, R., Munzer, S., and Kozaki, A.** (2000). Molecular cloning and characterization of ATP-phosphoribosyl transferase from Arabidopsis, a key enzyme in the histidine biosynthetic pathway. *Plant Physiology* **122**, 907-914.
- Olczak, M., Morawiecka, B., and Watorek, W.** (2003). Plant purple acid phosphatases - genes, structures and biological function. *Acta biochimica Polonica* **50**, 1245-1256.
- Osmont, K.S., Sibout, R., and Hardtke, C.S.** (2007). Hidden branches: developments in root system architecture. *Annu Rev Plant Biol* **58**, 93-113.

- Pant, B.D., Pant, P., Erban, A., Huhman, D., Kopka, J., and Scheible, W.R.** (2015). Identification of primary and secondary metabolites with phosphorus status-dependent abundance in Arabidopsis, and of the transcription factor PHR1 as a major regulator of metabolic changes during phosphorus limitation. *Plant Cell Environ* **38**, 172-187.
- Pant, B.D., Musialak-Lange, M., Nuc, P., May, P., Buhtz, A., Kehr, J., Walther, D., and Scheible, W.R.** (2009). Identification of nutrient-responsive Arabidopsis and rapeseed microRNAs by comprehensive real-time polymerase chain reaction profiling and small RNA sequencing. *Plant Physiol* **150**, 1541-1555.
- Park, B.S., Seo, J.S., and Chua, N.H.** (2014). NITROGEN LIMITATION ADAPTATION recruits PHOSPHATE2 to target the phosphate transporter PT2 for degradation during the regulation of Arabidopsis phosphate homeostasis. *Plant Cell* **26**, 454-464.
- Peng, M.S., Hannam, C., Gu, H.L., Bi, Y.M., and Rothstein, S.J.** (2007). A mutation in NLA, which encodes a RING-type ubiquitin ligase, disrupts the adaptability of Arabidopsis to nitrogen limitation. *Plant Journal* **50**, 320-337.
- Peoples, M.B., and Gifford, R.M.** (1993). Long-distance transport of carbon and nitrogen from sources to sinks in higher plants. In DT Dennis, DH Turpin, eds, *Plant physiology, biochemistry and molecular biology*. John Wiley & Son, Inc., New York, pp. 21434-447.
- Peret, B., Clement, M., Nussaume, L., and Desnos, T.** (2011). Root developmental adaptation to phosphate starvation: better safe than sorry. *Trends in plant science* **16**, 442-450.
- Peret, B., Desnos, T., Jost, R., Kanno, S., Berkowitz, O., and Nussaume, L.** (2014). Root Architecture Responses: In Search of Phosphate. *Plant Physiology* **166**, 1713-1723.
- Perini, S., Mambro, R., and Sabatini, S.** (2012). Growth and development of the root apical meristem. *Current opinion in plant biology* **15**, 17-23.
- Petricka, J.J., Winter, C.M., and Benfey, P.N.** (2012a). Control of Arabidopsis Root Development. *Annual Review of Plant Biology*, Vol 63 **63**, 563-590.
- Petricka, J.J., Winter, C.M., and Benfey, P.N.** (2012b). Control of Arabidopsis root development. *Annu Rev Plant Biol* **63**, 563-590.
- Pineros, M.A., Cancado, G.M.A., and Kochian, L.V.** (2008). Novel properties of the wheat aluminum tolerance organic acid transporter (TaALMT1) revealed by electrophysiological characterization in *Xenopus* oocytes: Functional and structural implications. *Plant Physiology* **147**, 2131-2146.
- Pinson, B., Kongsrud, T.L., Ording, E., Johansen, L., Daignan-Fornier, B., and Gabrielsen, O.S.** (2000). Signaling through regulated transcription factor interaction: mapping of a regulatory interaction domain in the Myb-related Bas1p. *Nucleic Acids Res* **28**, 4665-4673.
- Pinson, B., Vaur, S., Sagot, I., Couplier, F., Lemoine, S., and Daignan-Fornier, B.** (2009). Metabolic intermediates selectively stimulate transcription factor interaction and modulate phosphate and purine pathways. *Genes & development* **23**, 1399-1407.
- Plaxton, W.C., and Tran, H.T.** (2011). Metabolic adaptations of phosphate-starved plants. *Plant Physiol* **156**, 1006-1015.
- Poethig, R.S.** (2013). Vegetative phase change and shoot maturation in plants. *Current topics in developmental biology* **105**, 125-152.
- Poirier, Y., and Bucher, M.** (2002). Phosphate transport and homeostasis in Arabidopsis. *The Arabidopsis book/American Society of Plant Biologists* **1**.
- Poirier, Y., Thoma, S., Somerville, C., and Schiefelbein, J.** (1991). Mutant of Arabidopsis deficient in xylem loading of phosphate. *Plant Physiol* **97**, 1087-1093.
- Polkinghorne, M., and Hynes, M.J.** (1975). Effect of L-histidine on the catabolism of nitrogenous compounds in *Aspergillus nidulans*. *Journal of general microbiology* **87**, 185-187.

- Puga, M.I., Mateos, I., Charukesi, R., Wang, Z., Franco-Zorrilla, J.M., de Lorenzo, L., Irigoye, M.L., Masiero, S., Bustos, R., Rodriguez, J., Leyva, A., Rubio, V., Sommer, H., and Paz-Ares, J.** (2014). SPX1 is a phosphate-dependent inhibitor of PHOSPHATE STARVATION RESPONSE 1 in Arabidopsis. *Proceedings of the National Academy of Sciences of the United States of America* **111**, 14947-14952.
- Raghothama, K.G.** (1999). Phosphate acquisition. *Annu Rev Plant Phys* **50**, 665-693.
- Remy, E., Cabrito, T.R., Batista, R.A., Teixeira, M.C., Sa-Correia, I., and Duque, P.** (2012). The Pht1;9 and Pht1;8 transporters mediate inorganic phosphate acquisition by the Arabidopsis thaliana root during phosphorus starvation. *New Phytologist* **195**, 356-371.
- Reymond, M., Svistonoff, S., Loudet, O., Nussaume, L., and Desnos, T.** (2006). Identification of QTL controlling root growth response to phosphate starvation in Arabidopsis thaliana. *Plant Cell Environ* **29**, 115-125.
- Richardson, A.E.** (2009). Regulating the phosphorus nutrition of plants: molecular biology meeting agronomic needs. *Plant Soil* **322**, 17-24.
- Richardson, A.E., Lynch, J.P., Ryan, P.R., Delhaize, E., Smith, F.A., Smith, S.E., Harvey, P.R., Ryan, M.H., Veneklaas, E.J., Lambers, H., Oberson, A., Culvenor, R.A., and Simpson, R.J.** (2011). Plant and microbial strategies to improve the phosphorus efficiency of agriculture. *Plant and Soil* **349**, 121-156.
- Richardson, A.E., Hocking, P.J., Simpson, R.J., and George, T.S.** (2009). Plant mechanisms to optimise access to soil phosphorus. *Crop Pasture Sci* **60**, 124-143.
- Robinson, N.J., Procter, C.M., Connolly, E.L., and Guerinot, M.L.** (1999). A ferric-chelate reductase for iron uptake from soils. *Nature* **397**, 694-697.
- Rogers, E.E., and Guerinot, M.L.** (2002). FRD3, a member of the multidrug and toxin efflux family, controls iron deficiency responses in Arabidopsis. *Plant Cell* **14**, 1787-1799.
- Rosas, U., Cibrian-Jaramillo, A., Ristova, D., Banta, J.A., Gifford, M.L., Fan, A.H., Zhou, R.W., Kim, G.J., Krouk, G., Birnbaum, K.D., Purugganan, M.D., and Coruzzi, G.M.** (2013). Integration of responses within and across Arabidopsis natural accessions uncovers loci controlling root systems architecture. *Proceedings of the National Academy of Sciences of the United States of America* **110**, 15133-15138.
- Roschzttardtz, H., Conejero, G., Curie, C., and Mari, S.** (2009). Identification of the Endodermal Vacuole as the Iron Storage Compartment in the Arabidopsis Embryo. *Plant Physiology* **151**, 1329-1338.
- Rosemarin, A., Schroder, J., Dagerskog, L., Cordell, D., and Smit, A.** (2011). Future supply of phosphorus in agriculture and the need to maximise efficiency of use and reuse.
- Rouached, H., Stefanovic, A., Secco, D., Bulak Arpat, A., Gout, E., Bligny, R., and Poirier, Y.** (2011). Uncoupling phosphate deficiency from its major effects on growth and transcriptome via PHO1 expression in Arabidopsis. *The Plant journal : for cell and molecular biology* **65**, 557-570.
- Ruan, W., Guo, M., Cai, L., Hu, H., Li, C., Liu, Y., Wu, Z., Mao, C., Yi, K., and Wu, P.** (2015). Genetic manipulation of a high-affinity PHR1 target cis-element to improve phosphorous uptake in *Oryza sativa* L. *Plant molecular biology* **87**, 429-440.
- Rubio, V., Linhares, F., Solano, R., Martin, A.C., Iglesias, J., Leyva, A., and Paz-Ares, J.** (2001). A conserved MYB transcription factor involved in phosphate starvation signaling both in vascular plants and in unicellular algae. *Genes Dev* **15**, 2122-2133.

- Ryan, P., Delhaize, E., and Jones, D.** (2001). Function and Mechanism of Organic Anion Exudation from Plant Roots. *Annu Rev Plant Physiol Plant Mol Biol* **52**, 527-560.
- Sabatini, S., Heidstra, R., Wildwater, M., and Scheres, B.** (2003). SCARECROW is involved in positioning the stem cell niche in the Arabidopsis root meristem. *Genes & development* **17**, 354-358.
- Sanchez-Calderon, L., Lopez-Bucio, J., Chacon-Lopez, A., Gutierrez-Ortega, A., Hernandez-Abreu, E., and Herrera-Estrella, L.** (2006). Characterization of low phosphorus insensitive mutants reveals a crosstalk between low phosphorus-induced determinate root development and the activation of genes involved in the adaptation of Arabidopsis to phosphorus deficiency. *Plant Physiology* **140**, 879-889.
- Sanchez-Calderon, L., Lopez-Bucio, J., Chacon-Lopez, A., Cruz-Ramirez, A., Nieto-Jacobo, F., Dubrovsky, J.G., and Herrera-Estrella, L.** (2005). Phosphate starvation induces a determinate developmental program in the roots of Arabidopsis thaliana. *Plant Cell Physiol* **46**, 174-184.
- Santi, S., and Schmidt, W.** (2009). Dissecting iron deficiency-induced proton extrusion in Arabidopsis roots. *New Phytologist* **183**, 1072-1084.
- Sasaki, T., Yamamoto, Y., Ezaki, B., Katsuhara, M., Ahn, S.J., Ryan, P.R., Delhaize, E., and Matsumoto, H.** (2004). A wheat gene encoding an aluminum-activated malate transporter. *Plant Journal* **37**, 645-653.
- Satbhai, S.B., Ristova, D., and Busch, W.** (2015). Underground tuning: quantitative regulation of root growth. *Journal of experimental botany* **66**, 1099-1112.
- Sasahara, I., Fujimura, N., Nozawa, Y., Furuhashi, Y., and Sato, H.** (2015). The effect of histidine on mental fatigue and cognitive performance in subjects with high fatigue and sleep disruption scores. *Physiol Behav.* **147**, 238-244.
- Scheres, B., Benfey, P., and Dolan, L.** (2002). Root development. In: Somerville CR, Meyerowitz EM, eds. *The Arabidopsis book*. Rockville: America Society of Plant Biologists.
- Schmidt, S., and Stewart, G.R.** (1999). Glycine metabolism by plant roots and its occurrence in Australian plant communities. *Aust J Plant Physiol* **26**, 253-264.
- Secco, D., Wang, C., Shou, H., and Whelan, J.** (2012a). Phosphate homeostasis in the yeast *Saccharomyces cerevisiae*, the key role of the SPX domain-containing proteins. *FEBS letters* **586**, 289-295.
- Secco, D., Wang, C., Shou, H.X., and Whelan, J.** (2012b). Phosphate homeostasis in the yeast *Saccharomyces cerevisiae*, the key role of the SPX domain-containing proteins. *FEBS letters* **586**, 289-295.
- Shin, H., Shin, H.S., Dewbre, G.R., and Harrison, M.J.** (2004). Phosphate transport in Arabidopsis: Pht1;1 and Pht1;4 play a major role in phosphate acquisition from both low- and high-phosphate environments. *Plant Journal* **39**, 629-642.
- Shin, H., Shin, H.S., Chen, R., and Harrison, M.J.** (2006). Loss of At4 function impacts phosphate distribution between the roots and the shoots during phosphate starvation. *Plant Journal* **45**, 712-726.
- Sokalingam, S., Raghunathan, G., Soundrarajan, N., and Lee, S.G.** (2012). A Study on the Effect of Surface Lysine to Arginine Mutagenesis on Protein Stability and Structure Using Green Fluorescent Protein. *PloS one* **7**.
- Stefanovic, A., Arpat, A.B., Bligny, R., Gout, E., Vidoudez, C., Bensimon, M., and Poirier, Y.** (2011). Over-expression of PHO1 in Arabidopsis leaves reveals its role in mediating phosphate efflux. *Plant Journal* **66**, 689-699.

- Su, T., Xu, Q., Zhang, F.C., Chen, Y., Li, L.Q., Wu, W.H., and Chen, Y.F.** (2015). WRKY42 Modulates Phosphate Homeostasis through Regulating Phosphate Translocation and Acquisition in Arabidopsis. *Plant Physiology* **167**, 1579-U1717.
- Sun, X., Feng, R., Li, Y., Lin, S., Zhang, W., Li, Y., Sun, C., and Li, S.** (2014). Histidine supplementation alleviates inflammation in the adipose tissue of high-fat diet-induced obese rats via the NF- κ B- and PPAR γ -involved pathways. *Br J Nutr.*, **112**(4),477-85.
- Svistoonoff, S., Creff, A., Reymond, M., Sigoillot-Claude, C., Ricaud, L., Blanchet, A., Nussaume, L., and Desnos, T.** (2007). Root tip contact with low-phosphate media reprograms plant root architecture. *Nature genetics* **39**, 792-796.
- Takabatake, R., Hata, S., Taniguchi, M., Kouchi, H., Sugiyama, T., and Izui, K.** (1999). Isolation and characterization of cDNAs encoding mitochondrial phosphate transporters in soybean, maize, rice, and Arabidopsis. *Plant molecular biology* **40**, 479-486.
- S.N., Li, T.H., Cong, P.S., Xiong, W.W., Wang, Z.H., and Sun, J.M.** (2013). PlantLoc: an accurate web server for predicting plant protein subcellular localization by substantiality motif. *Nucleic Acids Res* **41**, W441-W447.
- Thibaud, M.C., Arrighi, J.F., Bayle, V., Chiarenza, S., Creff, A., Bustos, R., Paz-Ares, J., Poirier, Y., and Nussaume, L.** (2010). Dissection of local and systemic transcriptional responses to phosphate starvation in Arabidopsis. *Plant Journal* **64**, 775-789.
- Ticconi, C.A., and Abel, S.** (2004). Short on phosphate: plant surveillance and countermeasures. *Trends in plant science* **9**, 548-555.
- Ticconi, C.A., Delatorre, C.A., and Abel, S.** (2001). Attenuation of phosphate starvation responses by phosphite in arabidopsis. *Plant Physiology* **127**, 963-972.
- Ticconi, C.A., Delatorre, C.A., Lahner, B., Salt, D.E., and Abel, S.** (2004). Arabidopsis pdr2 reveals a phosphate-sensitive checkpoint in root development. *Plant Journal* **37**, 801-814.
- Ticconi, C.A., Lucero, R.D., Sakhonwasee, S., Adamson, A.W., Creff, A., Nussaume, L., Desnos, T., and Abel, S.** (2009). ER-resident proteins PDR2 and LPR1 mediate the developmental response of root meristems to phosphate availability. *Proceedings of the National Academy of Sciences of the United States of America* **106**, 14174-14179.
- Ticebaldwin, K., Fink, G.R., and Arndt, K.T.** (1989). Bas1 Has a Myb Motif and Activates His4 Transcription Only in Combination with Bas2. *Science* **246**, 931-935.
- Tomscha, J.L., Trull, M.C., Deikman, J., Lynch, J.P., and Gultinan, M.J.** (2004). Phosphatase under-producer mutants have altered phosphorus relations. *Plant Physiology* **135**, 334-345.
- Tran, H.T., and Plaxton, W.C.** (2008). Proteomic analysis of alterations in the secretome of Arabidopsis thaliana suspension cells subjected to nutritional phosphate deficiency. *Proteomics* **8**, 4317-4326.
- Tran, H.T., Hurley, B.A., and Plaxton, W.C.** (2010). Feeding hungry plants: The role of purple acid phosphatases in phosphate nutrition. *Plant Science* **179**, 14-27.
- Trull, M.C., and Deikman, D.** (1998). An Arabidopsis mutant missing one acid phosphatase isoform. *Planta* **206**, 544-550.
- Turner, B.L., Lambers, H., Condon, L.M., Cramer, M.D., Leake, J.R., Richardson, A.E., and Smith, S.E.** (2013). Soil microbial biomass and the fate of phosphorus during long-term ecosystem development. *Plant Soil* **367**, 225-234.
- Tzafirir, I., Pena-Muralla, R., Dickerman, A., Berg, M., Rogers, R., Hutchens, S., Sweeney, T.C., McElver, J., Aux, G., Patton, D., and Meinke, D.** (2004). Identification of genes required for embryo development in Arabidopsis. *Plant Physiology* **135**, 1206-1220.
- Valdes-Lopez, O., Arenas-Huertero, C., Ramirez, M., Girard, L., Sanchez, F., Vance, C.P., Reyes, J.L., and Hernandez, G.** (2008). Essential role of MYB transcription factor: PvPHR1 and microRNA: PvmiR399 in phosphorus-deficiency signalling in common bean roots. *Plant Cell Environ* **31**, 1834-1843.

- Vance, C.P.** (2001). Symbiotic nitrogen fixation and phosphorus acquisition. *Plant nutrition in a world of declining renewable resources. Plant Physiology* **127**, 390-397.
- Vance, C.P.** (2010). Quantitative Trait Loci, Epigenetics, Sugars, and MicroRNAs: Quaternaries in Phosphate Acquisition and Use. *Plant Physiology* **154**, 582-588.
- Vance, C.P., Uhde-Stone, C., and Allan, D.L.** (2003). Phosphorus acquisition and use: critical adaptations by plants for securing a nonrenewable resource. *New Phytologist* **157**, 423-447.
- vandenBerg, C., Willemsen, V., Hendriks, G., Weisbeek, P., and Scheres, B.** (1997). Short-range control of cell differentiation in the Arabidopsis root meristem. *Nature* **390**, 287-289.
- Varotto, C., Maiwald, D., Pesaresi, P., Jahns, P., Salamini, F., and Leister, D.** (2002). The metal ion transporter IRT1 is necessary for iron homeostasis and efficient photosynthesis in Arabidopsis thaliana. *Plant Journal* **31**, 589-599.
- Veneklaas, E.J., Lambers, H., Bragg, J., Finnegan, P.M., Lovelock, C.E., Plaxton, W.C., Price, C.A., Scheible, W.R., Shane, M.W., White, P.J., and Raven, J.A.** (2012). Opportunities for improving phosphorus-use efficiency in crop plants. *New Phytologist* **195**, 306-320.
- Versaw, W.K., and Metzenberg, R.L.** (1995). Repressible Cation-Phosphate Symporters in Neurospora-Crassa. *Proceedings of the National Academy of Sciences of the United States of America* **92**, 3884-3887.
- Versaw, W.K., and Harrison, M.J.** (2002). A chloroplast phosphate transporter, PHT2;1, influences allocation of phosphate within the plant and phosphate-starvation responses. *Plant Cell* **14**, 1751-1766.
- Vert, G., Grotz, N., Dedaldechamp, F., Gaymard, F., Guerinot, M.L., Briat, J.F., and Curie, C.** (2002). IRT1, an Arabidopsis transporter essential for iron uptake from the soil and for plant growth. *Plant Cell* **14**, 1223-1233.
- Vincent, J.B., Crowder, M.W., and Averill, B.A.** (1992). Hydrolysis of Phosphate Monoesters - a Biological Problem with Multiple Chemical Solutions. *Trends Biochem Sci* **17**, 105-110.
- Voll, L.M., Allaire, E.E., Fiene, G., and Weber, A.P.** (2004). The Arabidopsis phenylalanine insensitive growth mutant exhibits a deregulated amino acid metabolism. *Plant Physiol* **136**, 3058-3069.
- Wagatsuma, T., Khan, M.S.H., Watanabe, T., Maejima, E., Sekimoto, H., Yokota, T., Nakano, T., Toyomasu, T., Tawaraya, K., Koyama, H., Uemura, M., Ishikawa, S., Ikka, T., Ishikawa, A., Kawamura, T., Murakami, S., Ueki, N., Umetsu, A., and Kannari, T.** (2015). Higher sterol content regulated by CYP51 with concomitant lower phospholipid content in membranes is a common strategy for aluminium tolerance in several plant species. *Journal of experimental botany* **66**, 907-918.
- Wang, C., Ying, S., Huang, H.J., Li, K., Wu, P., and Shou, H.X.** (2009). Involvement of OsSPX1 in phosphate homeostasis in rice. *Plant Journal* **57**, 895-904.
- Wang, R.C., Okamoto, M., Xing, X.J., and Crawford, N.M.** (2003). Microarray analysis of the nitrate response in Arabidopsis roots and shoots reveals over 1,000 rapidly responding genes and new linkages to glucose, trehalose-6-phosphate, iron, and sulfate metabolism. *Plant Physiology* **132**, 556-567.
- Ward, J.T., Lahner, B., Yakubova, E., Salt, D.E., and Raghothama, K.G.** (2008). The effect of iron on the primary root elongation of Arabidopsis during phosphate deficiency. *Plant Physiol* **147**, 1181-1191.
- Wildwater, M., Campilho, A., Perez-Perez, J.M., Heidstra, R., Blilou, I., Korthout, H., Chatterjee, J., Mariconti, L., Gruijsem, W., and Scheres, B.** (2005). The

RETINOBLASTOMA-RELATED gene regulates stem cell maintenance in Arabidopsis roots. *Cell* **123**, 1337-1349.

Williamson, L.C., Ribrioux, S.P., Fitter, A.H., and Leyser, H.M. (2001). Phosphate availability regulates root system architecture in Arabidopsis. *Plant Physiol* **126**, 875-882.

Wissler, R.W., Steffee, C.H., and et al. (1948). Studies in amino acid utilization; the role of the indispensable amino acids in maintenance of the adult albino rat. *The Journal of nutrition* **36**, 245-262.

Wolf, P.A., and Corley, R.C. (1939). Significance of amino acids for the maintenance of nitrogen balance in the adult white rat. *American Journal of Physiology--Legacy Content* **127**, 589-596.

Woo, J., MacPherson, C.R., Liu, J., Wang, H., Kiba, T., Hannah, M.A., Wang, X.J., Bajic, V.B., and Chua, N.H. (2012). The response and recovery of the Arabidopsis thaliana transcriptome to phosphate starvation. *BMC plant biology* **12**.

Wu, P., Ma, L.G., Hou, X.L., Wang, M.Y., Wu, Y.R., Liu, F.Y., and Deng, X.W. (2003). Phosphate starvation triggers distinct alterations of genome expression in Arabidopsis roots and leaves. *Plant Physiology* **132**, 1260-1271.

Yates, C.M., Filippis, I., Kelley, L.A., and Sternberg, M.J.E. (2014). SuSPect: Enhanced Prediction of Single Amino Acid Variant (SAV) Phenotype Using Network Features. *J Mol Biol* **426**, 2692-2701.

Yu, B., Xu, C.C., and Benning, C. (2002). Arabidopsis disrupted in SQD2 encoding sulfolipid synthase is impaired in phosphate-limited growth. *Proceedings of the National Academy of Sciences of the United States of America* **99**, 5732-5737.

Zakhleniuk, O.V., Raines, C.A., and Lloyd, J.C. (2001). *pho3*: a phosphorus-deficient mutant of Arabidopsis thaliana (L.) Heynh. *Planta* **212**, 529-534.

Zavaliev, R., Ueki, S., Epel, B.L., and Citovsky, V. (2011). Biology of callose (β -1, 3-glucan) turnover at plasmodesmata. *Protoplasma* **248**, 117-130.

Zeng, X.Q., Chow, W.S., Su, L.J., Peng, X.X., and Peng, C.L. (2010). Protective effect of supplemental anthocyanins on Arabidopsis leaves under high light. *Physiologia plantarum* **138**, 215-225.

Zhang, G.C., Slaski, J.J., Archambault, D.J., and Taylor, G.J. (1996). Aluminum-induced alterations in lipid composition of microsomal membranes from an aluminum-resistant and an aluminum-sensitive cultivar of *Triticum aestivum*. *Physiologia plantarum* **96**, 683-691.

Zhang, Y., Wang, X.Y., Lu, S., and Liu, D. (2014). A major root-associated acid phosphatase in Arabidopsis, AtPAP10, is regulated by both local and systemic signals under phosphate starvation. *Journal of experimental botany* **65**, 6577-6588.

Zhou, J., Jiao, F.C., Wu, Z.C., Li, Y.Y., Wang, X.M., He, X.W., Zhong, W.Q., and Wu, P. (2008). OsPHR2 is involved in phosphate-starvation signaling and excessive phosphate accumulation in shoots of plants. *Plant Physiology* **146**, 1673-1686.

Zhou, Y., and Ni, M. (2010). SHORT HYPOCOTYL UNDER BLUE1 Truncations and Mutations Alter Its Association with a Signaling Protein Complex in Arabidopsis. *Plant Cell* **22**, 703-715.

Ziegler, J., and Abel, S. (2014). Analysis of amino acids by HPLC/electrospray negative ion tandem mass spectrometry using 9-fluorenylmethoxycarbonyl chloride (Fmoc-Cl) derivatization. *Amino Acids* **46**, 2799-2808.

LIST OF ABBREVIATION

AA - Amino acid	NH₄Cl - Ammonium chloride
ACP5 - Acid phosphatase	(NH₄)₂SO₄ -Ammonium sulfate
ALMT - Aluminum-activated malate transporter 1	NO₃⁻ - Nitrate
AM - Arbuscular mycorrhizal	P - Phosphorus
Arg (R) - Arginine	Pi -Phosphate
Asn - Asparagine	P1BS - PHR1 binding sequences
ATP-PRT1 - ATP-phosphoribosyl transferease 1	PDR1 -Phosphate deficiency response 1
bHLH - Basic helix-loop-helix	PEPC -Phosphoenolpyruvate carboxylase
Col-0 - <i>Arabidopsis thaliana</i>	Phe - Phenylalanine
dCAPS - derived cleaved-amplified polymorphic sequences	PHF1 -Transporter traffic facilitator 1
DNA - Deoxyribonucleic acid	Phi -Phosphite
EMS - Ethyl methanesulfonate	PHO2 -Phosphate2
ER - Endoplasmic reticulum	PHR1 -Phosphate starvation response 1
Fe - Iron	PI - Propidium iodide
FW - Fresh weight	PR - Primary root
Gln - Glutamine	Pro - Proline
Glu -Glutamate	PSI -Phosphate Starvation induced
His - Histidine	QC - quiescent center
KNO₃ . Potassium nitrate	RBR -Retinoblastoma-related
Ler-0 - <i>Landsberg erecta</i>	RNS -Ribonuclease
LPR1 -Low phosphate root1	RSA -Root system architecture
LPI -low phosphate insensitive	SCN - Stem cell niche
LR -Lateral root	SCR -Scarecrow
Lys or K - lysine	SD -standard deviation
M - Molar	SHR - Short-root
miRNA - microRNA	SNP -Single nucleotide polymorphism
mM -millimolar	Trp - Tryptophan
μM - micromolar	Val - Valine
N -Nitrogen	WT - Wild-type
NH₄⁺ -Ammonium	Xpr1 -Xenotropic and polytropic retrovirus receptor 1

Acknowledgement

I am expressing *Sukria* to my Allah for granting the wish of my late father, Delower Hossen who wanted me to be graduated with a PhD degree. His advice, inspiration and encouragement still act as a tonic for me to go ahead. He left us forever on 2nd December, 2007 but still I feel his presence behind me. I am remembering my beloved mother Halima Delower who continuously supports me through her inspiration and prayer to complete my study smoothly.

I would like express my sincere gratitude to my supervisor Professor Steffen Abel for giving me the opportunity to work with nice and exciting projects. His continuous support, guidance and patience during the course of my work have made it possible to write this thesis. I appreciate all his contributions of time, intellectual ideas, and amicable discussions throughout the whole period to shape the present format of this thesis. His outstanding and innovative ideas along with inspiration enthusiastically propelled me to complete the work successfully.

I would like to thank my guide Dr. Jens Müller for his insightful suggestions, guidance and criticism to improve the work. His tireless effort on reading my draft and valuable comments on my writing has improved my writing capability. Next person deserve the credit is Dr. Katharina Bürstenbinder for her help, advice and encouragement.

I also would like to thank Dr. Jörg Ziegler for his help to determine amino acid and phosphate content that has added valuable information to my thesis work.

Thanks to Professor Dr. Marcel Quint and Dr. Carolin Delker for their valuable guidelines to design the experiment for the initiation of the suppressor screening.

Many people in the Department of Molecular Signal Processing of IPB helped me in many ways at least with a smile. The names that need to mentions are Dinesh and Kalidoss, Anshu, Amar and Masum. Thanks to Kalidoss Ramamoorthy for sharing his experience that speeded up my work to identify the *PDR1* gene. Thanks to Dinesh Dhurvas Chandrasekaran specially for helping me to purify the herring sperm DNA that was crucial of the experiments and helped to do the homology modelling of ATP-PRT1. The reading of my thesis and passing the comments by Anshu Khatri helped to avoid the stupid mistakes. I am also thankful to Msum Haq and Ammer Jaber for reading a part of the thesis.

Thanks to the authority of the Shahjalal University of Science and Technology for granting me the study leave to complete the PhD work. Specially thanks to Professor Dr Narayan Saha, chairman of the Department of Forestry and environmental Science, for his administrative help and continuous inspiration. I am thankful to DAAD for awarding me the scholarship for PhD.

Finally, I want to acknowledge my wife Most Masuma Khanum for her love, encouragement and patience. Indeed it would have not been possible to complete the work so fast without her continuous support. Thanks to my special gift Jesita Delu, my little Mommy, who relieve my all the tiredness by giving a sweet smile.

Curriculum Vitae

Personal information

First name(s) / Surname(s) **Romel Ahmed**
Address Department of Forestry and Environmental Science, Shahjalal University of Science and Technology Sylhet (Bangladesh)
E-mail(s) romelahmed76@yahoo.com
Nationality Bangladesh
Date of birth 12/12/1976
Gender Male

Work experience

Dates 13/12/2005 →
Occupation or position held Assistant Professor
Main activities and responsibilities Teaching and research
Name and address of employer Shahjalal University of Science and Technology Department of Forestry and Environmental Science, 3114 Sylhet (Bangladesh)

Education and training

Dates 12/09/2008 - 01/09/2010
Title of qualification awarded M. Sc. in Horticulture,
Thesis Biochemical, molecular and analytical investigations of the study of the flavone formation in *Dahlia variabilis*
Supervisor: Professor Karl Stich, Vienna University of Technology Getreidemarkt 9,, 1060 Vienna (Austria)
University Degree awarded by Alma Mater Studiorum -University of Bologna (Italy), Technical University of Munich and BOKU, Vienna (Erasmus Mundus Joint Master degree programme)
Dates 10/07/2001 - 31/12/2003
Title of qualification awarded Graduation in Forestry
Principal subjects covered Allelopathy
University Chittagong University Institute of Forestry and Environmental Science,, 4331 Chittagong (Bangladesh)

Publications

Thill, J., Miosic, S., Ahmed, R., Schlangen, K., Muster, G., Stich, K. and Halbwirth, H. 2012. 'Le Rouge et le Noir': A decline in flavone formation correlates with the rare color of black dahlia (*Dahlia variabilis* hort.) flowers. BMC Plant Biology, 12:225.
Ahmed, R., Hoque A. T. M. R., and Hossain, M. K. 2008. Allelopathic effects of leaf litters of *Eucalyptus camaldulensis* on some forest and agricultural crops. Journal of Forestry Research. 19(1):19–24.
Ahmed, R., Uddin, M. B., Khan, M.A.S.A., Mukul, S. A., and Hossain, M.K. 2007. Allelopathic effects of *Lantana camara* L. on germination and growth behavior of some agricultural crops. Journal of Forestry Research. 18 (4):301- 304.

Scholarship awarded

Erasmus Mundus (2008-2010) and DAAD (2011-2015).